



Durham E-Theses

Analysis of noise in the Rookhope area

Halls, H. C.

How to cite:

Halls, H. C. (1964) *Analysis of noise in the Rookhope area*, Durham theses, Durham University.
Available at Durham E-Theses Online: <http://etheses.dur.ac.uk/10036/>

Use policy

The full-text may be used and/or reproduced, and given to third parties in any format or medium, without prior permission or charge, for personal research or study, educational, or not-for-profit purposes provided that:

- a full bibliographic reference is made to the original source
- a [link](#) is made to the metadata record in Durham E-Theses
- the full-text is not changed in any way

The full-text must not be sold in any format or medium without the formal permission of the copyright holders.

Please consult the [full Durham E-Theses policy](#) for further details.

ANALYSIS OF NOISE IN THE ROOKHOPE AREA.

by

H.C.Halls, (1964)

ABSTRACT.

The main purpose of this research has been to investigate the attenuation and frequency characteristics of noise generated by a single source.

About seven weeks were spent from October to late November, 1963 measuring the vertical ground velocity of the noise over a network of recording stations on the southern slopes of the valley at Rookhope, County Durham.

Special recording methods were used to eliminate the effects of any variation in noise level with time. This was necessary as the ground velocity at all stations over the network had to be normalised to values that would be obtained for a constant source, before they could be used in the construction of attenuation curves.

Two methods of frequency analysis were performed on a number of the station records: one a power spectral analysis using a computer to facilitate calculations, and the other employing a range of band-pass filters on records obtained on magnetic tape. Both techniques showed that the noise consisted essentially of two frequency components, 6 c.p.s. and 11-12 c.p.s., the latter being confined to an area in the immediate vicinity of the source.

Attenuation analyses revealed the presence of two areas to the west and south of the source which showed noticeably different rates of attenuation.

Two possible hypotheses were put forward to explain this phenomenon: one embodying a change in subsurface conditions between the two areas, and the other constant subsurface conditions, but a change in the predominant wave types propagating over the two regions.

Since no knowledge could be obtained on the precise distribution and nature of the wavetypes, as the vertical ground velocity only was measured, both theories were considered to be open to some doubt, and thus preference was given to neither.

It was found that the values of the rate of absorption obtained for the two areas were generally consistent with those usually found from laboratory experiments on sedimentary rocks.

ANALYSIS OF NOISE IN THE ROOKHOPE AREA

Being a Thesis submitted for the degree of
Master of Science
in
The University of Durham

by

Henry C. Halls, B.Sc.

Durham 1964



CONTENTS

	<u>PAGE</u>
ABSTRACT.....	1
 <u>CHAPTER I - INTRODUCTION AND GEOLOGY</u>	
1. Introduction	4
Seismic Attenuation in the Rookhope area	
The Nature of Absorption	
2. Geology	10
 <u>CHAPTER II - FIELDWORK PROCEDURE AND RECORDING TECHNIQUES</u>	
1. Field Procedure	14
Construction of the Station Network	
Description of Stations	
Seismometer-ground coupling	
2. Recording Techniques	19
The Method of Recording at Individual	
Stations	
Recording Techniques used over the Field	
Network	
Recording Caravan Experiments	
 <u>CHAPTER III - INSTRUMENTATION</u>	
1. Instrumentation of Field Equipment	25
Willmore Seismometer	
Neocardiograph Pen-recorder	
Instrumental Calibration	
Frequency Response of the Seismograph	
2. Caravan Instrumentation	43
 <u>CHAPTER IV - FREQUENCY AND ATTENUATION ANALYSES</u>	
1. General Description of Field Records	46
2. Frequency Analysis	48
Power Spectrum Analysis	
Frequency Analysis using Caravan Filters	
Comparison of results Obtained by Filter	
and Power Spectrum Analyses	
3. Attenuation Analysis	62
Method of Measuring Average Peak-to-peak	
amplitude	
Observations on Noise Variation	
Plotting of Attenuation Curves	
Comparison of Attenuation Results Obtained	
from Record Measurements and Power	
Frequency Analysis	

CONTENTS
(continued)

	<u>PAGE</u>
<u>CHAPTER V - INTERPRETATIONS AND CONCLUSIONS</u>	
1. Interpretations	83
The Nature of the Noise Source	
The Cause of the Difference in Attenuation	
2 Conclusions	92
APPENDIX A	I
APPENDIX B	II
APPENDIX C	III
APPENDIX D	IV
APPENDIX E	V
ACKNOWLEDGMENTS	VI
BIBLIOGRAPHY	VII

LIST OF ILLUSTRATIONS

<u>FIGURE NO.</u>	<u>DESCRIPTION</u>	<u>FOLLOWING PAGE</u>
1	Map of Rookhope area showing position of recording stations	4
2	Wavefronts of body and surface waves from a surface source	5
3	Geological map of Rookhope area	10
4	Carboniferous succession in the Rookhope area	10
5	Willmore seismometer	25
6	Amplifier and seismometer calibration, and damping circuits used in the seismograph	27
7	Neocardiograph	28
8	Seismometer response curve	39
9	Amplifier response curve	41
10	Seismograph response curve	42
11	Records of local and background noise.	46
12	Records of local noise	48
13	a. Amplitude measurements of a random waveform	49
	b. Spectral window	49
	c. Cause of increased side lobes in spectral windows	49
14	Computer programme for Power frequency analysis.....	54
15	Computer programme for sine wave summation	54
16	Power spectrum for station 9	55
17	Power spectrum for station 6	55
18	Filter channels for station 25, recorded from caravan	58

LIST OF ILLUSTRATIONS

(continued)

<u>FIGURE NO.</u>	<u>DESCRIPTION</u>	<u>FOLLOWING PAGE</u>
19	Filter channels for stations 24, 19 and 10, recorded from caravan.....	58
20	Relative amplitudes of frequency components filtered from noise	58
21	Caravan recordings showing variation in noise level	69
22	Scatter diagram of ground velocity V as function of distance R from source, for all stations	76
23	Variation of ground velocity along lowest arc profile	76
24	Variation of ground velocity along middle and upper arc profiles	76
25	Plot of V.R against R on logarithmic graph paper, for two lowest arc profiles	77
26	Plot of V.R against R on linear graph paper, for two lowest arc profiles....	77
27	Contour map showing ground velocity variation over Rookhope area.....	78
28	Record made by caravan during termination of source output	83

ABSTRACT

The main purpose of this research has been to investigate the attenuation and frequency characteristics of noise generated by a single source.

About seven weeks were spent from October to late November, 1963 measuring the vertical ground velocity of the noise over a network of recording stations on the southern slopes of the valley at Rookhope, County Durham.

Special recording methods were used to eliminate the effects of any variation in noise level with time. This was necessary as the ground velocity at all stations over the network had to be normalised to values that would be obtained for a constant source, before they could be used in the construction of attenuation curves.

Two methods of frequency analysis were performed on a number of the station records: one a power spectral analysis using a computer to facilitate calculations, and the other employing a range of band-pass filters on records obtained on magnetic tape. Both techniques showed that the noise consisted essentially of two frequency components, 6 cps. and 11-12 cps., the latter being confined to an area in the immediate vicinity of the source.

A study of the waveform, frequency content and level variation of the noise, showed that the source was of a composite nature, consisting of a cluster of individual mechanical noise generators.

Attenuation analyses revealed the presence of two areas to the west and south of the source which showed noticeably different rates of attenuation.

Two possible hypotheses were put forward to explain this phenomenon: one embodying a change in subsurface conditions between the two areas, and the other constant subsurface conditions, but a change in the predominant wave types propagating over the two areas.

Since no knowledge could be obtained on the precise nature and distribution of the wave types as the vertical ground velocity only was measured, both theories were considered to be open to some doubt, and thus preference was given to neither.

It was found that the values of the rate of absorption obtained were generally consistent with those usually found from laboratory experiments. **on rock materials.**

CHAPTER I

INTRODUCTION and GEOLOGY

1. INTRODUCTION

General Statement

This thesis is the result of one year's work in the Geology Department of the University of Durham, and concerns a seismic survey made over the southern slopes of the Rookhope Valley, Rookhope, County Durham. Measurements were made on noise, locally derived from a single source.

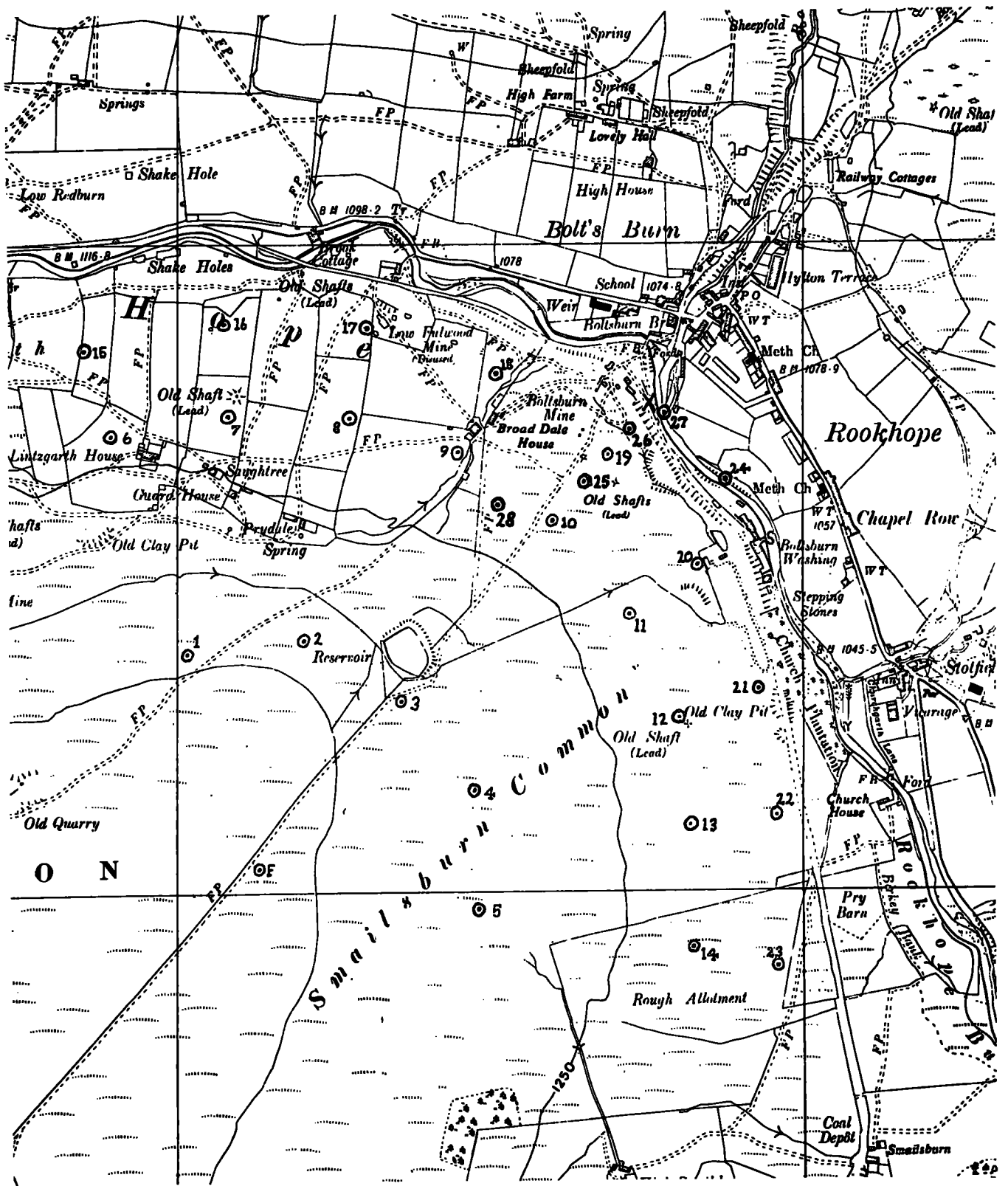
The principal aims of this research have been to measure the horizontal rate of absorption of the noise as a function of distance from its source, and to analyse the frequency spectrum of the noise. The purpose of the latter has been to assist in the attenuation measurements, and to give some idea of the frequency composition of the noise and the nature of the noise source.

Seismic Attenuation in the Rookhope Area

The seismic survey was conducted on Smailsburn and adjoining commons, (Fig. 1), just to the south of Rookhope, a village in the Northern Pennines, about 30 miles west of Durham. The village is situated in the valley of Rookhope Burn which flows eastwards from the Pennine watershed.

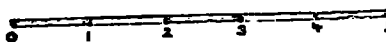
The preliminary results of the survey showed that almost all of the locally derived noise was generated by a single source. This source was found to be the Boltsburn Washing plant*, the position of which is about 300 metres south-east from the Rookhope

* The function of the plant is to reduce the raw fluorspar, mined from Stotfield, into a fine powder for use as a flux in furnaces.



- ⊙ Stations recorded by portable seismograph.
- Stations recorded by caravan unit only.

FIG. 1

Scale: 
Metres x 100.

borehole, (marked 'X' in Fig. 1), and coincident with the break of slope between the floor and southern slopes of the valley.

The material through which the noise is propagating consists mostly of rapid alternations of shale, sandstone and limestone, with a roughly homogeneous aspect, (the Geology of the Rookhope area will be described on page 10).

The seismic setting at Rookhope is thus similar to the simplified model in which there is a point source of energy, situated on the surface of a homogeneous medium. If the point source is at 0, (Fig. 2), then at any instant the wavefront of the body waves emitted from the source will be a hemisphere centred upon 0. The wavefront of surface waves on the other hand, will approximate to a vertical cylinder of height h with axis passing through 0, where h is the depth of penetration of the surface waves.

As the spherical or cylindrical wavefront spreads out from the source, the energy must be distributed over an increasing surface area. Thus as the distance from the source increases, the energy per unit area must decrease and thus the amplitude of the wave motion must also decrease. The argument is analagous to that of a light source; the luminous intensity per unit area falling off with increasing distance from the source.

It can be shown, (Ewing, Jardetsky and Press, 1957), that for a surface source on a homogeneous medium, the amplitude, A , of body waves falls off as $\frac{1}{R} 3/2 \rightarrow 2$, and that of surface waves as $\frac{1}{R} 1/2$, where R is the distance from the source.

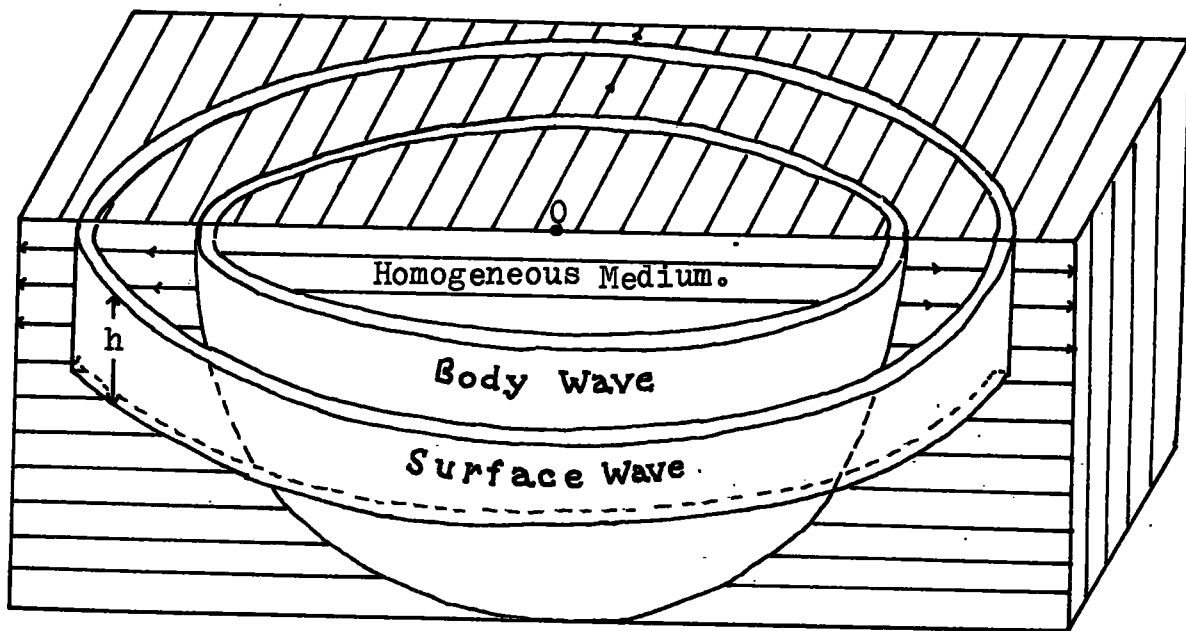


FIG. 2

Now, in addition to the attenuation of amplitude due to geometrical spreading of the wavefront, there will also be a certain loss from absorption, scattering, and diffraction. Knopoff and Macdonald (1960) have considered that appreciable scattering will only take place if the wavelength of the seismic wave is of the same magnitude as the dimensions of an individual rock grain. It will be shown later that the frequency of the noise components at Rookhope are such that their wavelength is many orders of magnitude greater than this, and thus scattering must be considered negligible.

Diffraction effects can also be regarded as small due to the absence of "edge" structures such as faults and intrusions in the geological structure at Rookhope.

However, absorption is considered to play an important role in the attenuation since it will be present whenever any type of wave is propagated through a medium which is not perfectly elastic.

Born (1941) has given a general formula relating the amplitude A_0 of a seismic wave at the source to the amplitude, A_R , at a distance R from the source, assuming absorption to be the only cause of attenuation. It is:

$$A_R = A_0 e^{-\alpha R}, \text{ where } \alpha \text{ is the attenuation constant}^* \dots (1.1)$$

This equation states that for each unit of distance travelled, the wave suffers the same percentage reduction in amplitude.

* For derivation of this formula, see Appendix A.

If the effects of geometric spreading of the wave and absorption are combined then the complete equation describing the attenuation is for body waves:

$$A_R = \frac{A_0}{R^{3/2}} e^{-\alpha R} \dots\dots\dots (1.2)$$

and for surface waves:

$$A_R = \frac{A_0}{R^{1/2}} e^{-\alpha R} \dots\dots\dots (1.3)$$

The Nature of Absorption

Many field and laboratory experiments have been performed in an attempt to explain the mechanisms which control absorption of seismic energy. For instance, the exponential decay of amplitude with distance has been found by many workers (e.g., Born(1941), Sezawa and Kanai (1935)).

In addition it has been found by Fortch (1956) that the elastic wave velocity is unaffected by attenuation, and also that according to Knopoff and Macdonald (1960) the attenuation is independent of the amplitude of vibration. However, Howell (1961) has suggested that the attenuation may be greater if the source is emitting continuous waves than if it is emitting discrete pulses (e.g., as on impact).

Now Born (1941) has expressed the attenuation constant as a function of frequency thus:

$$= \quad \xi .f.t. \dots\dots\dots (1.4)$$

where ξ is a constant; f is frequency and t is the time taken

along the wavepath. For a constant time path the attenuation is thus proportional to frequency. If there is a source emitting an impulse which has a frequency spectrum covering a wide band of frequencies, then the higher frequency components will be more rapidly attenuated than the lower frequency ones, in other words the earth acts as a low pass filter.

The nature of absorption is often described in terms of the logarithmic decrement δ , or the Q factor. Both these quantities are related to the amount of energy lost during one cycle of wave motion, i.e., -

$$\frac{1}{Q} = \frac{\Delta E}{2\pi E} \text{ where } \Delta E = \text{energy loss/cycle,}$$

and $E = \text{maximum stored energy,}$

and

$$\delta = \frac{\pi}{2Q} = \frac{1}{4} \cdot \frac{\Delta E}{E} \quad (= \alpha/\text{ft.}, \text{ from equn. (1.4)).}$$

Q and δ have the same meaning as when they are used in LCR electronic circuits.

Now it has been found by Birch and Bancroft (1938); Knopoff and Macdonald (1958), Born and others that for dry specimens of rock, there is a constant 'Q' law for absorption, that is, there is an amount of energy lost per cycle which is independent of frequency (up to about 10^8 cps.). The process responsible for such an occurrence necessitates some non-linear mechanism according to Knopoff and Macdonald (1958) and O'Brien (1961); Donato et al (1962) favour hysteresis as a possible mechanism. However, at low frequencies Donato et al and Usher (1962) have found that $\Delta E/E$ increases by a factor of two from about 2 cps.

to 40 cps., and remains constant thereafter. Usher considers that, whereas at high frequencies the loss process is mainly frictional, at low frequencies a viscous effect associated with the grain boundaries is in operation.

O'Brien has stated that laboratory measurements indicate that seismic absorption in sedimentary rocks lies in the range of 0.1 - 1.0 decibels per wavelength.

Measurement of absorption by rocks in situ are few, though Ricker (1953) has found that Q was inversely proportional to the frequency, (i.e., $\alpha \propto f^2$). For the same rock however Macdonald et al (1958) concluded a constant ' Q ' relationship (i.e., $\alpha \propto f$).

Ewing and Press (1954) indicate that from the study of earthquake records, surface waves follow a constant ' Q ' law. Due to the absence of moisture, a frictional mechanism is held responsible for this relation. Born has considered that the frictional losses are of the solid friction type, caused by adjacent particles rubbing together when the region is excited by wave energy. Knopoff and Macdonald (1958 and 60) have demonstrated the importance of grain surface area and conclude that sliding friction may be the answer. In support of their constant ' Q ' model, they prefer a frictional force which varies as the gradient of the local stress instead of the Coulomb-type friction proposed by Fortch and others (this latter mechanism would lead to $Q \propto f^2$). The frictional force is thought of as taking place along the grain boundaries.

Now if the moisture content of the rock is increased, it is found that the energy loss/cycle also rises and becomes

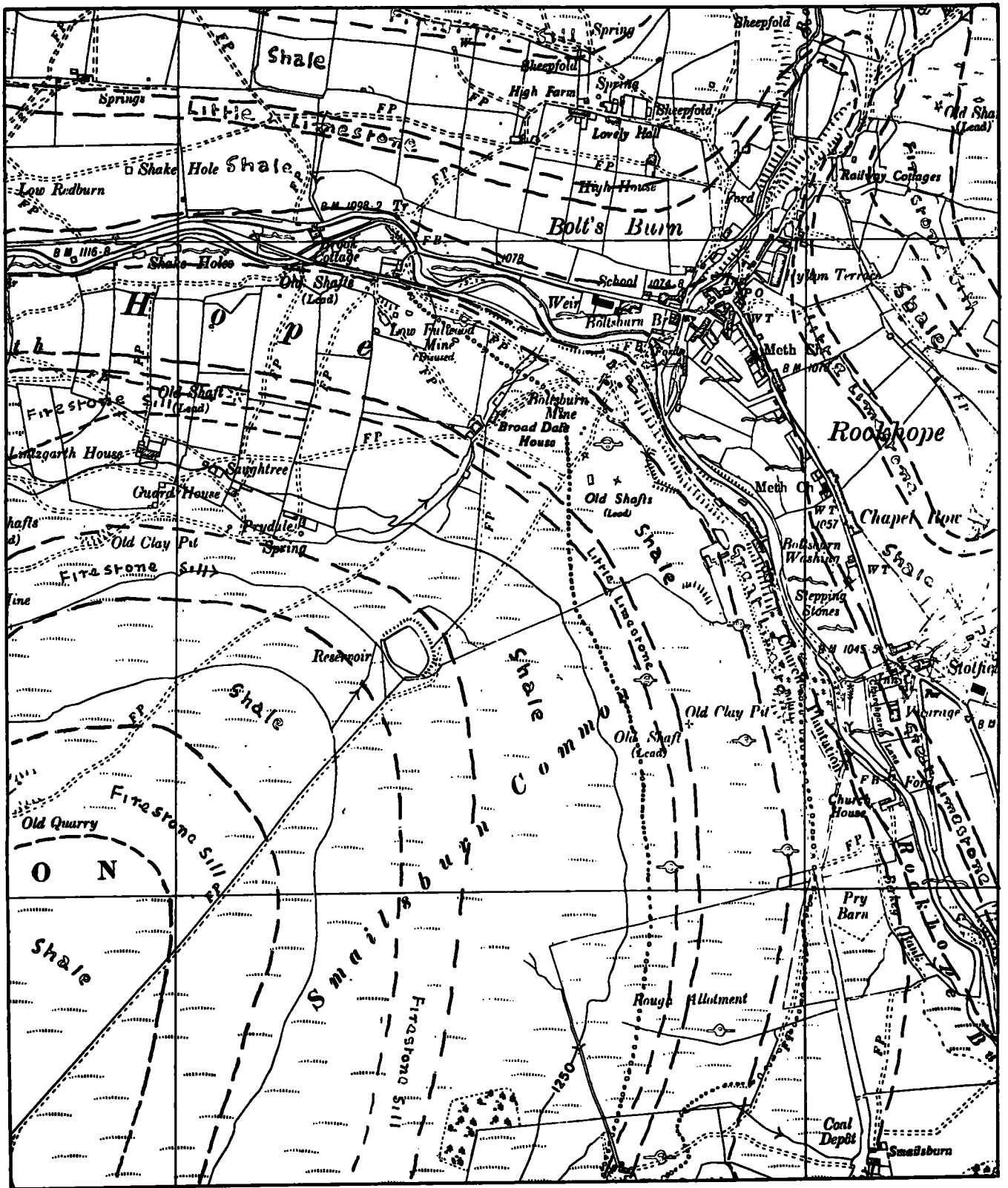
increasingly dependent upon frequency (Born, Usher). A constant value of the energy loss is normally reached at a water content of about 2.4%. This constant value is attained more quickly and there is a faster rise of ΔE with liquid content if water is substituted by oil (Usher). It thus appears that the mechanism responsible for absorption when a liquid is present is a viscous one. Born believes that the nature of the viscous effects are due to the drag exerted upon an excited grain by the liquid surrounding it. Usher modifies this by stating that the losses are caused by fluid being forced from compressed to dilated regions. However Wyllie et al (1962) assume that the losses are due to the chemical and physical effect of the fluid on the cementing material of the rock, and in addition prefer the loss model proposed by Biot (1956) which supports the dissipation of energy by means of a "sloshing" mechanism in which a pore space is only partially filled with fluid which is "sloshed about" in the cavity.

2. GEOLOGY

Though there is no published paper dealing specifically with the geology of the Rookhope area, sufficient information for our purposes has been obtained from unpublished borehole data and the Geological Survey memoir on the North Pennine Orefield (Dunham, 1948).

Geological Structure

The rocks present at Rookhope are Carboniferous shales, limestones and sandstones of the Middle and Upper Limestone groups.



Geological Map of the Rookhope area.
 (Same scale as Fig.1).


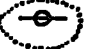
-  Alluvium.
-  Drift.

FIG.3

CARBONIFEROUS SUCCESSION AT ROOKHOPE

(Only those beds are given which outcrop over, or which underlie the area studied.)

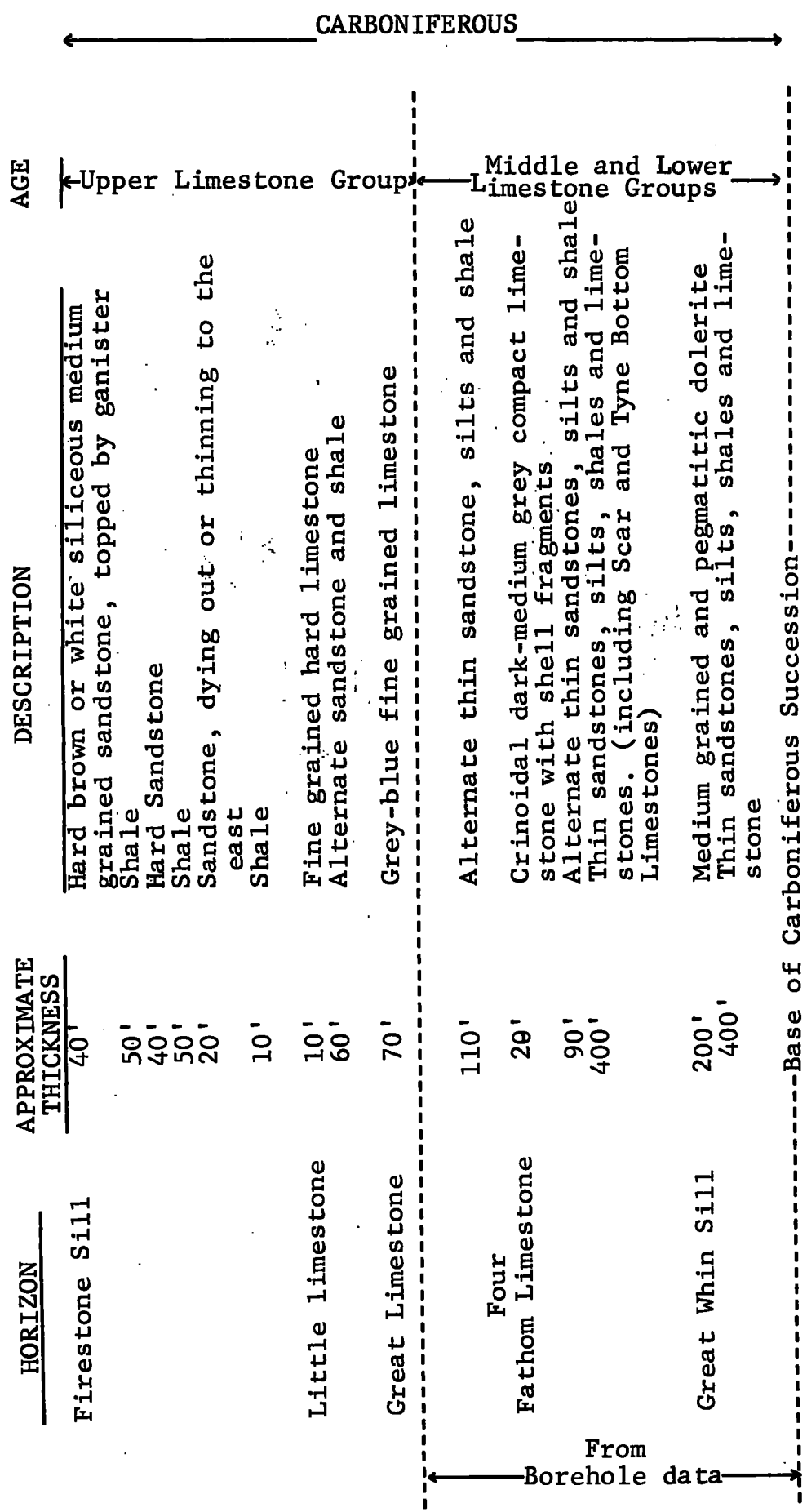


FIG. 4

They are almost horizontal everywhere over the area, there being a very slight dip to the north. Faulting of any major scale is absent though small scale throws do occur along mineral veins traversing the area. A geological map of the area is shown in Fig. 3.

Detailed Succession

The detailed succession is shown in Fig. 4.

Drift thickness has not been included as this is variable over the area; from the Rookhope borehole a thickness of 12 feet of glacial valley fill was proved. Over the southern side of the valley, drift is mainly confined to the lower slopes, approximately to the South of the Washing plant. An old filled-in clay pit about 300 metres SSW of the plant may point to a thickness of drift of at least 10 feet. From the limited size of the area of drift it is estimated that the maximum possible thickness that it can have is about 30 feet.

Peat and clay subsoil cover almost the whole of the area surveyed.

Mineralisation

A number of thin mineral veins containing lead, fluorite and iron traverse the area but these are regarded as having no effect on the propagation of seismic waves and thus are not discussed in detail.

CHAPTER II

FIELDWORK PROCEDURE and RECORDING TECHNIQUES

GENERAL STATEMENT

The experimental procedure for the noise survey was to have a network of recording stations covering the area to be studied and adjacent to the main noise source. At each station the vertical ground velocity was measured, using a Willmore seismometer and a transistorised portable pen-recorder (Neocardiograph). Since the vertical component of motion only was recorded, precise knowledge of the seismic wavetypes propagating could not be obtained.

1. FIELD PROCEDURE

Construction of the Station Network

A network of recording stations, in the shape of a circle segment, was established on Smailsburn and adjoining commons, Fig. 1. Such a pattern was adopted so that if changes in geology or topography effected the propagation of the seismic waves generated by the source, then along arc profiles there would be a minimum change in subsurface and surface conditions, and along radial profiles there would be a maximum change.

The reason for this is that at Rookhope the main valley has a roughly semicircular course, the surface contours running parallel to it on the southern (Smailsburn Common) side. Due to the geological structure of the area the pattern of outcrop of the individual layers in the rock sequence follows that of the contours. Thus arc profiles everywhere are approximately at the same height and remain for the most part on the same geological horizon. Conversely radial profiles run parallel to lines along which there is a maximum change in geology and topography.

The network consists of 5 radii emanating at 30° to each other from a focal point, F, situated about 1000 metres South-west from the washing plant.

Stations were spaced along each radius at intervals of about 400 metres. In order to increase the accuracy of ground velocity studies around the washing plant, this distance was reduced to about 150 metres near the edge of the valley, and 4 further subsidiary network radii were introduced between the main ones in this area. Thus a final network was produced such that the station coverage could provide 5 radial profiles each of four stations, all tied to a common station at the focus, and three arc profiles, the highest one consisting of 5 stations and the lower two each of 9 stations.

The dimensions of the network are controlled by:

(a) the topography and geology (these determine the curvature of the network arcs), and (b) the position of the washing plant and the likely attenuation rate of noise with distance from it. The furthest stations from the plant should receive only a small amount of noise that is recognisable as coming from the plant. It should then be possible to plot a graph of the attenuation of the plant noise down to a level that is near to that of the background noise.

Description of Stations

Each station was so constructed to provide protection for the seismometer from wind and rain, and consisted of a pit

of dimensions two feet by one foot, with a depth of about two feet. A flat stone was embedded in the earth at the bottom of each pit, its upper surface approximately horizontal. Each stone was about three inches thick and sufficiently large so that a Willmore tripod stand could be placed on it. With the Willmore in position on the stand, the pit was covered over by two roofing slates suitably weighted down by earth to ensure minimum wind vibration. The pit and cover combined thus afforded complete protection for the seismometer from wind or rain. The site of each seismometer station was selected so as to avoid if possible marshes, man-made features and trees. Marshes were avoided as these would cause inaccessibility and needless flooding of holes. Roads, dumps, or other man-made objects were also unsuitable sites as these may have caused undesirable coupling effects, as will be discussed in the next section. Stations had to be kept well away from trees and stone walls as these would cause spurious vibrations on the recording trace during windy weather.

Seismometer-ground Coupling

The quality of coupling between the ground and seismometer is important because it controls the amount of attenuation and distortion suffered by the ground motion when it is transferred across the coupling junction to the seismometer. In the present work, an attempt has been made to keep the coupling conditions as constant as possible at all stations in the recording network. This is desirable since the readings obtained at each station are used subsequently in the construction of attenuation curves.

Since the seismometer and stone can be considered to be one unit, with little attenuation across the junction between them, then the function of the stone is to increase the area of contact between the earth material and the seismometer, thereby improving the coupling between them. Stones of similar dimensions were used for all stations. Each stone was firmly embedded in the hole so that coupling conditions would remain constant with time (i.e., no settling of the stone causing increased compaction and hence rigidity of the earth material in contact with the stone.)

Now it can be shown (Fail, Grau and Lavergne, 1962) that the degree of coupling depends upon the admittance of the earth material in contact with the seismometer system.

The coupling is given by:

$$\frac{V_{g-s}}{V_g} = \frac{1}{1 + jmwY} \dots\dots\dots (2.1)$$

where V_{g-s} is the velocity assumed by the ground-seismometer system; V_g is the velocity the ground would have in the absence of the seismometer; m is the mass of the seismometer case; w is the frequency of the ground motion; Y is the admittance of the ground, and $j = \sqrt{-1}$. Bycroft (1956) has related the admittance to the rigidity of the ground thus:

$$Y = \frac{w(f''-f'.j)}{\mu.r^0} \dots\dots\dots (2.2)$$

where f'', f' are functions of $w.r^0/V_t$, r^0 is the radius of the seismometer case; μ is the modulus of rigidity; and V_t is the transverse wave velocity. Thus from (2.1) and (2.2) it can be seen that a decrease in the rigidity of the ground would also

decrease the coupling between it and the seismometer (assuming V_t is unaffected).

Since the design of the stations has been kept constant, it would only remain for all stations to be dug in a material with the same admittance to retain constant coupling conditions throughout the station network. Since all stations could be dug in clay subsoil, sites on man-made features were avoided as these would introduce a variety of coupling materials with different transmission properties. Despite the apparent constancy of the coupling clay material at each station, some variation in the coupling properties can be expected, since, for example, the station at the focus F, and also numbers 1 and 5, flooded immediately on being dug, thus preventing the stone from being imbedded in firm clay. From equations (2.1) and (2.2), it is probable that this loss in rigidity of the clay would decrease the coupling at these stations, and thus reduce the magnitude of the recorded signal.

Now for those stations in which the clay is in the same state of rigidity, dispersion of the damping constant and resonance frequency of the seismometer may occur but this effect only becomes appreciable at high frequencies of ground motion. Since the frequencies that are recorded at Rookhope are low (about 1 → 30 c.p.s.), then such effects as these can be neglected. Thus it can be concluded that the only major modifications of the recorded signal due to coupling will come from differences in the rigidity of the coupling clay material.

Unfortunately, it was not possible to predict the magnitude of this effect, due to the uncertainty in the relative magnitudes of the rigidity of the wet and dry clay in contact with the coupling stone.

2. RECORDING TECHNIQUES

The Method of Recording at Individual Stations

At each station the Willmore tripod stand was placed on the stone at the bottom of the pit, and the seismometer placed in an upright position on the stand.

The stand was levelled by means of its adjustable screw legs, using the spirit level on the seismometer as a guide. In the levelled position the seismometer mass was thus constrained to move only in a vertical direction.

Once the levelling procedure had been completed, the seismometer was connected to the Neocardiograph pen recorder, and the seismometer mass unclamped. The pit was then covered over and recordings made.

All recordings were hampered by frequent interference from temporary extraneous sources of noise, such as motor vehicles passing through the village and farmland; high-flying aircraft and sheep grazing over the hills. The first two gave rise to high frequency signals (often of large amplitude in the case of motor vehicles), while sheep caused sporadic low frequency bursts on the records. Noise sources such as these must be minimised, as only recordings of ground disturbance generated by permanent

sources are required (i.e., background noise and locally derived noise from the Boltsburn Washing plant). Unwanted noise signals create errors in the amplitude and frequency analyses of the records, especially if measurements are averaged over short lengths of time (40 → 60 seconds, for example). Longer averaging times would tend to nullify this effect, but normally to prevent rapid run-down of the batteries in the Neocardiograph, recordings were made over a period of about a minute only, during intervals free from unwanted interference.

After each station recording, the seismometer and Neocardiograph were calibrated (the details of this will be discussed in the next chapter).

Recording Techniques Used over the Field Network

The noise measured can be considered to consist of two parts: the local noise generated by the Boltsburn Washing plant, and the background noise due to distant sources.

Since the prime object of this work is to measure the frequency content and attenuation characteristics of noise derived from the local source, only a minority of recordings were made of isolated background noise. Over the area studied the local noise was about 5 → 50 times the level of the background noise, the difference in magnitude between the two decreasing with increasing distance from the source.

Now before attenuation calculations can be made on the local noise, corrections or allowance must be made for any source

variation with time. The velocity values obtained at all stations over the area must be normalised to values which would correspond to those for a constant source.

Two recording methods designed for this purpose were used:

(a) Two stations were recorded simultaneously, one at a fixed location and the other variable in the field. Provided both stations received noise from the same source, the ratio of the ground velocity at the two stations would correspond to a source of constant amplitude.

(b) Stations were recorded one at a time in a random sequence, along a profile or over the station network as a whole.

If the amplitude of the recorded values are plotted against their respective source-station distances, then by smoothing the resulting attenuation curve, a true graph independent of time variation of the source may be obtained, providing that sufficient readings have been taken.

Since this method is statistical in nature, as many samples are required as possible. Ideally several stations should be measured rather than repeated observations at only a few. This method then tends to average out any station response variation as well as variation in the amplitude of the source. Thus provided sufficient measurements are taken this method is superior to (a).

However, the number of recordings required is far in excess of the number that time would allow. Nevertheless, in many cases this method was employed mainly due to difficulties.

encountered in the retention of two stations operating simultaneously.

The obvious objection that too few readings were taken is offset by the use of method (a) to support method (b); provided greater significance is placed on points obtained by method (b) during the averaging process the method is satisfactory.

Three recording techniques which implicate method (b) were used in the field:

(1) Stations were recorded in a random sequence along a profile, each station being measured only once during the day.

(2) Along those profiles in which there were only a limited number of stations (e.g., the topmost arc profile), method (1) was extended by repeating observations at most stations using a looping technique. The recording sequence used for the topmost arc profile, for example, was Station 1, 2, 4, 3, 2, 3, 4, 5, 2, and 1. Systematic changes in ground velocity values at these stations which were recorded more than once would then reflect any change in noise level with time.

(3) Stations were recorded in a random sequence over the network, most stations being measured only once.

Only methods (a) and (b2) are capable of giving direct indication as to the nature and magnitude of any noise level change with time.

Frequent interruptions due to instrumental failures and adverse weather conditions were the main sources of difficulty in the execution of the fieldwork.

Recording Caravan Experiments

Continuous recording over a period of one week, of two stations (Nos. 24 and 28 in Fig. 1) was made possible using the A.W.R.E. recording caravan unit, which was made available to Durham University towards the middle of the field survey. By this means, an insight could be obtained into the variation of the noise level throughout the period of recording and the magnitude of any change ascertained. It will be seen in Chapter IV that this experiment can show indirectly the general pattern and order of magnitude of noise level variation that might be expected in the field.

A second short project using the caravan equipment was also carried out. The purpose of this was to obtain record samples from a number of stations and perform on them a frequency analysis using various band-pass filters. Fuller details of this will be given in Chapter IV.

The major shortcoming of the caravan recording system was that the area studied by it was confined to a very small fraction of the total region surveyed. This restriction was due to there being a limited supply of connecting cable at the time that recordings were made.

CHAPTER III

INSTRUMENTATION

GENERAL STATEMENT

This chapter is divided into two parts: the first discussing the mechanics, calibration and frequency response of the field equipment, and the second briefly describing the instrumentation in the recording caravan.

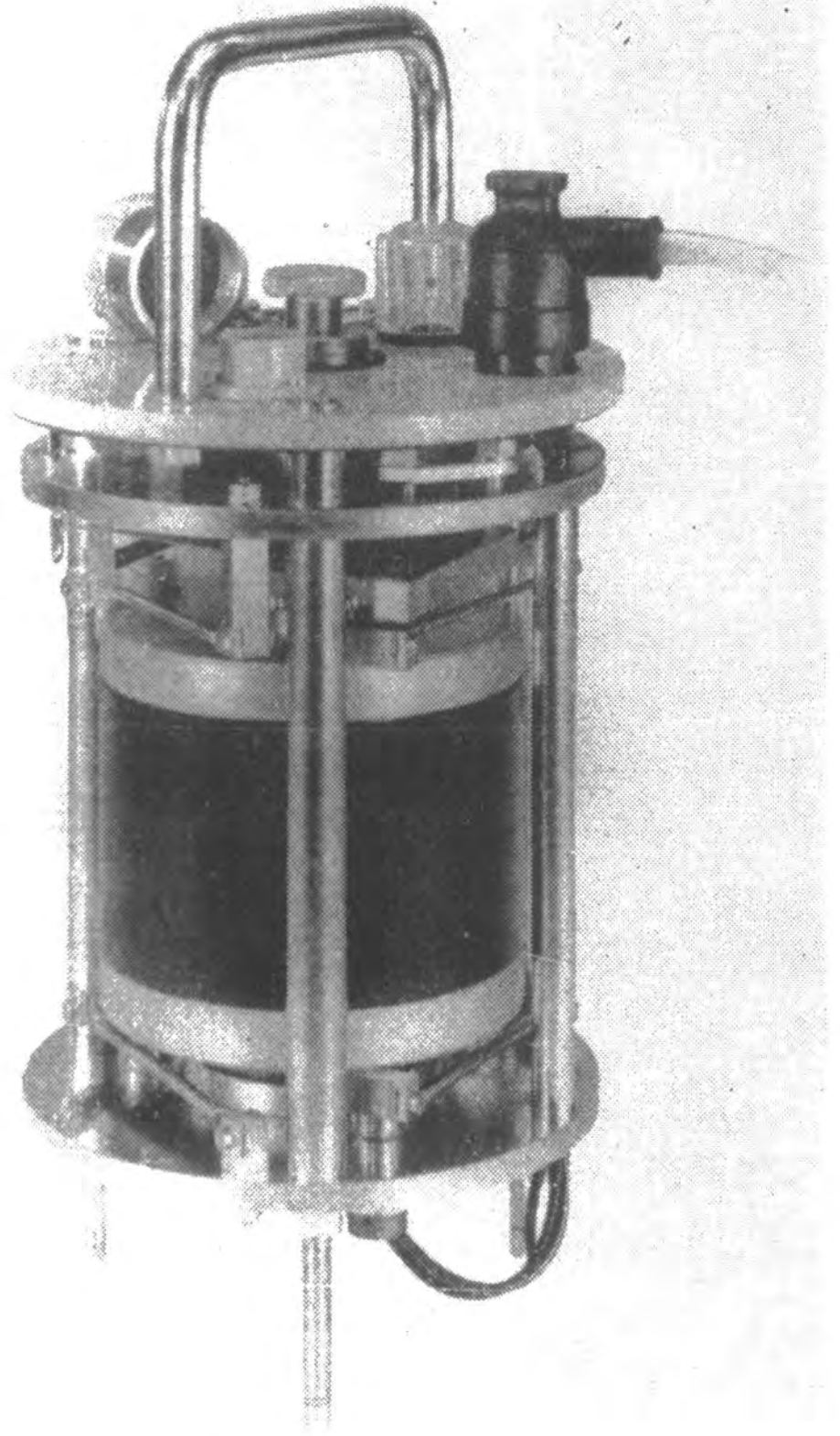
1. INSTRUMENTATION OF FIELD EQUIPMENT

Most of the survey was conducted using a single Willmore Mark I seismometer and Neocardiograph recorder. A second instrument of each was used for a short time at the beginning of the survey so that simultaneous recordings at two stations could be made.

The Willmore Seismometer

The seismometer, first described by Willmore (1950) and shown in Fig. 5, consists of a large permanent magnet suspended from a system of leaf springs in a frame, and so constrained by them that it is free to move only in a direction parallel to the axis of the frame. A coil of wire is fixed to the frame and enters a circular gap between the pole pieces of the magnet.

Relative motion occurs between the coil and the magnet, since coil is attached to the frame and moves with the ground, and the magnet motion is controlled by the natural period of its suspension as well as the ground movement. The E.M.F. generated in the coil by electromagnetic induction is then amplified and



Willmore seismometer.

FIG.5

recorded. Since it is proportional to the rate at which the lines of force are cut by the coil, it is thus proportional to the relative velocity of the magnet and coil. Providing that the natural frequency of the seismometer is not too far outside the range of frequencies of the impressed force, the output is approximately proportional to the true velocity of the ground motion, the output lagging behind the motion of the ground. The output from the seismometer coil is about 1.1 volts for a ground velocity of 1 cm./second.

The natural frequency of the two seismometers used are approximately 1.24 and 1.6 cps. (the higher frequency seismometer was only used in simultaneous recording (field method (a)) and in caravan experiments).

The total weight of each seismometer is about 21 pounds, almost half of this being the weight of the magnet.

Damping in the seismometer

Damping is essential to all seismometers so that the vibration of the magnet has ceased before the arrival of each successive pulse in the ground motion. If this was not the case, then the output at any instant would be a function of the velocity of the ground motion at that instant, plus some function due to the undamped motion of the previous displacement. Since the seismometer must give an output proportional to the actual ground velocity at any instant, then some form of damping must be present. The Willmore is designed so that it has a damping

factor 0.7 times the critical value.*

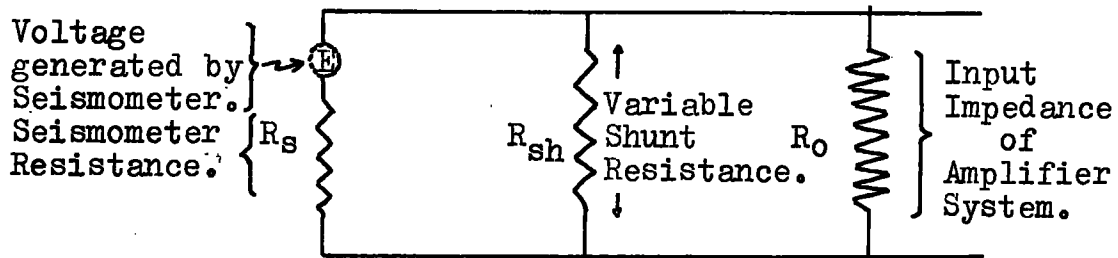
It has been found that this degree of damping gives the highest response coupled with the least distortion. In addition the resonance peak found** when lower values of damping are used, is eliminated; thus frequencies near the natural frequency of the seismometer should not "show through" on the records obtained. Damping in the Willmore is caused by electromagnetic induction between the coil and the magnet. The size of the current in the coil controls the amount of damping applied to the motion of the magnet; the larger the current, the greater the damping.

The degree of damping may thus be controlled by means of the circuit shown in Fig. 6a. R_s and R_o are the resistances of the seismometer and the amplifier, where R_o is much greater than R_s . R_{sh} is the shunt resistance connected in parallel across the seismometer and is of the same order of magnitude as R_s , (about 500 ohms). Now if R_{sh} is not switched into the circuit, then a small current flows from the seismometer as there is a high resistance in the circuit (R_o), and thus the degree of damping is small. This is used when the seismometer is being calibrated.

If R_{sh} is connected, then a larger current is drawn through the seismometer, around the circuit containing R_{sh} , since R_{sh} affords a low resistance path to the current in comparison with R_o . This degree of damping is used during recording.

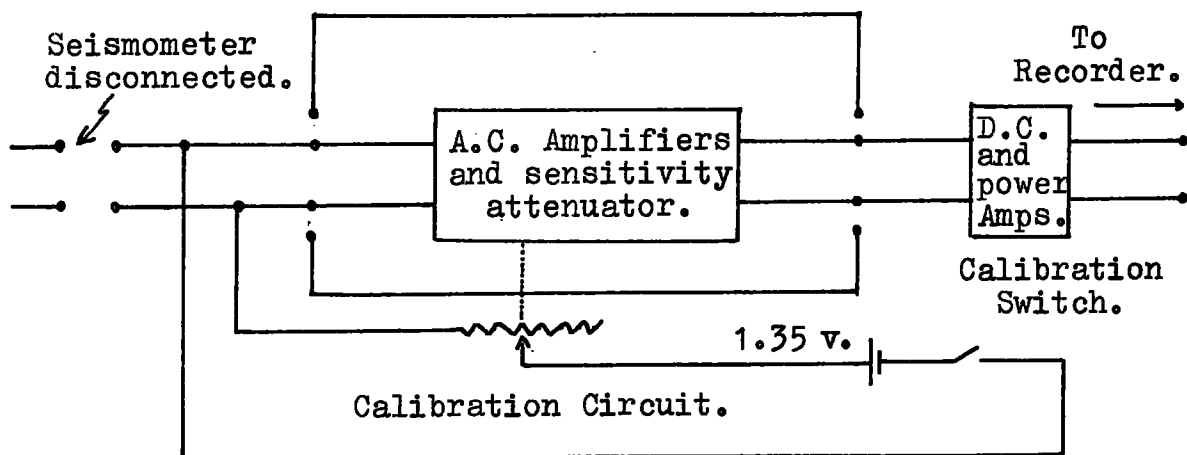
* The critical value is the maximum amount of damping that can be applied without destroying the oscillatory character of the seismometer response.

** "Methods and Techniques in Geophysics", Ed. Runcorn, p.239, (Willmore).



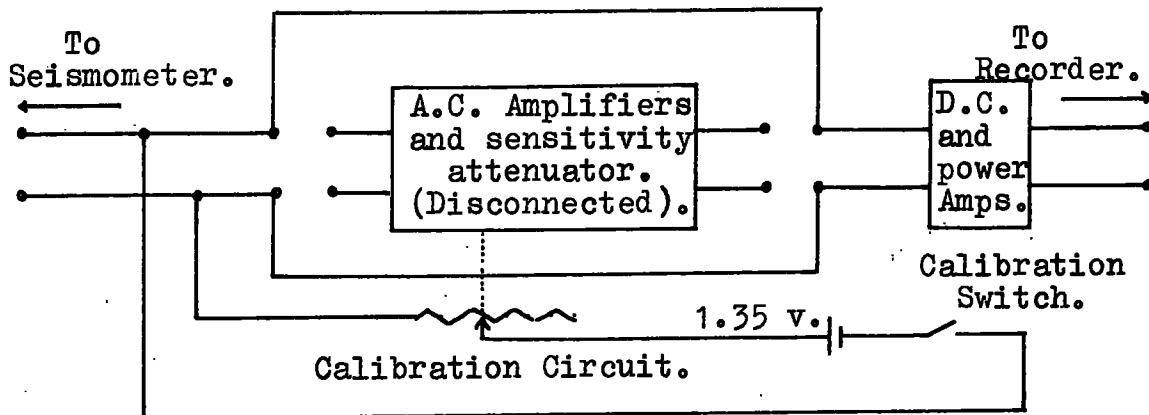
Seismograph damping circuit.

(a)



Amplifier calibration circuit.

(b)



Seismometer calibration circuit.

(c)

The Neocardiograph Pen-recorder

This instrument, designed for use with the Willmore seismometer, was constructed by the Atomic Weapons Research Establishment, and originally used by them to record background noise of about 2 c.p.s.

The Neocardiograph is basically a transistorised portable amplifying system and pen-recording unit, and may thus be described in terms of these two parts. The complete instrument is shown in Fig. 7.

Amplifying Unit

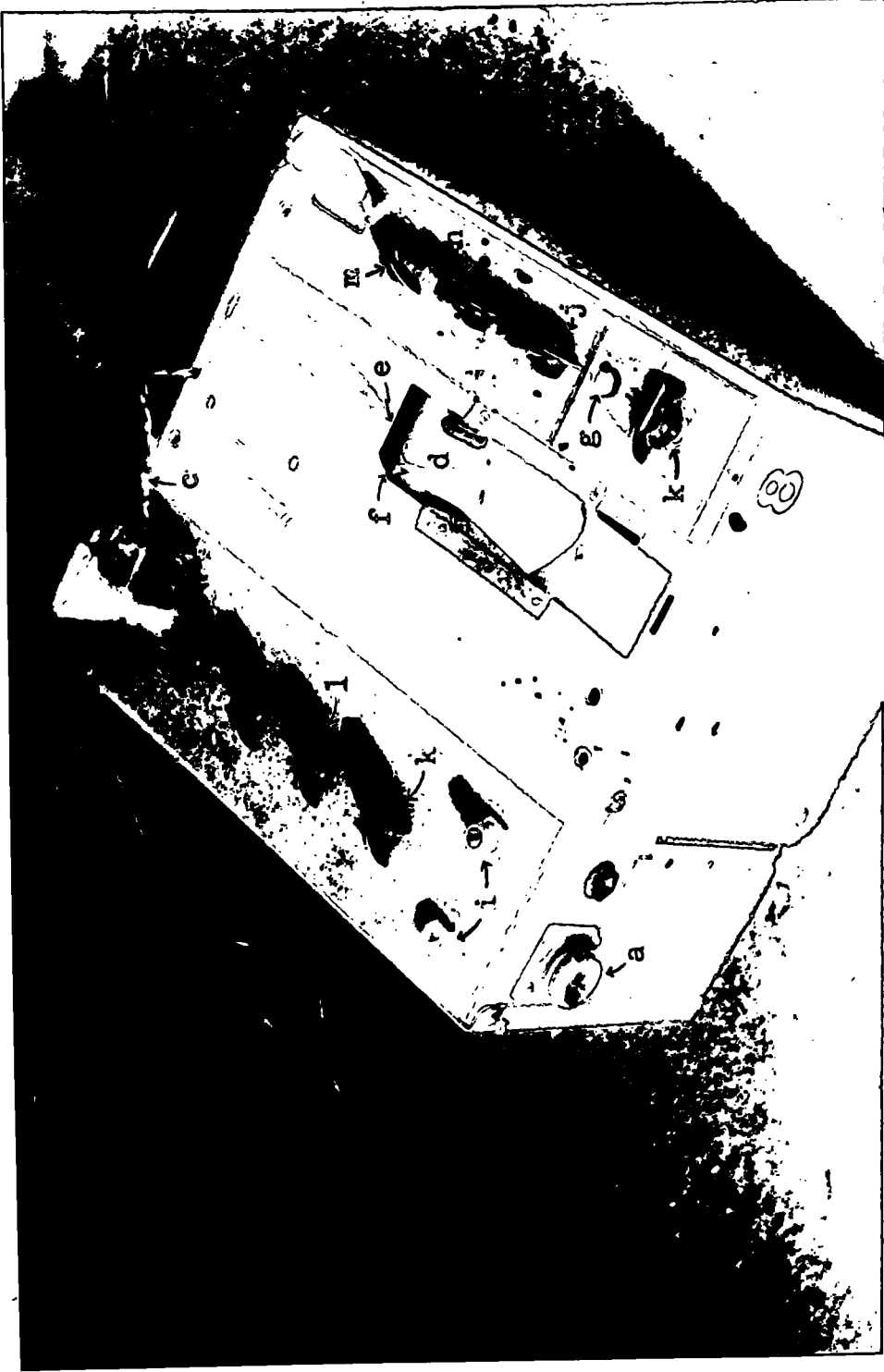
It is sufficient for our purposes, to regard the amplifying unit as an electronic "black box"^{*}, with a given input impedance. The input impedance must be large enough to prevent attenuation of the seismometer output, and also to enable control of the damping of the seismometer. The frequency characteristics of the amplifier unit contribute to the overall response of the seismograph.^{**}

Normally all the individual amplifying circuits contained within the "black box" are used when the Neocardiograph is recording. However a number of them may be switched out of the amplifying unit in order to reduce the amplification by a large degree. This is done in the calibration of the seismometer, where the input to the seismometer is very much bigger than that due to

*"Black Box" is a name that can be given to any amplifying system, when the details of its construction are not discussed.

**The term "Seismograph" is here used to denote the combined seismometer and amplifier-recorder system.

FIG. 7



a: connection to Willmore; b: connection to battery supplying current to recording pens; c: connection to timer; d: drum; e: signal pen; f: timing pen; g: calibration switch; h: gain control; i: pen current adjustments; j: zero control; k: calibration selectors; l: sensitivity selector; m: record switch.

Neocardiograph pen recorder.

ground motion and thus less magnification is needed. An important feature of the amplifying unit is a variable attenuator which adjusts the nominal sensitivity. The sensitivity decreases by multiples of two from 2^{μ}v/cm to 0.2 mv/cm . A nominal sensitivity of 64^{μ}v/cm for example, means that a pen deflection of one centimetre will result if the amplifier input is 64^{μ}volts .

However in practice this is seldom the case, because in addition to the attenuator there is a variable gain control which can magnify or suppress the deflection of the pen. The attenuator is equivalent to a coarse adjustment in that it can only alter the size of pen deflection by large fixed increments. The gain control is the finer adjustment and this determines the amplitude of the signal trace on the recording paper (usually about half a centimetre).

Recording Unit

A heated recording pen is activated by the amplified signal, and its movement synchronised with any change in signal magnitude. The displacement of the pen is traced out on heat-sensitive recording paper, conveyed by a motor driven drum at a constant speed beneath the pen and in contact with it, Fig. 7.

The recording paper is itself black in colour but its surface is coated with a very thin layer of white wax. The recording pen is made of a thin nickel-chromium wire which is heated by a 3 volt battery.

Since the heated pen is in continual contact with the paper, then the wax immediately beneath the pen is melted, and

thus a black line is traced on the paper which follows the exact movement of the pen.

As the paper is travelling in a direction at right angles to the direction of pen displacement, a continual record of the pen movement with time is obtained.

Exact time intervals must be marked on the paper so that a frequency analysis can be performed on the trace (time intervals are also required in the analysis of the seismometer calibration curves, as we shall see later). Thus at the top edge of the recording paper there is a timing pen which operates on exactly the same principal as the recording pen except that it is activated by pulses generated by a make-and-break system attached to a clockwork timepiece. The time between the opening and closing of the circuit should be a quarter of a second. Thus the appearance of the trace caused by the timing pen is a square waveform of half second period.

The recording pen moves in an arc (of maximum length 1 centimetre), with a radius of 12.5 centimetre. The recording paper is graduated in millimetre squares, the ordinate lines being parallel to the arc inscribed by the recording pen; this facilitates amplitude measurement of the recorded signal.

The intensity of the timing and signal traces may be adjusted by controlling the size of the current passing through the pens, using a rheostat which is present in each of the pen circuits.

Instrumental Calibration

In order to derive the ground velocity from the recorded trace, it is necessary to calibrate the system. This calibration was performed as described in the succeeding section, after each station recording so as to eliminate the effects of variation of the natural period of the seismometer and the performance of the amplifiers.

Two calibrations were necessary:

- (a) Calibration of the seismometer output in terms of the ground motion, and
- (b) Calibration of the amplifiers, so that the amplitude of pen motion may be interpreted in terms of the output of a the seismometer.

Amplifier Calibration

When the amplifiers are calibrated, a calibration voltage is injected into the input of the amplifier system, with the seismometer disconnected, Fig. 6b. Fig. 6b also shows that the calibration circuit consists of a battery supplying a voltage of 1.35 volts, a press button switch and an attenuator.

Now suppose that the amplifier attenuator is switched to a certain nominal input voltage, then by depressing the calibration button switch, a voltage equal to this nominal value is inserted at the input of the amplifier. The switch is then released, the circuit is thus opened, and the D.C. level returns to zero. Thus by repeating this a number of times a square wave

signal is put into the amplifier. The resultant trace observed on the recording paper is the amplifier calibration curve:



The magnitude of the pen deflection, p , depends upon the performance of the amplifiers and the setting of the gain control.

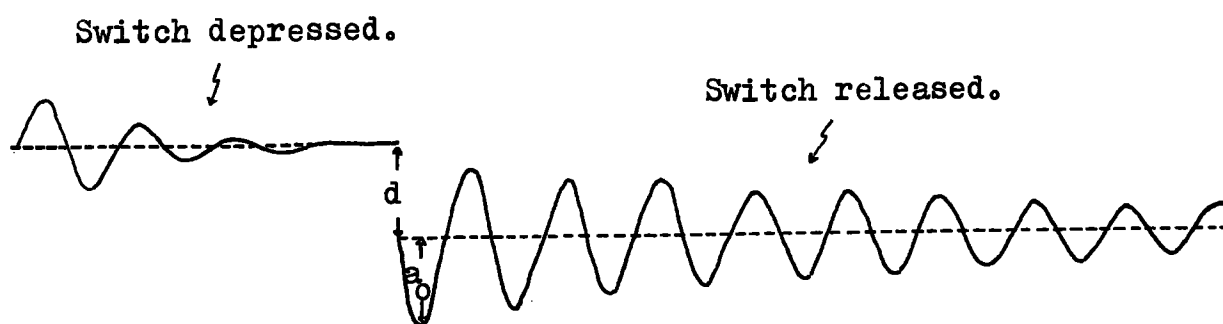
It will also be noticed that the D.C. portion of the curves are only transmitted with distortion owing to the presence of the coupling capacitor in the amplifying circuit. The discharge or charging time of the amplifier capacitance gives the time constant which is the time taken for the capacitor to charge to $2/3$ or to discharge to $1/3$ of its peak voltage. An approximate value for the time constant can be measured from the amplifier calibration curves. It will be seen later that from this and ordinary amplifier theory it is possible to get some idea of the frequency response of the coupling capacitor as this is a contributory factor in the overall response curve of the amplifier.

Seismometer Calibration

The circuit used for the calibration is shown in Fig. 6c. The differences between this circuit and the one for the amplifier

calibration are that the seismometer is connected into the circuit, the amplification is reduced and the damping shunt resistance R_{sh} , (Fig. 6a), is removed so that there is only very slight damping on the seismometer.

On depressing the calibration switch a current step is fed across the seismometer by the process of electromagnetic induction. The sudden change in the E.M.F. through the seismometer coil results in a force being exerted on the magnet, causing it to oscillate. The oscillations die away only very slowly due to the small amount of damping present, but once they have done so, the switch is released, opening the circuit and returning it to zero potential. Again the change in E.M.F. causes the magnet to oscillate freely but this time the initial displacement is in the opposite direction. The calibration curves are shown below:



It will be noticed that there is a greater degree of damping present in the depressed switch position than in the released position, since in the former case the calibration circuit resistance is switched into the main circuit, whereas in the latter it is not.

It can thus be seen that the seismometer calibration curves consist of two components: D.C. voltage changes across the amplifier due to the calibration circuit, and an A.C. voltage generated by the seismometer.

Now from the seismometer calibration curves a number of measurements are made which are subsequently used in the calculation of the vertical ground velocity; these are:

- (1) The frequency, f_o , of the oscillations.
- (2) The deflection of the pen d corresponding to the change in D. C. level.
- (3) The amplitude a_o of the first peak of the oscillations in the released switch position.

Now a_o and f_o should be values of amplitude and frequency at zero damping. In the present case, only a very small amount of damping is present, so that the error in taking the amplitude of the first peak and the frequency of the oscillation obtained is small, an underestimation probably not greater than about 2%.

Conversion of the Seismometer Voltage Output into Units of Ground Velocity using Calibration Curves

It can be proved (see Appendix B) that the sensitivity S of the seismometer in the "record" position is given by:

$$S = 0.58\sqrt{a_o f_o / d} \text{ volts/cm./sec.} \dots\dots\dots (3.1)$$

where a_o , f_o and d are as defined in the previous section.

From (3.1) it can be seen that:

1 volt corresponds to a ground velocity of $1/0.58\sqrt{a_0 f_0/d}$ cm./sec.
 (3.2).

Now if V volts are put into the amplifier and a pen deflection of p cm. is obtained (measured from the amplifier calibration curve) then

1 cm. of pen deflection corresponds to V/p volts (3.3).

Thus from (3.2) and (3.3):

1 cm. of pen deflection corresponds to $V/0.58.p\sqrt{a_0 f_0/d}$ cm./sec.
 (3.4).

Equation (3.4) is the basis on which all amplitude measurements taken from the records are converted into values of ground velocity. It should be pointed out at this stage that equation (3.4) only calculates the relative velocity between the coil and the magnet of the seismometer.

The size of the relative velocity is determined by the velocity of the ground motion and its frequency. Thus the values that we are calculating are not strictly of ground velocity but for a constant frequency of ground motion they may be considered to be proportional to the actual vertical ground velocity. Since the quantities calculated are required for attenuation studies, we are only interested in their relative values, providing that amplitude measurements are made on peaks of a single frequency.

For convenience we will continue to use the expression "vertical ground velocity" instead of "relative coil/magnet velocity", bearing in mind that they are not exactly equivalent.

Variation in Instrumental Parameters

The measured value, f_0 , of the natural frequency of the longer period seismometer (the one that was mostly used) gradually decreased during the fieldwork from 1.24 cps. at the beginning to 1.16 cps. at the end.

It was found that the observed change in f_0 could be explained by a gradual lengthening of the period of the timing signal on the Neocardiograph records throughout the field survey. It was noticed that for the same length of recording paper, the ratio of the time in seconds given by the earliest recordings to that of the final ones was 10:9. It would thus appear that there was a gradual increase in the speed of the rotation of the drum or in the period of the clockwork timepiece, as the fieldwork progressed. Such variation in mechanical parts of the Neocardiograph probably result from its continual use over an extended period of time.

Since the variation in f_0 appears to be related to mechanical changes within the Neocardiograph, other factors affecting f_0 , such as thermoelastic changes in the leaf springs supporting the seismometer magnet, and loosening of mechanical parts in the seismometer, must be absent or negligible by comparison.

Now as the variation in the value of f_0 has been concluded to be due to the instability of the timing mechanism of the Neocardiograph, then errors will occur in the relative values of the ground velocity since any variation of f_0 in equation (3.4) must be due only to changes in the natural period

of the seismometer. It has been estimated that, on the average, a 3% increase in values of ground velocity, calculated from equation (3.4), would occur if f_0 decreases from 1.24 to 1.16 cps. Since stations have been recorded in a random sequence throughout the total duration of the fieldwork, then such errors should be averaged out in any subsequent attenuation curves drawn.

In addition to the apparent change in the natural frequency of the seismometer, it was also found that the Neocardiograph amplification was gradually lowered throughout a full recording day due to the running-down of the batteries powering the amplifiers.

This change is often large, the amplification being reduced by as much as 20% at the end of the day. Such an effect as this must be allowed for by repeatedly calibrating the amplifiers after each station recording. Since the pen deflection, p , appears in equation (3.4), then the value of it after each station recording must be known in order that true relative values of ground velocity are obtained at each station.

Frequency Response of the Seismograph

The frequency response of the seismograph is the variation of the output with input frequency. A knowledge of this is essential before the true relative amplitudes of the component frequencies present in the noise analysed can be assessed.

An ideal seismograph should be equally sensitive to all frequencies of ground motion, but in practice this is never the case.

The seismograph used at Rookhope consists of an electronic amplifier-pen recorder (Neocardiograph) coupled to an electromagnetic seismometer (Willmore).

Unlike galvanometer coupled seismographs, where the frequency response is controlled by the mutual interaction between the seismometer and galvanometer, the amplifier and seismometer in this case can be regarded as separate systems once allowance has been made for the effect of the input impedance of the amplifier on the damping current through the seismometer coil (Fig.6a).

The overall frequency response of the seismograph may thus be considered as the product of the individual responses of the amplifier and seismometer.

The response for the Willmore has been worked out from simple theory using the differential equation of motion of the seismometer magnet and the known values of the damping and natural frequency of the seismometer. Modifications have been made to the resulting response curve in an attempt to correct for approximations made in the theory.

The response of the Neocardiograph amplifier has been found experimentally for input frequencies above 4 cps., and theoretically for those frequencies below 4 cps.

Frequency Response of the Seismometer

The frequency response of the seismometer may be obtained from a plot of its velocity sensitivity against the input frequency.

The velocity sensitivity of the Willmore may be expressed in two ways: either as the ratio of the voltage output to the relative magnet/coil velocity, or as used here, the ratio of the velocity of the magnet to that of the ground.

Thus in order to obtain the response curve of the Willmore, it is necessary to derive an expression relating the velocity sensitivity to the input frequency. Such an expression can be shown (Appendix C) to be:

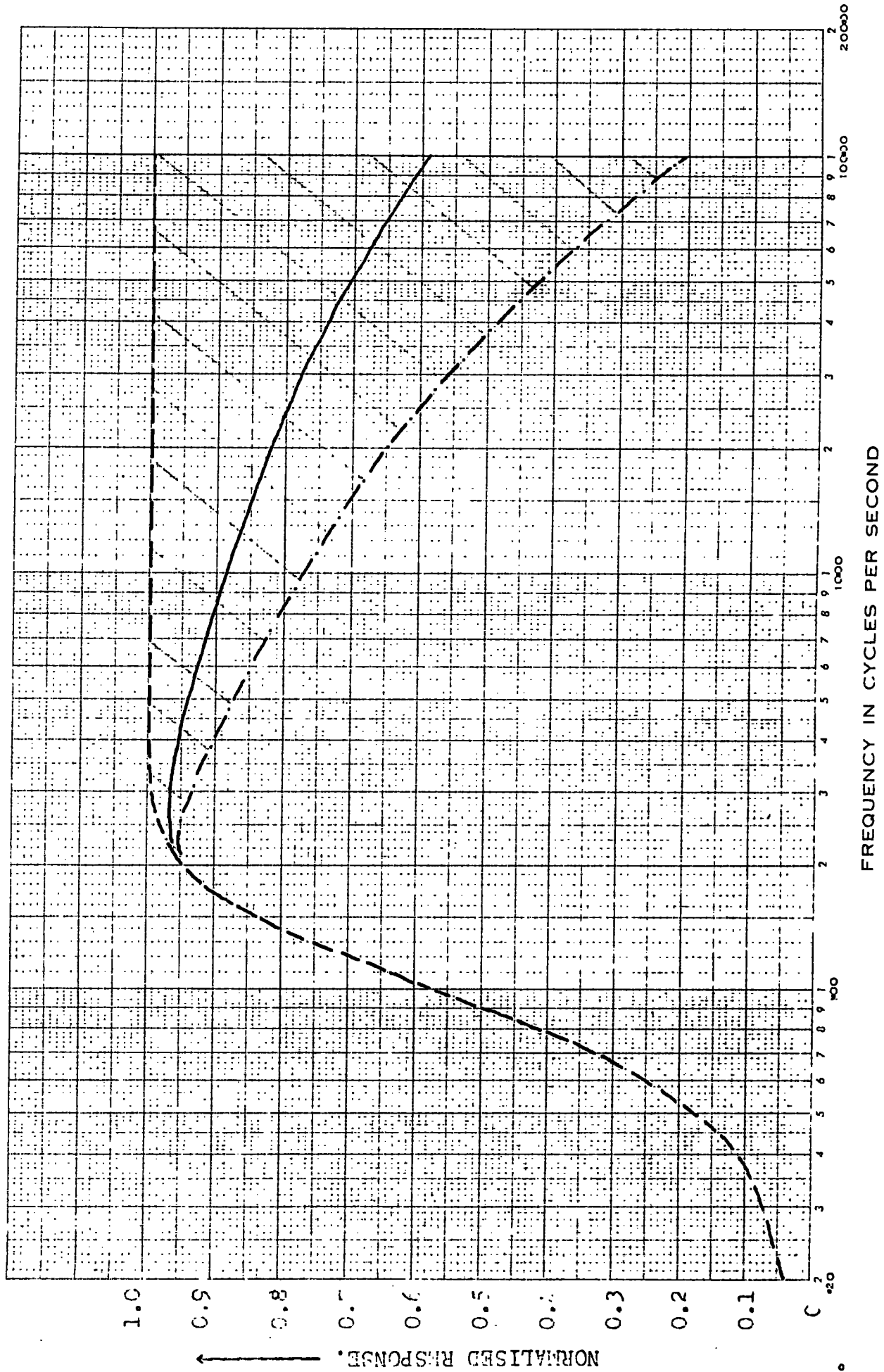
$$\frac{\dot{x}}{\dot{X}} = f/f_0 \sqrt{(f_0/f - f/f_0)^2 + 4n^2} \dots\dots\dots (3.5)$$

where \dot{x}/\dot{X} gives a measure of the velocity sensitivity of the instrument, \dot{x} = the velocity of the magnet; \dot{X} = the vertical ground velocity; f_0 = the natural frequency of the seismometer; n = the damping factor, and f is the frequency of the ground motion. Thus the shape of the response curve depends upon two of the fixed parameters of the instrument, f_0 and n . For the Willmore, f_0 has been taken as 1.24 cps. Since the Willmore is almost critically damped, a value of $n = 0.7$ has been taken. The theoretical response curve for the Willmore using these values is shown in Fig. 8.

Two points to note from the graph are, firstly, that the damping of the instrument is such that no maximum occurs at the natural frequency of the seismometer, the graph instead approaching its maximum value asymptotically. A second feature of the graph is that for frequencies lower than about 4 cps., the sensitivity of the seismometer falls off rapidly. For frequencies

SEISMO-METER RESPONSE CURVE.

Fig. 5.



higher than this the response curve remains almost constant. This can be seen from equation (3.5) in that when f becomes very much greater than f_0 , the sensitivity approaches unity; thus the response at the natural frequency is smaller than that for all higher frequencies.

Now though it has been shown theoretically that the response remains constant for all frequencies above about 8 cps., (fig. 8), it is usually found in practice that the response gradually drops as the frequency increases.

This discrepancy between the theoretical and practical response curves is due to the approximations made in the derivation of equation (3.5). No allowance has been made for the inductive effect of the seismometer coil. Since the size of the inductive E.M.F. is proportional to the rate of change of current through the coil, then as the frequency of ground motion increases the current rate of change through the coil also increases and thus the greater the opposing inductive E.M.F. This has the effect of increasing the damping of the instrument and thus lowering its response. In addition to the frequency, the magnitude of the inductive E.M.F. depends upon the resistance of the seismometer and the external damping circuit.

Unfortunately the magnitude of the response fall-off due to the inductive effect was not supplied by the Willmore manufacturers. However, published response curves of a number of seismometers similar in design to the Willmore were compared, and the curve showing the steepest fall-off taken to represent the maximum decay that might be expected in the Willmore.

Unsatisfactory as this method is, it does provide us with an approximate lower limit, the true response curve being taken as lying somewhere between it and the theoretical response curve.

More precise response determinations such as by Maxwell bridge, or shaking table methods were not possible in the limited time available for research.

Frequency Response of the Amplifier

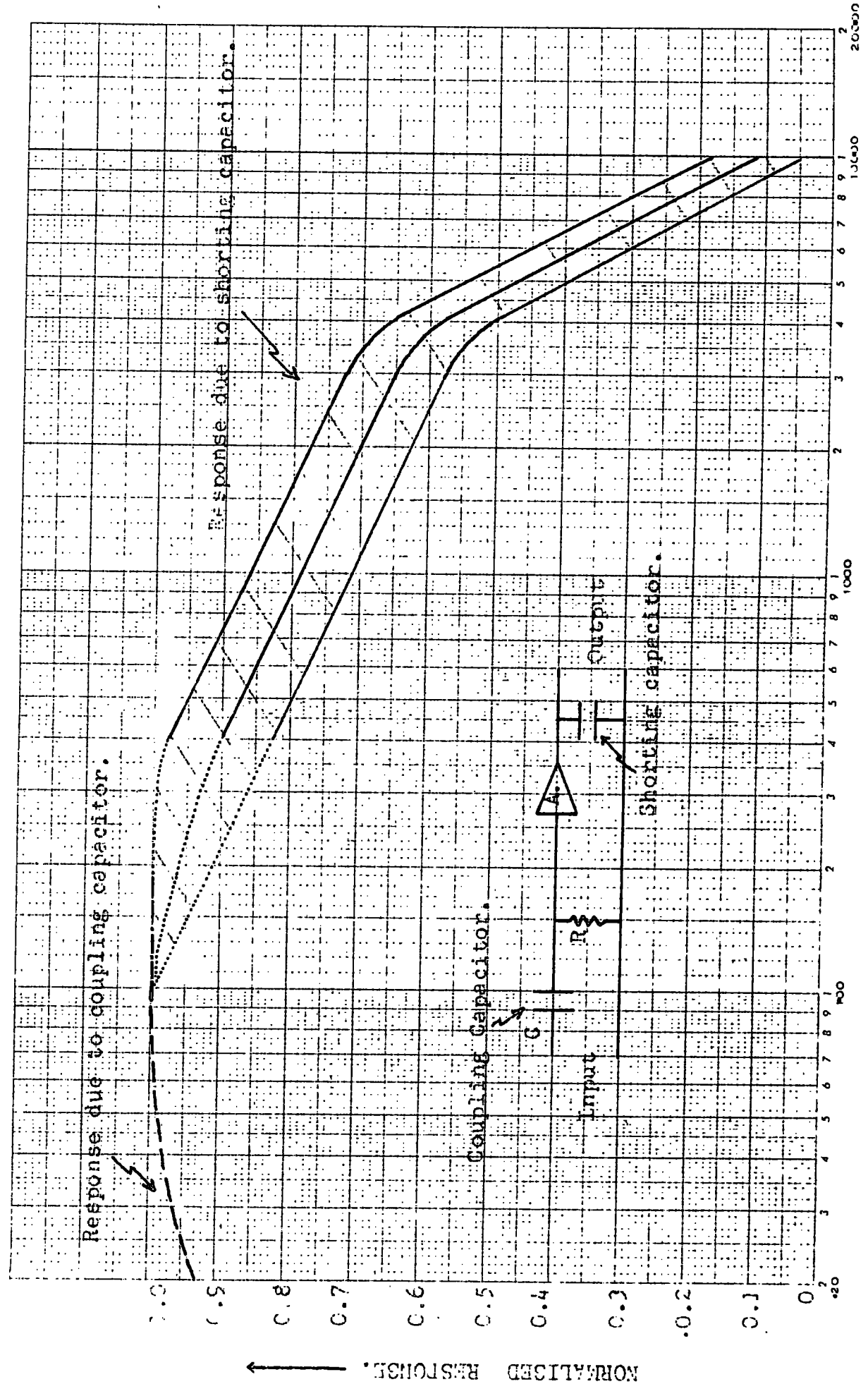
The response of the amplifier system is controlled principally by two capacitors; by input coupling capacitor at low frequencies and a shorting capacitor connected across the output of the amplifier at higher frequencies (Fig. 9). A low frequency oscillator was used to test the response of the amplifier between the frequency range 4 → 100 cps. An oscilloscope showed that the output voltage of the oscillator remained constant while the frequency was altered through the required range. The experimental response curve derived in this way decreases with increasing frequency due to the gradually lowered resistance of the shorting capacitor.

It can be shown theoretically (Appendix D) that the response begins to fall off at frequencies below about 1 cps. due to the increased resistance of the coupling capacitor at low frequencies.

Both the capacitor response curves are shown in Fig. 9.

AMPLIFIER RESPONSE CURVE.

Fig. 9



• FREQUENCY IN CYCLES PER SECOND

Frequency Response of the Seismograph

Now the part of the response curve with which we are mainly concerned is that lying within the frequency range 1 + 30 cps., since, as we shall see in the next chapter, most of the recorded noise components lie within these limits.

The frequency response of the seismograph (Fig. 10) has been found by taking the product of the amplifier and seismometer response over this frequency range. Since the lowest frequency that could be produced by the oscillator was 4 cps., it was necessary to extrapolate the measured amplifier response curve from 4 cps. back to 1 cps.

Estimation of the Accuracy of the Seismograph Response Curve

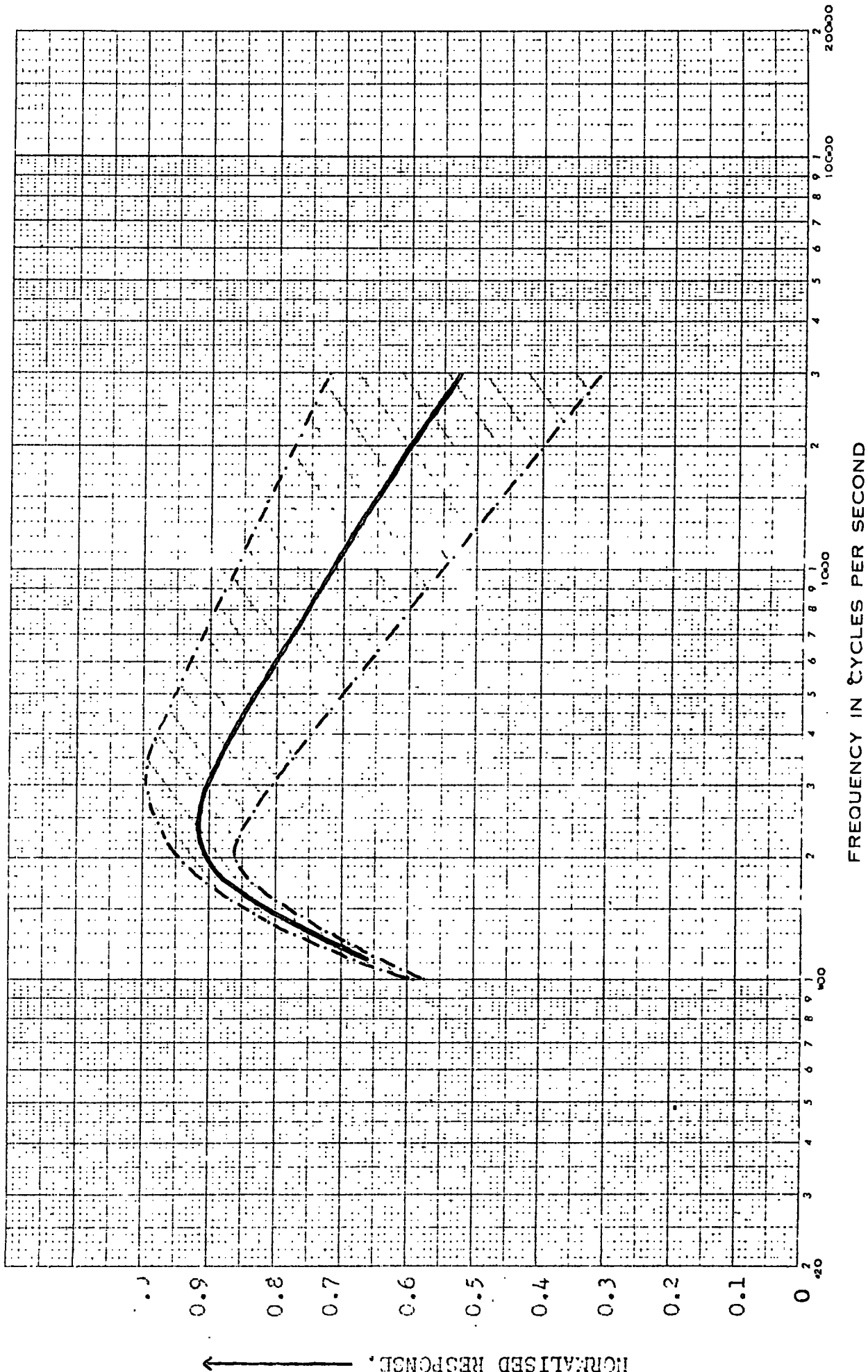
Two major sources of error are present in the derivation of the seismograph response curve.

The first and most important one is the uncertainty associated with the seismometer response curve. Since the value of the fall-off rate chosen to represent the response at the higher frequencies is considered to be near the maximum value that may be expected, there is a high probability that the true response curve occurs somewhere within the shaded portion of Fig. 8 defined by the theoretical and postulated response curves.

A second error occurs in the extrapolation of the measured amplifier response curve over the frequency range of 1 + 4 cps. The limits of the possible extrapolation are drawn in Fig. 9; the enclosed area between the resulting curves representing the region

SEISMOGRAPH RESPONSE CURVE.

FIG. 10



of uncertainty. In both the amplifier and seismometer response curves, an average value of the response has been drawn through the shaded areas.

Both the above errors will thus be incorporated in the final seismograph response curve of Fig. 10, with the resultant shaded portion defining the region within which the true response curve may lie. If the solid line in Fig. 10 represents an average value of the response curve, then it will be noticed that, relative to the response at 1 cps., there may be as much as 40% error in the response at 30 cps., 20% at 10 cps., and about 10% at 3 cps.

Finally, it must be mentioned that the overall response curve has been derived assuming that the seismometer-ground coupling remains constant for all frequencies. This is in fact not the case since both the coupling equations given on page 17, are frequency dependent. The magnitude of this effect is unknown and thus it has not been possible to allow for it.

2. CARAVAN INSTRUMENTATION

Caravan recordings were all made on 24-channel magnetic tape which could be monitored on playback by a four-channel pen-recorder. Three Willmore seismometers were used at various stations in the immediate vicinity of the caravan. A fourth seismometer, designed by A.W.R.E., was also used and maintained at a fixed position (Sta.26) throughout the period of caravan recording.

An added feature of the caravan was that band-pass filters could be connected to the output from the magnetic tape, when it was played back, and in this way frequency components present in the noise could be almost isolated.

CHAPTER IV

FREQUENCY AND ATTENUATION ANALYSES

GENERAL STATEMENT

The methods used in the record analysis are primarily designed to separate the frequency components of the local noise, and to study its horizontal attenuation from the source.

Before we enter into a description of these techniques, a short section dealing with the appearance of the records themselves is given.

1. GENERAL DESCRIPTION OF FIELD RECORDS

The character of the records obtained in the field depends upon whether noise is being generated by the Boltsburn Washing plant. The plant is maintained in continuous operation, except for one day each week and when it is closed down and does not generate any noise.

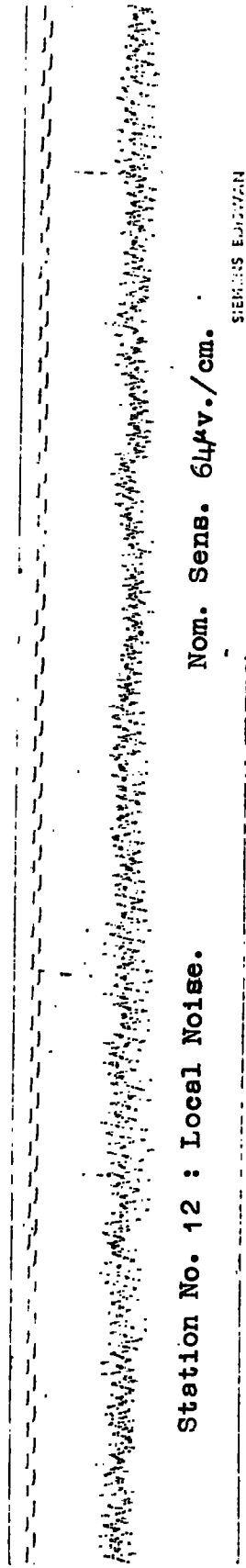
Since nearly all local noise is generated by the plant, then during this "quiet" period only background noise is recorded and thus its character and magnitude may be studied.

When the noise source is present, the background is largely obscured by higher frequency components except for those recordings at the most distant stations from the source.

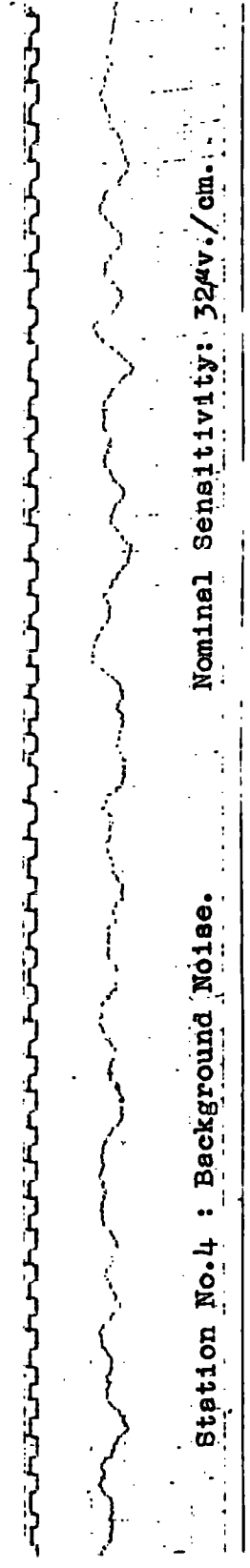
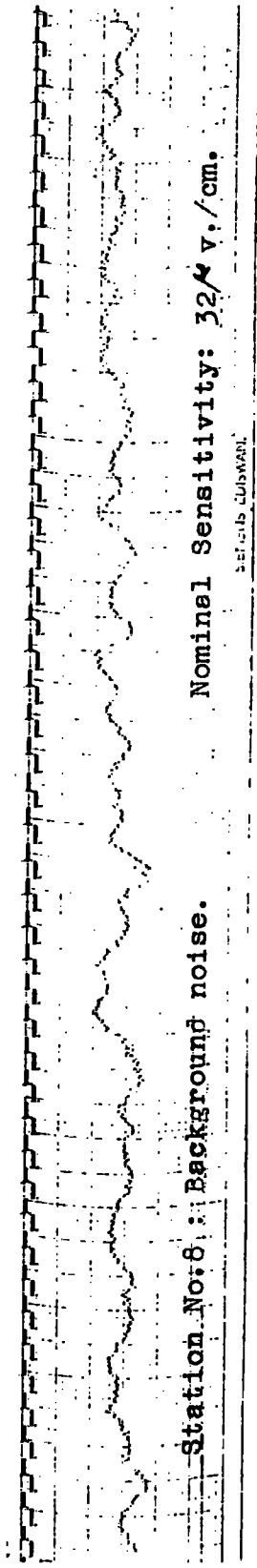
Records Obtained When the Noise Source is Absent

The characteristic appearance of the background noise is a prominent low frequency variation of about 0.5-1.0 cps., on which there is superimposed minor fluctuations of very small amplitude with frequencies ranging from about 15 - 20 cps. There are also short bursts of even higher frequencies. Two typical records of the background noise are shown in Fig. 11b.

FIG. 11



(a)



(b)

Now it was found that, whereas the high frequency fluctuations were markedly reduced when recordings were made well away from civilization, the low frequency variation remained almost constant (compare the two records in Fig. 11 b).

From this it can be deduced that most of the high frequency components originate from small local man-made sources of noise, whereupon the low frequency variation is probably the natural microseismic noise.

Records Obtained When the Noise Source is Present

General Frequency Content

It was found that at all stations where the source noise could be readily distinguished from the background, the predominant frequency was about 6 cps. The only exceptions to this were for stations very close to the noise source. Here the 6 cps. component, though present, was almost obscured by higher frequencies of about 11 to 30 cps. These higher frequencies rapidly died out with increasing distance from the source, until at about a distance of 500 metres a fairly high quality 6 cps. signal was recorded, with only minimal amounts of higher frequency. Now for those marginal stations, situated some distance from the source, at which the difference between the source noise and background levels became small, the interference between the two levels caused distortion in the 6 cps. signal and made it often difficult to recognise.

While the source was in operation, the only station not to receive any noise from it was the one at the focus, F, of the recording network which seemingly recorded an uncontaminated background trace.

The frequency characteristics of the noise, mentioned above, are illustrated in Figs. 12a → g, where a number of examples are taken from actual records.

Waveform Characteristics

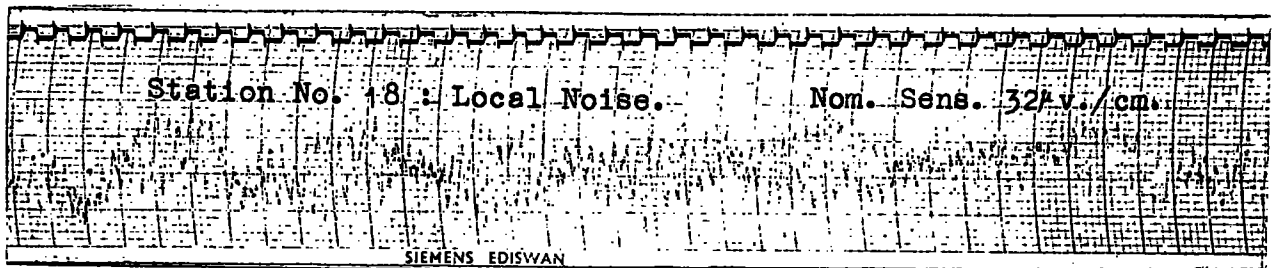
Amplitude modulation of the 6 cps. signal is a common feature of the records. The period of modulation recorded ranges from about 4 → 5 seconds, and may occasionally be as high as 9 seconds. This variation is thought to be due to changes in the mechanical nature of the source and will be discussed later.

Fig. 12h → j shows a selection of traces exhibiting variable modulation.

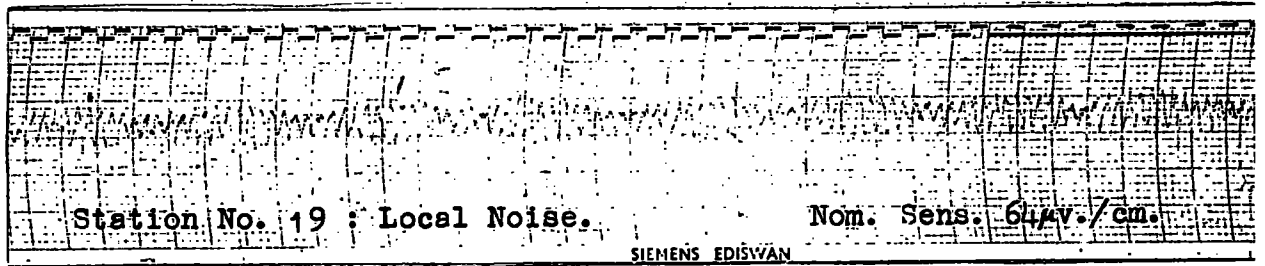
2. FREQUENCY ANALYSIS

An analysis was performed on samples of seismic noise to discover its frequency content and also to assist (1) in establishing the nature of the noise source, and (2) in the measurement of attenuation of the noise with increasing distance from the source.

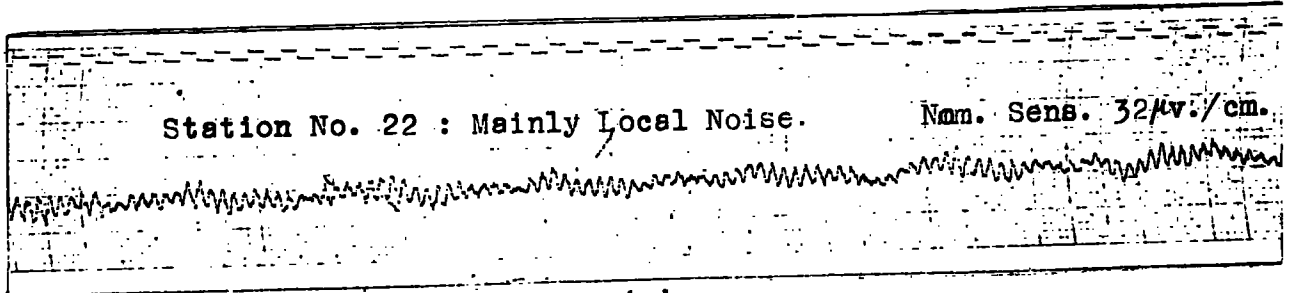
The analytical technique used involved direct amplitude measurement of the field records and subsequent conversion of the data so obtained into a power frequency spectrum using a digital computer.



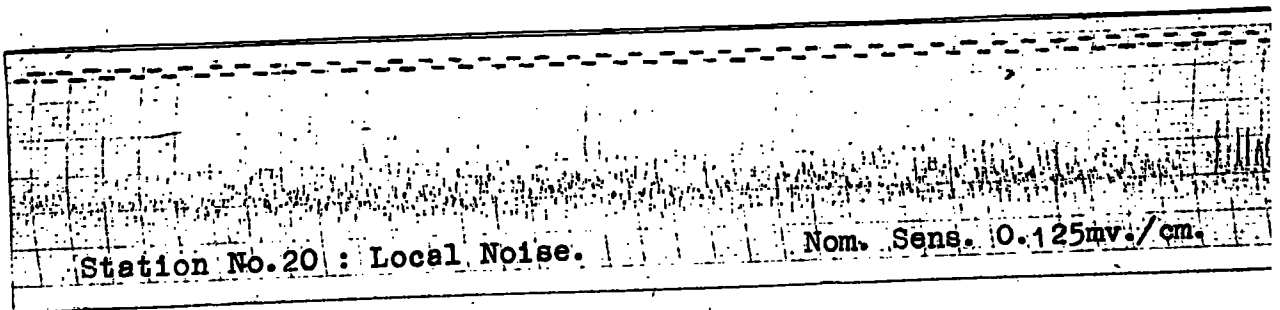
(a)



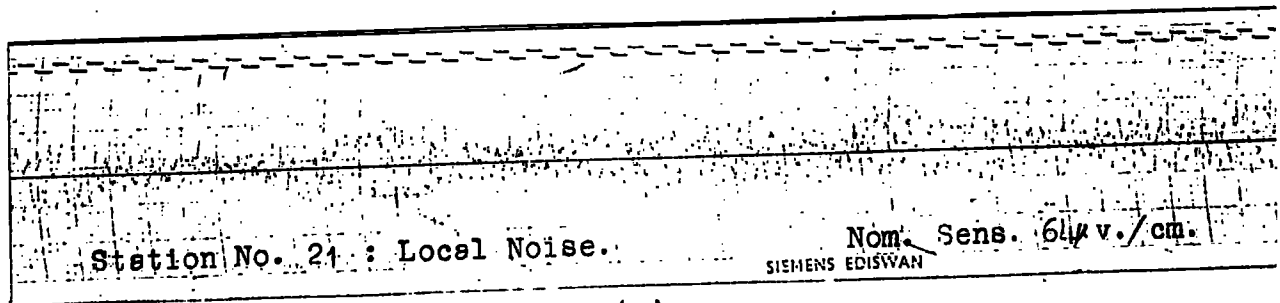
(b)



(c)

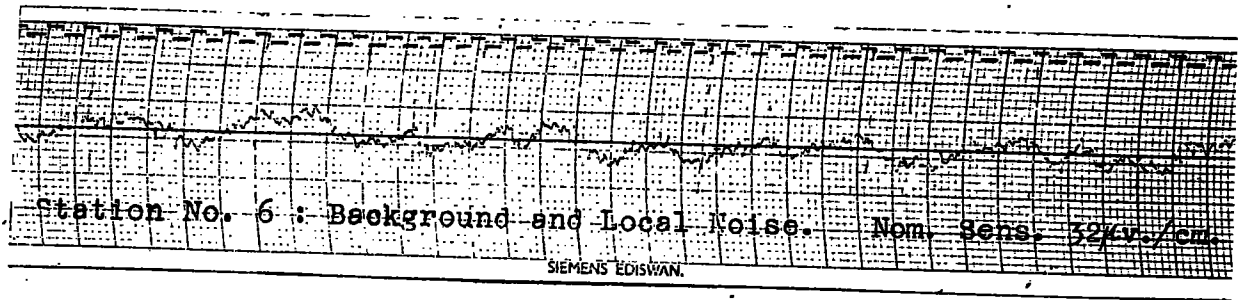


(d)

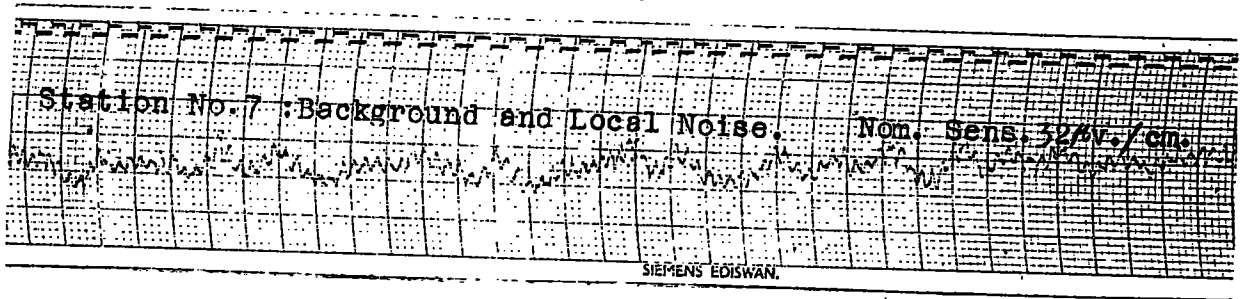


(e)

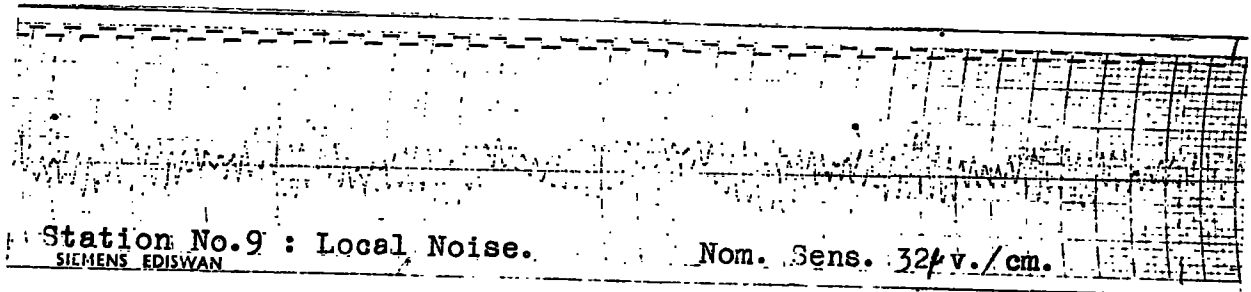
FIG. 12



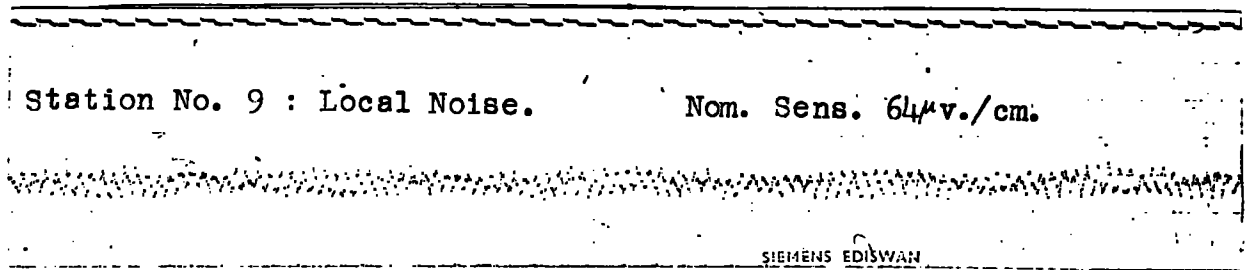
(f)



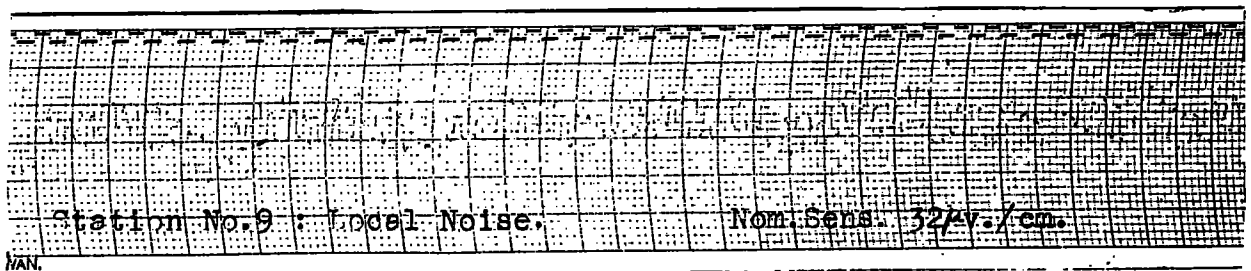
(g)



(h)



(i)



(j)

FIG. 12

However the power spectrum analysis is prone to statistical faults inherent in any process where a random waveform is sampled at a number of equally spaced intervals. Thus in order to supplement and test the validity of the results a further analysis was performed in which the frequency components of the noise obtained on records from the caravan unit were separated by the use of band-pass filters.

Power Spectrum Analysis

General Statement

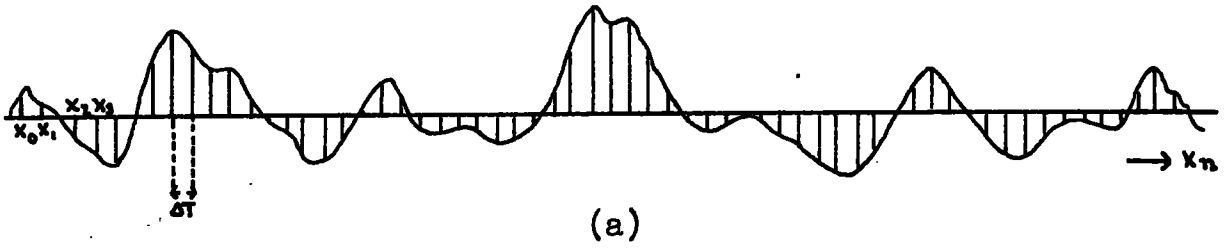
This method is designed to estimate the Power Density, $P(f)$, for each frequency component of a stationary random waveform.

Sample autocovariances are calculated, modified and the results Fourier transformed to give values of the Power Density for each frequency.

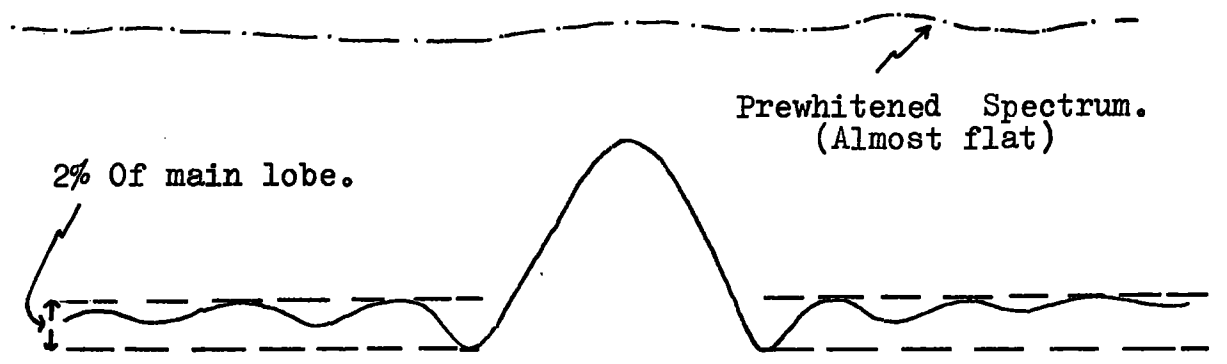
Only a brief summary of the method will be given; for a more rigorous account the reader is referred to the work by Blackman and Tukey (1958).

Theory

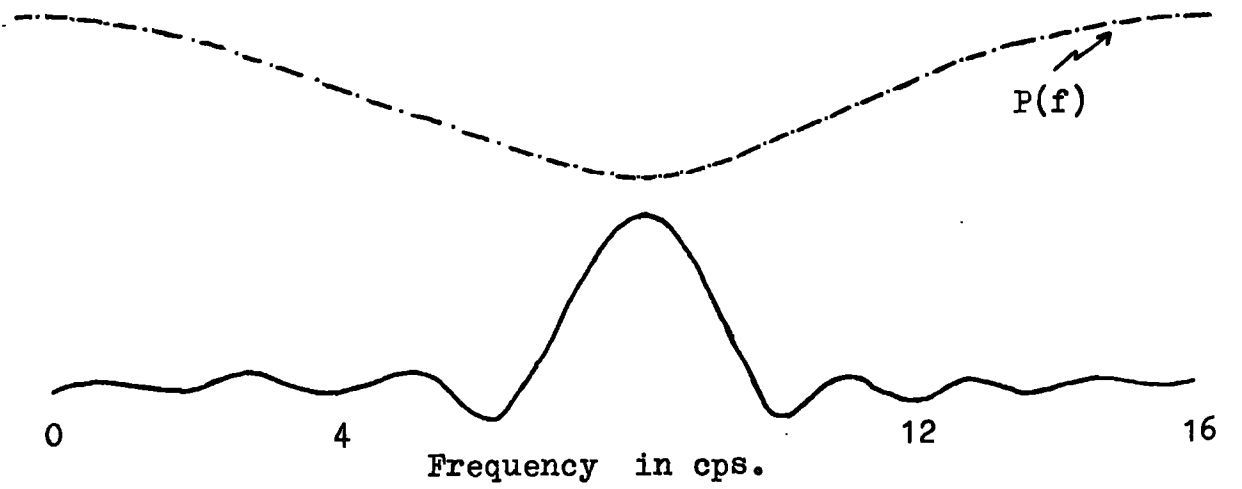
A number of amplitude readings, X_t , are taken, each at a fixed interval DT from the next, along a stationary random waveform, Fig. 13a; $t = 0, 1, 2, 3, \dots, n$, where $n + 1$ is the number of readings.



(a)



(b)



(c)

Minor lobes, from all spectral windows between about 4 and 12 cps., become prominent and thus contribute appreciable power density to their respective frequencies.

FIG. 13

Using this data it is possible to describe such a waveform in terms of (a) the average value \bar{X} of X_t where

$$\bar{X} = \frac{X_0 + X_1 + X_2 + \dots + X_n}{n+1}$$

and (b) the autocovariance function, C , which is defined as a measure of the linear common variation between two quantities, equal to the average product of deviations from the averages, and is a function of the lag between the two quantities (in this case amplitude measurements).

Thus, for example, the covariance of X_i and X_j where the lag = $j-i=1$, and $n=6$, is given by:

$$C_{j-i} = \frac{(X_i - \bar{X})(X_j - \bar{X})}{6}$$

If we can assume for the moment that \bar{X} approximately equals zero, then C_{j-i} equals the average of $X_i X_j$. However in order to specify the waveform more completely, the interval between i and j must be variable.

If $r = j-i = 0, 1, 2, 3, \dots, m$, where m is approximately equal to $n/10$, then there will be $m+1$ values of the covariance given by:

$$C_r = \frac{1}{n-r} \sum_0^{n-r} X_t \cdot X_{t+r} \dots \dots \dots (4.1)$$

where C_r is the autocovariance function.

Thus covariances are obtained between two quantities separated by a range of time intervals $0, DT, 2DT, 3DT, \dots, mDT$.

There can thus be only m possible frequency bands extending from $1/2mDT$to $m/2mDT$.

Now the maximum autocovariance for a fixed r will occur when $rDT = \lambda$ where λ is the wavelength of the frequency component, and DT is very much less than λ . Low values of r used will thus tend to show up the higher frequencies and high values, low frequencies.

Now it is necessary to modify the values of C_r obtained in equn. (4.1) in two ways:

(1) If $X \neq 0$, then an adjustment for the mean must be made. The need for modification becomes clear when we consider the effect of small displacements of the average. If most of the observations, say 999 in 1000, lie between -100 and +100 with a few falling outside one limit or the other, then the standard deviation approximately equals 30 and the variance about 900. Now suppose the average of the observations was not zero as we have assumed but say about 10, then the total power = (average D.C. power)² + the variance = $10^2 + 900 = 1000$. Now all the D.C. power will belong to the low frequency bands. Since $m = n/10$, there will be a hundred frequency bands and as a result the power density in the lowest frequency band will be nine times that of the 99 others. Since this will cause distortion in the values of $P(f)$ for these higher bands, the lowest frequency bands must be eliminated. This can be done by subtracting from each value of the autocovariance obtained in equn. (4.1), the square of the mean of all the data.

(2) Strong variations of $P(f)$ are ironed out by prewhitening. This effectively makes the power spectrum flat, that is, $P(f)$ independent of frequency. The reason for this procedure will be stated later.

Prewhitening modifies each value of X_t thus:

$X_t^* = X_t - 0.6X_{t-1}^*$ where X_t^* is the prewhitened value of X_t , (t now starts from 1 and not zero).

Thus after modification equn. (4.1) then becomes:

$$C'_r = \frac{1}{n-r} \sum_{t=1}^{n-r} X_t^* X_{t+r}^* - \left(\frac{1}{n} \sum_{t=1}^n X_t^* \right)^2 \dots\dots (4.2).$$

C'_r is the modified autocovariance function.

Now C'_r is a time function of lag, and in order to obtain $P(f)$ from this which is a frequency function, it is necessary to apply a cosine series transform to equn. (4.2):

$$V_r = (C'_0 + 2 \sum_{q=1}^{m-1} C'_q \cos(qr\pi)/m + C'_m \cos r\pi), \text{ where } V_r$$

is then a measure of $P(f)$.

Since $P(f)$ represents the measure of the variance contributed by each frequency, then $P(f)$ can be approximately thought of as the square of the amplitude of that frequency, (if \bar{X} approx. equals zero).

Now the contribution of the spectral density at each frequency is not only determined by the amplitude of the particular

frequency, but also by a function which is termed the spectral window. The spectral window used has the shape shown in Fig. 13b. The side lobes are made about 2% the height of the main peak. Previous prewhitening is necessary so that the density spectrum is roughly flat thereby minimising the contribution to the power density of the minor lobes. If as in Fig. 13c, prewhitening was omitted and the density spectrum was as shown then the contribution of the subsidiary lobes may be magnified in comparison with that of the main lobe. If the spectrum is fairly flat, then the power density for each frequency is controlled only by the main peaks, there being negligible additional contributions from minor lobes.

The actual values of the power density are smoothed out since the value of the power density at any frequency has contributions from adjacent windows.

As it is important to choose a spectral window which has only one major peak, adjustments are made (termed hanning) to V_r to gain this effect.

Finally the prewhitening, which was introduced purely to minimise the effect of the minor lobes, is removed after hanning and at the same time errors introduced in the adjustment for the mean (equn. (4.2)) are corrected.

Method and Results

An Algol programme based on the theory just given was constructed for use in a digital computer.

From the programme Fig. 14 it can be seen that each of the procedures outlined in the theory are taken in the order: prewhitening; calculation of the modified autocovariance function; Fourier transformation to a cosine series; hanning and corrections for both prewhitening and the mean.

The programme was tested first by feeding in data for a single sine wave and then for a mixture of sine waves. This latter test involved the construction of a second computer programme, Fig. 15, designed so that any number of sine waves of different frequency, amplitude or phase could be fed in. From these, the computer gave a series of values corresponding to amplitude measurements, at fixed intervals apart, for the waveform resulting from the superposition of the input sine waves. This data was then directly used for the power frequency analysis programme, and the resultant spectrum showed peaks corresponding to the original input frequencies. The amplitude ratio of the peaks was the same as that for the squared values of the input amplitudes. From these tests it was concluded that the programme would prove satisfactory for the analysis of seismic records.

Two records showing the same degree of amplification were analysed, from stations 9 and 6 (Figs. 12 f and h); in each case the record was photographed and a negative obtained, which was magnified by projection. Both records were analysed over a time interval of 20 seconds. For station 9, $DT =$ one-fiftieth of a second and n (the number of readings) = 1000. For station 6, $DT =$ one-eightieth of a second, and $n = 1200$.

COMPUTER PROGRAMME FOR POWER FREQUENCY ANALYSIS.

Programming System: Elliot 803 Algol (5 hole).

```
POWER SPECTRUM ANALYSIS (HCH)'
BEGIN INTEGER M,N,R,Q,T'
REAL F,G,A,L,SUM,D,E,DT'
ARRAY X(0:1200),C(0:120),V(0:120),U(0:120)'
READ N,M,DT'
F:=0'
FOR T:=0 STEP 1 UNTIL N DO
BEGIN READ X(T)'
G:=F'
F:=X(T)'
X(T):=X(T)-0.6*G'
END'
SUM:=0'
FOR T:=1 STEP 1 UNTIL N DO
BEGIN SUM := SUM+X(T)'
END'
A:=(SUM/N)**2'
FOR R:=0 STEP 1 UNTIL M DO
BEGIN SUM:=0'
FOR T:=1 STEP 1 UNTIL (N-R) DO
BEGIN L:=X(T)*X(T+R)'
SUM:=SUM+L'
END'
C(R):=(SUM/(N-R))-A'
END'
FOR R:=0 STEP 1 UNTIL M DO
BEGIN SUM:=0'
FOR Q:=1 STEP 1 UNTIL (M-1) DO
BEGIN D:=2*C(Q)*COS((Q*R*3.1416)/M)'
SUM:=SUM+D'
END'
E:=C(M)*COS(R*3.1416)'
V(R):=C(0)+SUM+E'
END'
U(0):=(V(0)+V(1))/2'
U(0):=U(0)*(N/(N-M))*1/((1.36-1.20*COS((2*3.1416)/(6*M)))'
FOR R:=1 STEP 1 UNTIL (M-1) DO
BEGIN U(R):=V(R-1)/4+V(R)/2+V(R+1)/4'
U(R):=U(R)/((1.36-1.20*COS((2*R*3.1416)/(2*M)))'
END'
U(M):=V(M-1)/2+V(M)/2'
U(M):=U(M)/((1.36-1.20*COS((1-1/(6*M))*2*3.1416))'
FOR R:=0 STEP 1 UNTIL M DO
PRINT SCALED(4),R/(2*M*DT), SAMELINE, U(R)'
END'
```

↑
Prewhitening.
↓

↑
Correction
for the mean.
↓

↑
Calculation
of modified
Autocovariance
functions.
↓

↑
Fourier
transformation
by Cosine Series.
↓

↑
Hanning
and

Corrections
for Pre-

whitening
and the mean.
↓

Time of duration of programme: Approx. 2 hours, 10 minutes.
(For N=1200, M=120 and DT=0.0125).

COMPUTER PROGRAMME FOR SINE WAVE SUMMATION.

Programming System: Elliot 803 Algol,(5 hole).

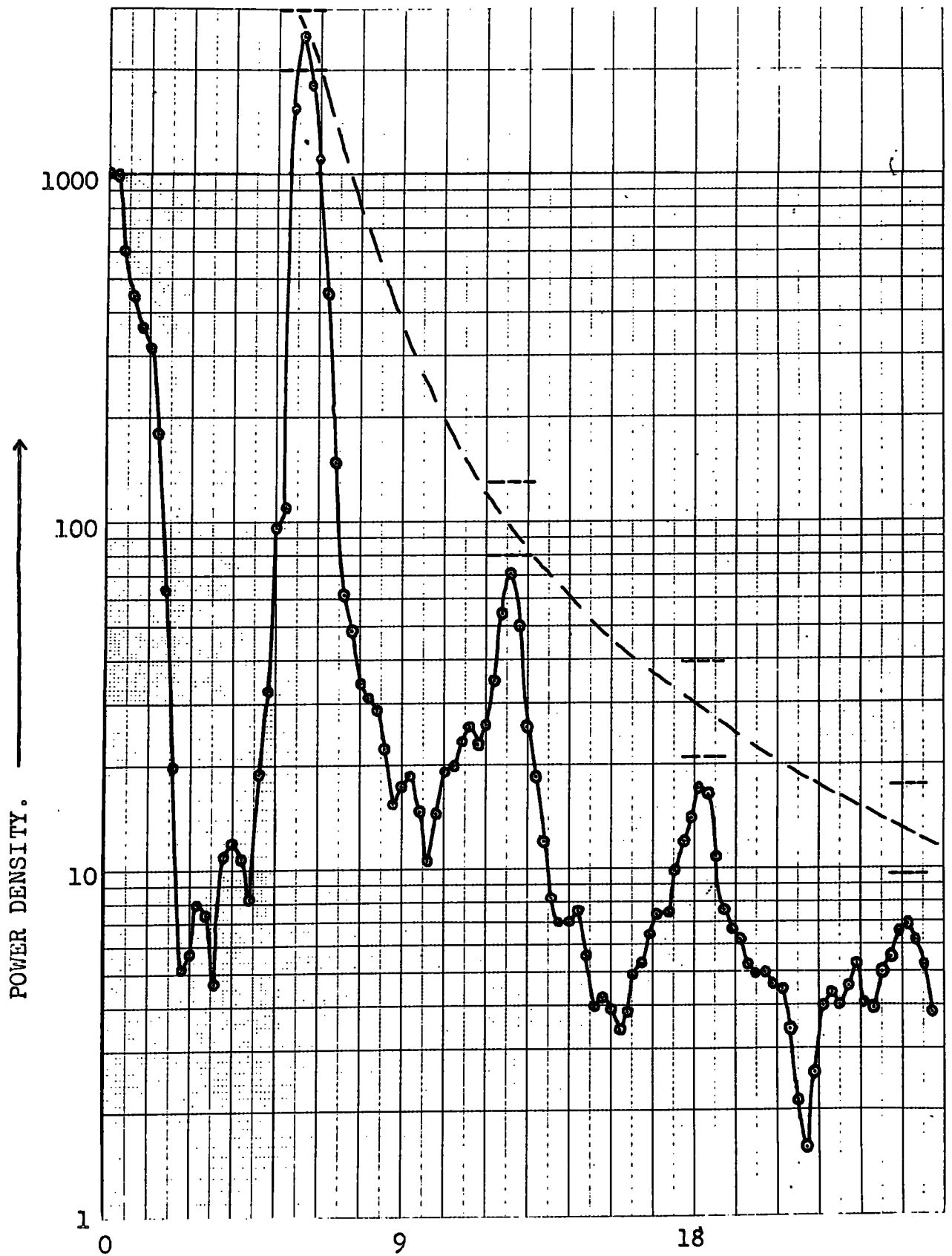
```
SINE WAVE SUMMATION (HCH)'
BEGIN ARRAY A(0:50),F(0:50),E(0:50)'
      INTEGER Q,I,N,M,J'
      REAL SUM,L,DT'
      SWITCH SS:=S1'
S1: READ Q,N,M,DT'
      PRINT N,M,DT'
      FOR I:=1 STEP 1 UNTIL Q DO
      BEGIN READ A(I),F(I),E(I)'
      END'
      FOR I:=0 STEP 1 UNTIL (N+1) DO
      BEGIN SUM:=0'
          FOR J:=1 STEP 1 UNTIL Q DO
          BEGIN L:=A(J)*SIN(6.2832*F(J)*I*DT+E(J))'
              SUM:=SUM+L'
          END'
          PRINT SUM'
      END'
      WAIT'
      GOTO S1'
END'
```

FIG. 15

The resulting power spectra for both the stations are shown in Figs. 16 and 17. Referring to Fig. 16, we see that there are four prominent peaks corresponding approximately to frequencies of 6, 12, 18, and 24 cps., the power density falling off with increasing frequency. The dotted line in Fig. 16 represents the true relative values of the power for each of these frequencies, estimated from applying the frequency response curve of the seismograph, Fig. 10, to the power spectrum. Since the difference between the power of adjacent peaks is large, errors in the response curve (possibly including those due to coupling) are not likely to alter the relative sizes of the peaks significantly.

Since the major peak at 6 cps. is almost 40 times the value of the next highest peak at 12 cps., it seems likely that the plant is generating a 6 cps. component with progressively minor amounts of higher order harmonics.

Now the power spectrum for station 6, Fig. 17, does not show such prominent frequency components. However the 6 cps. one can still be clearly distinguished. Minor peaks do occur at about 12.5, 16 and 21 cps. but their magnitude may be of a similar size to those at the very high frequencies, and thus may not be significant; the reason for this is that they form only subsidiary peaks to a much higher and broader peak extending from about 21 to 2 cps. which reaches a pronounced maximum at 6 cps. The broadness may be due to a true maximum occurring somewhere between about 9 and 14 cps., but there has not been sufficient resolution to separate it from the 6 cps. peak. The power spectrum shows a somewhat ragged appearance in comparison



FREQUENCY in CYCLES PER SECOND.

FIG. 16

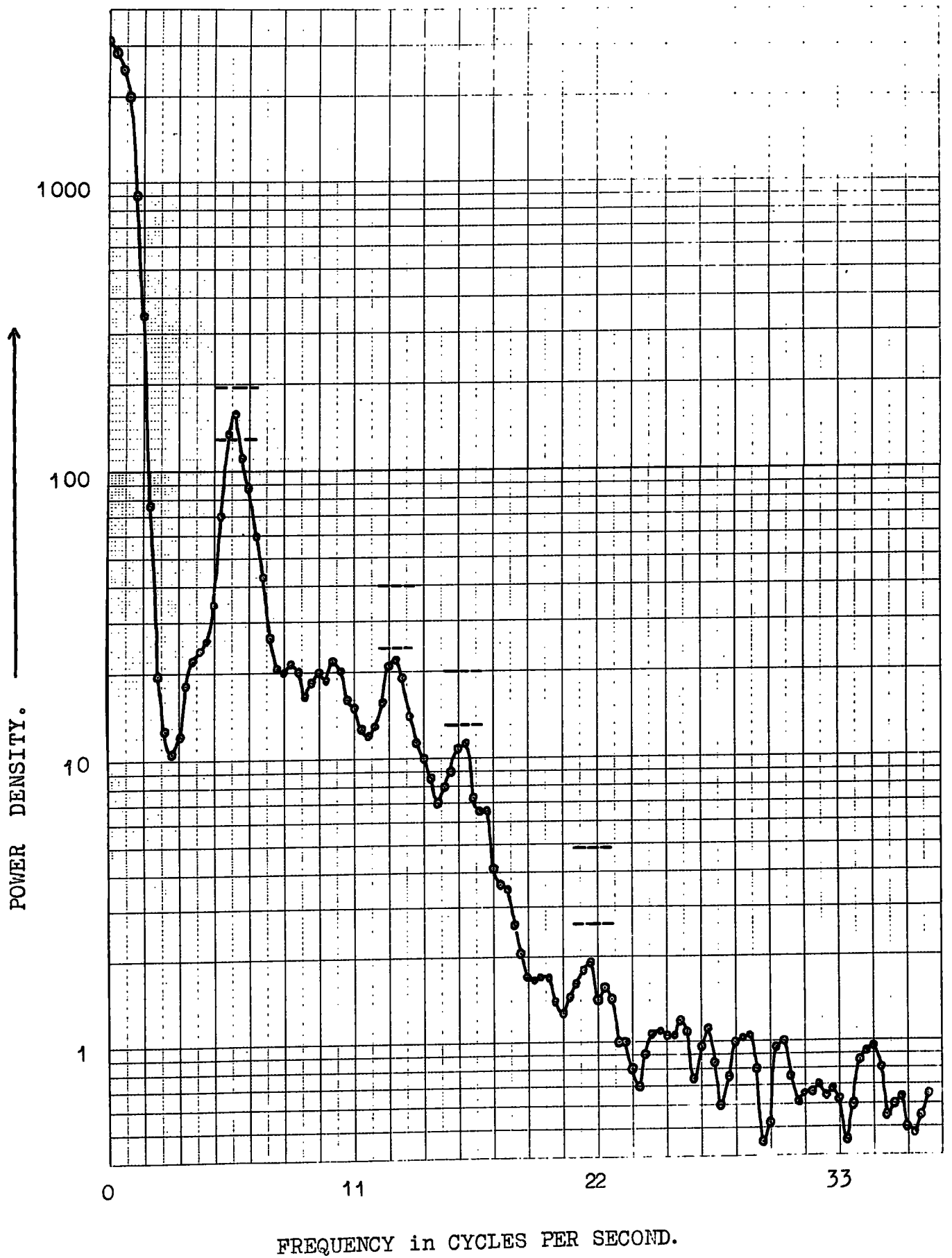


FIG. 17

with that of Fig. 17, due to the relative increase of the background noise in comparison with that from the source.

Now from Figs. 16 and 17, the ratio of the amplitudes, ($=\sqrt{\text{Power density}}$), of the 6 cps. component at stations 6 and 19 is 1:4. Since the other frequencies recognizable in Fig. 16 cannot be picked out with any certainty in Fig. 17, then the 6 cps. peak is the only one that can be safely compared between the two stations.

Now it will be noticed that in both the power spectra of Figs. 16 and 17, there is a steep rise in the power density towards the lower end of the frequency spectrum, reaching a maximum at zero frequency. Since the seismometer and amplifier response are almost negligible at these frequencies, it must be concluded that their existence in the power spectrum is fictitious.

The high values of power density at the low frequencies may be due to a number of cumulative factors:

- (1) The D.C. level may be much greater than that allowed for by the correction for the mean. This is very likely to arise, since the datum line from which the amplitude measurements were made was drawn through each trace in such a way that, purely from inspection, a value of \bar{X} close to zero might have been expected. In fact it is possible that \bar{X} is much greater than zero.
- (2) From Fig. 11b, it can be seen that the background noise level is mainly composed of frequencies at or below 1 cps.
- (3) Modulation of the noise (seen in Figs. 12a, b, c, e, h and i) may have some effect, since the frequency of the modulation

envelope is about 0.2 cps. This effect should only be present to any marked degree in the power spectrum of station 9, since here the 6 cps. component predominates.

Now if the low frequency part of the spectrum results from the wave modulating the 6 cps. noise, then the ratio of the power values at 6 cps. might be expected to equal that at the low frequencies for the two stations. If the low frequency power is due to the background noise, then the power value should remain almost constant for the two stations. Since neither of the above results are observed in Figs. 16 and 17, it must be concluded that modulation and background noise only play a minor role in the low frequency power spectrum; even their combined effect could not account for the greater value of the low frequency spectrum at station 6 in comparison with that at 9. It is considered instead that (1) is the most likely cause of the anomalous low-frequency spectrum; the reason for supposing this is that the value of the power density at zero frequency is much greater in Fig. 17 than Fig. 16 and this may arise out of the greater difficulty in fitting, by eye, a "zero" datum line to the trace for station 6 than for the more regular one of station 9.

There are two possible sources of error in the power spectrum analysis which may lessen the reliability of the results obtained:

(a) "Aliassing" of frequencies may occur if an insufficient number of amplitude measurements are made on each peak of the seismic trace. However in the present analysis such errors are

considered negligible since the interval between amplitude measurements is such that for every peak occurring on the records there are at least three amplitude values to define it.

(b) Errors may occur in the relative values of the power density for each prominent frequency component, because the values used in the prewhitening and the subsequent corrections may not be entirely suited to the type of waveform analysed. The formulae used in the computing, however, are considered by Blackman and Tukey "to work fairly well in many cases".

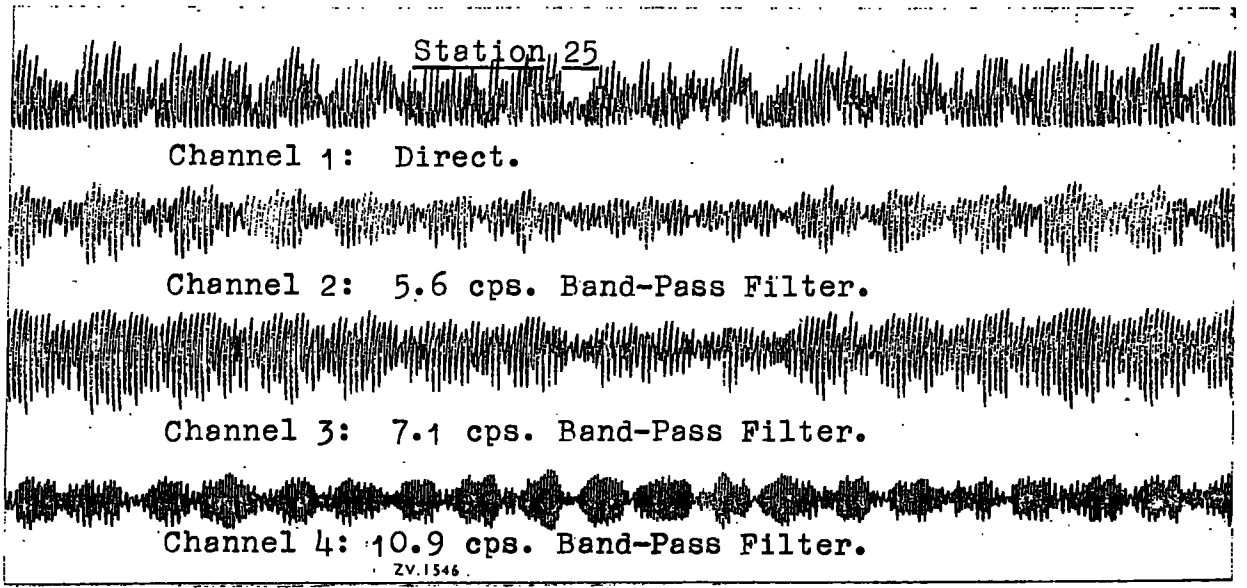
Frequency Analysis Using Caravan Filters

A number of recordings stored on magnetic tape were reproduced on playback, and the output fed through a band-pass filter at various frequency settings, to a pen recorder.

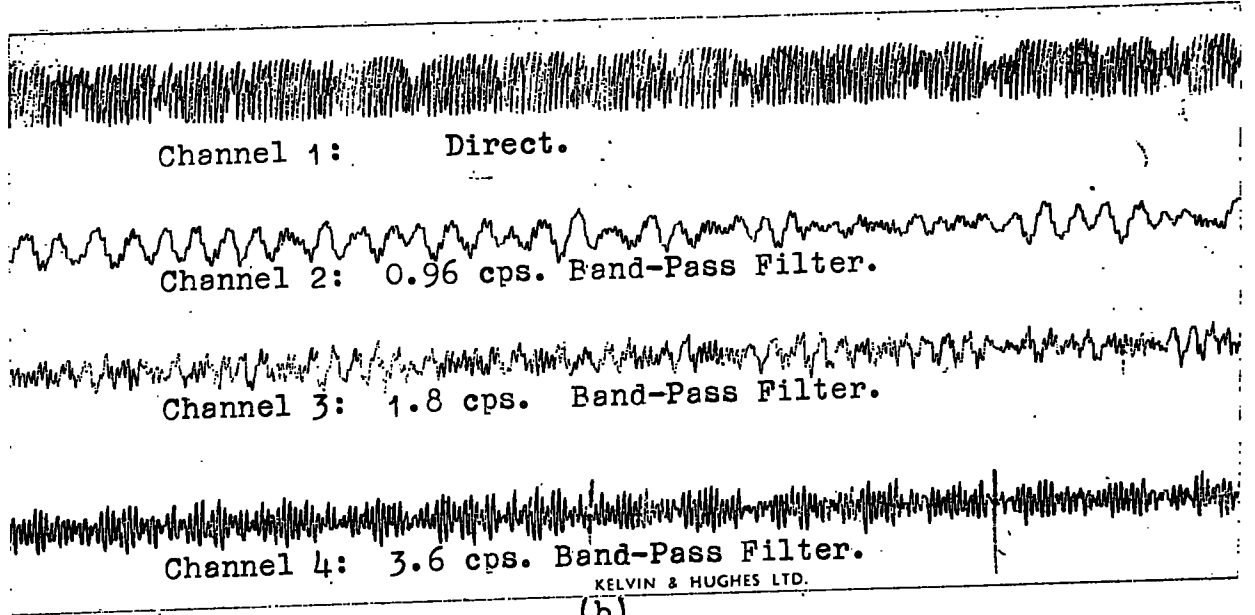
The magnetic tape recordings were made from stations 10, 25 and 19 (Fig. 1) along a radial profile. An additional station (No. 24), near the crushing plant, was also recorded simultaneously with station 10. For each of the profile recordings nine filter settings, ranging from 0.36 + 10.9 cps. were used. Only the top three filter settings were used on the record from station 24. All filters were maintained at a constant bandwidth.

Figs. 18 and 19 show all filter channels for station 25 and the three higher filter channels for stations 19, 10 and 24.

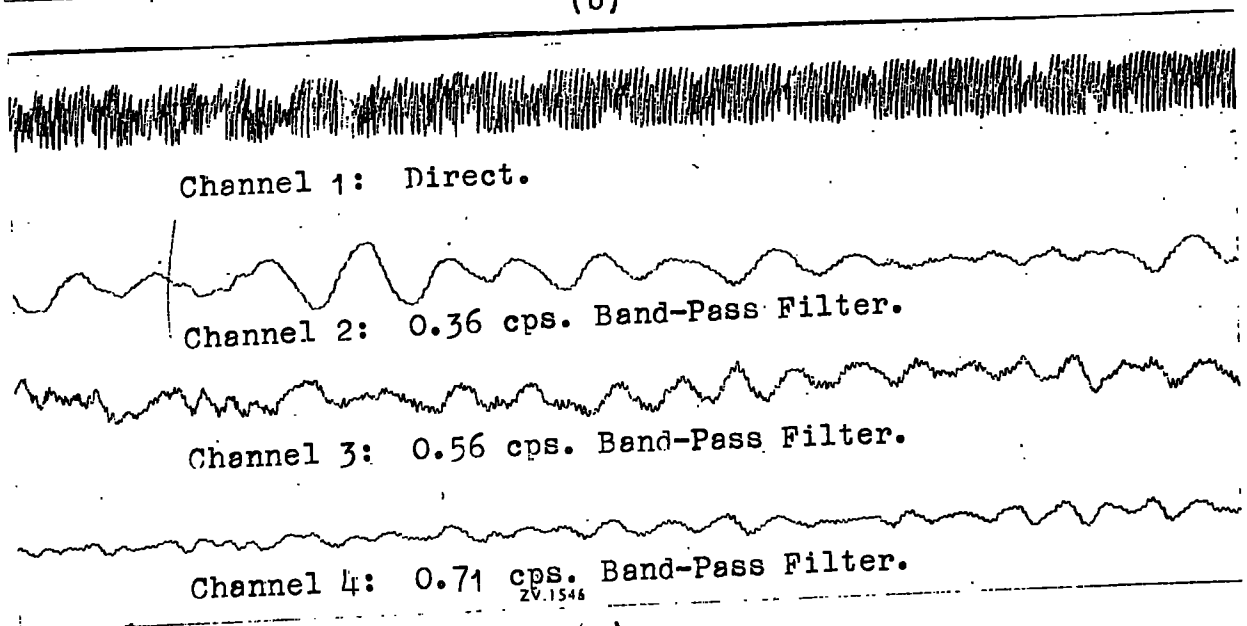
For each of the recorded stations, the normalised output from the filter for all detected frequencies is shown in Fig. 20;



(a)

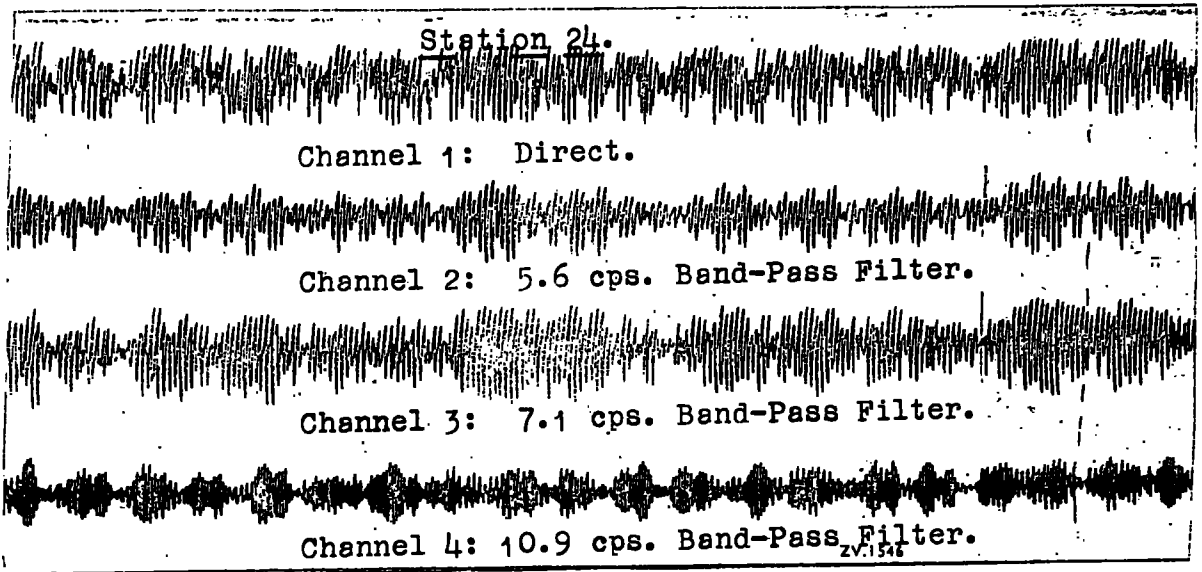


(b)

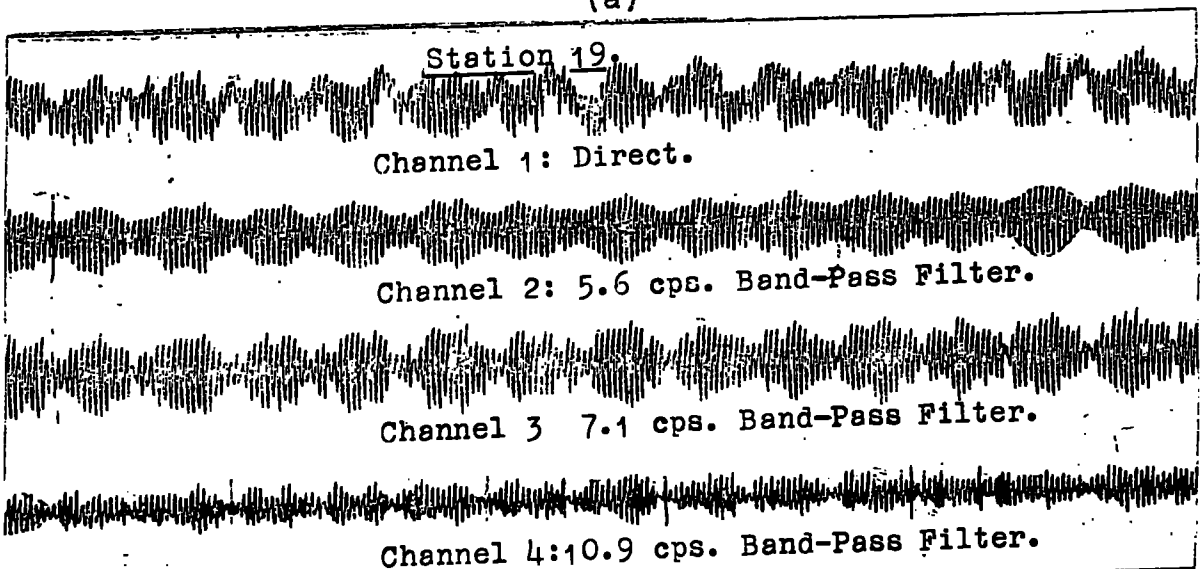


(c)

FIG.18

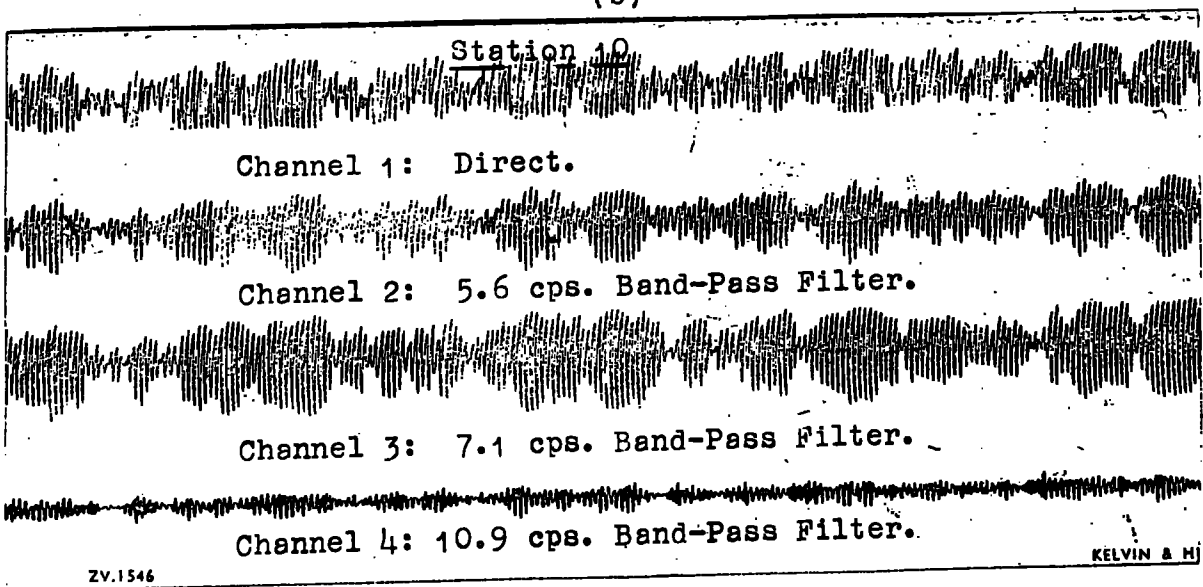


(a)



KELVIN & HUGHES LTD.

(b)



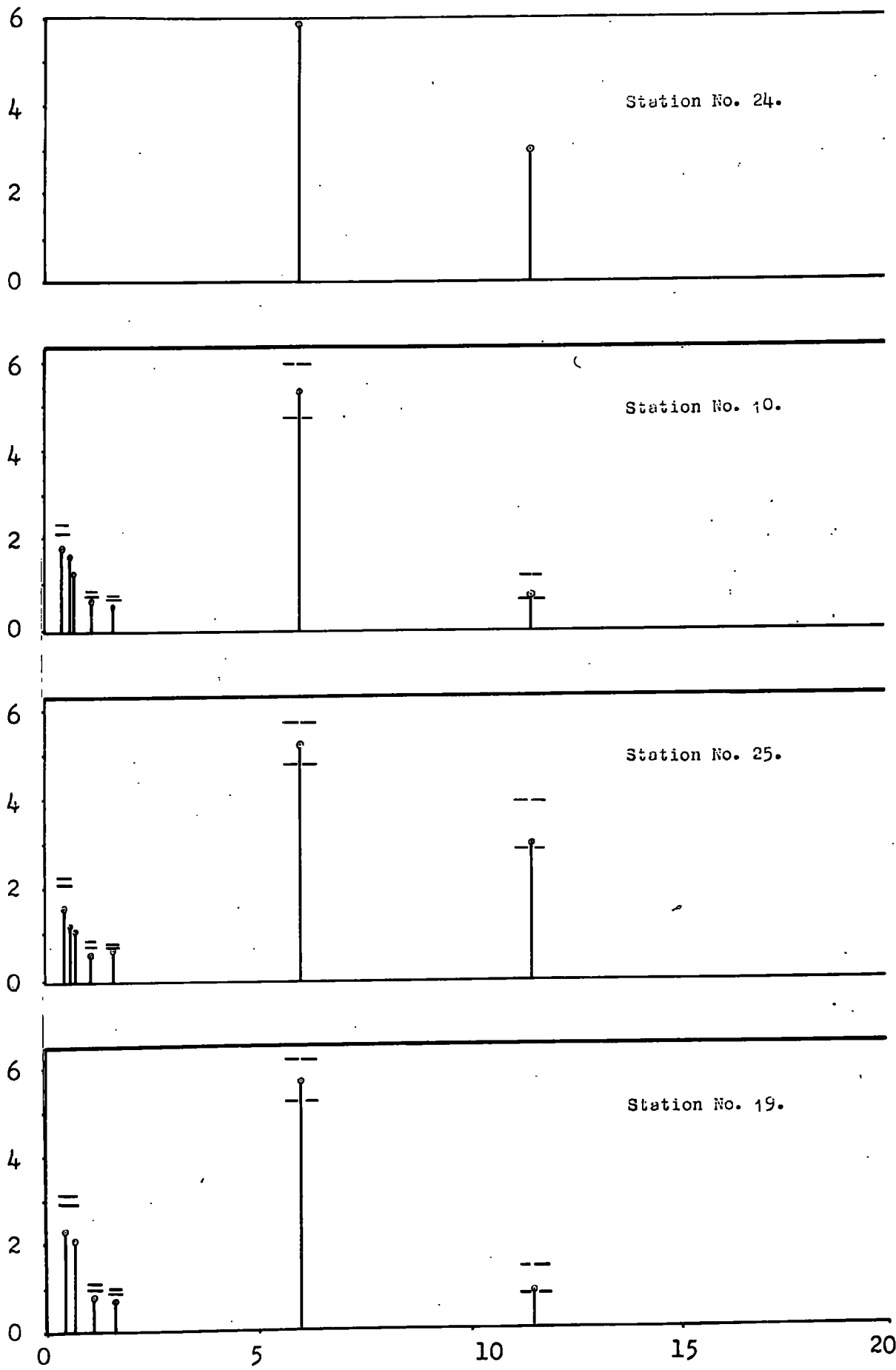
ZV.1546

KELVIN & H

(c)

FIG. 19

NORMALISED RESPONSE.



FREQUENCY in CYCLES PER SECOND.

FIG. 20

it will be noticed from this that, whereas the output for the 6 cps. and lower frequencies remains almost constant from station to station, there is a marked fluctuation in the 11-12 cps. component. For stations 19 and 10 the output ratio of the 6 cps. and 11-12 cps. components is about 7:1; for a similar source-station distance this decreases to just under 2:1 at station 25. The cause of this will be discussed later in the section on noise variation. Since stations 10 and 24 were recorded at the same time it will also be seen that there is a greater attenuation of the 11-12 cps. than of the 6 cps. component.

The lower frequencies around 1 cps. detected at stations 19, 25 and 10 belong to the background noise level; the output for such frequencies appears to remain fairly constant from station to station. The filters were calibrated by measuring their response to a sine wave input of constant amplitude, but varying frequency, generated by an oscillator.

The errors in the measurement of the output level for each detected frequency increase if (a) masking of the frequency occurs due to breakthrough of other frequencies not contained within the filter bandwidth, (b) the response of the filter to the measured frequency is small, and (c) the actual output for that frequency is small. In (a) it is likely that amplitude measurements not belonging to the desired frequency will be made, and in (b) and (c) the smaller the quantity, the greater the fractional error incurred in its measurement.

Large errors as high as 50% may occur in the estimation of the output level from the four lowest frequency filters, since

(1) the filter response to the measured frequency had to be calculated theoretically using the filter bandwidth as the oscillator used in the calibration could not produce frequencies lower than 1.25 cps. and (2) the estimate of the frequency measured on the filtered output must be accurate to at least 0.1 cps. Since this latter was not possible due to the large number of low frequencies present, errors result in the calculation of the filter response to the frequency measured.

Maximum errors of about 5% are likely in amplitude measurements of the 6 cps. frequency recorded through 5.6 and 7.1 cps. filters, and the 11-12 cps. frequency recorded through the 10.9 cps. filter.

Errors would be increased to about 20% if 6 cps. breakthrough was measured from the outputs of the 3.6 and 10.9 cps. filters (errors due to (a), (b) and (c)).

The output level of frequencies from the 1.8 and 0.96 cps. filters will probably be correct to about 10% (errors due to (a) and (c)).

Comparison of Results Obtained by Filter and Power Spectrum Analyses

Since records from two stations close together (9 and 10) were examined using the different frequency analyses, direct comparison of the results can be made. This, however, can only extend over the frequency range from zero to 12 cps.; higher frequencies could not be studied in the caravan since no filters above 10.9 cps. were available.

The existence of low frequency components seen in the records of the background noise (Fig. 11b) was confirmed by the filter analysis, since all filters from 0.56 to 0.96 cps. (Fig. 18b and c) gave definite output signals. Over the low frequency range, a small peak was registered at about 0.5 cps. in Fig. 20. The power spectrum analysis proved unsatisfactory for detecting these low frequency components, since they are probably obscured by the large D.C. level. However, despite this there is a distinct break of slope in the power density curve of Fig. 16 at about 1 cps. which may show the presence of this frequency.

Both frequency analyses show frequency components of 6 cps. and 11+12 cps. The ratio of the amplitude of the 6 cps. to the 11+12 cps. components is about 5:1 in both the filter and Power Spectrum analyses. The similarity in the results can be expected due to the proximity of the two stations analysed by the two methods.

Since the ratio is almost the same for the two analyses, it may be concluded that either (a) the frequency response of the recording unit at the caravan is not appreciably different from that of the portable field equipment, or (b) that the frequency response is significantly different but that a difference in results due entirely to the nature of the analysis used has compensated for this with a resultant apparent similarity in the results.

The contribution of the frequency analyses to the measurement of attenuation will be given in the next chapter.

ATTENUATION ANALYSIS

Method of Measurement of the Average Peak-to-peak Amplitude

Since the Willmore seismometer is a velocity sensitive instrument, then all the recordings obtained give a measure of the vertical ground velocity. Equation (3.4) shows that if the pen deflection is proportional to the ground velocity at any instant, then the average peak-to-peak amplitude of the trace taken over an interval of time should be proportional to the average peak-to-peak ground velocity over that time.

If the average peak-to-peak amplitude is A_p cm. then from equation (3.4) it follows that:

$$A_p \text{ cm. corresponds to } N.A_p \cdot 10^{-6} / 0.58 p/a_o f_o/d \text{ cm./second... (4.3)}$$

where N is the nominal sensitivity in $\mu\text{v./cm.}$

Thus by evaluating the average peak-to-peak amplitude for all records, a value for the vertical ground velocity at each station can be obtained. Average values were taken due to the wide variation in the amplitude of individual peaks along the trace, but they can only be used for attenuation measurements providing that proper allowance has been made for any variation of the noise level with time. This was done by using appropriate field recording methods supplemented with experiments made by the caravan unit. This was discussed fully in Chapter II.

The peak-to-peak amplitude for each record was averaged over a time interval of about a minute (see page 20). The graduated squares on the recording paper assisted in the rapid measurement of the peak-to-peak amplitude.

Sentence at bottom
and top of page 64: "Again,
attenuation for a number of
files can be easily observed."
should be deleted.

can be easily observed. Again, if the attenuation for a number of frequencies is measured over the same wavepath, the variation of attenuation with frequency could be studied.

It was mentioned on page 7 , that for a homogeneous medium, a simple mathematical expression for the rate of attenuation can be derived for surface and body waves. Thus, if the points forming the attenuation graph are scattered, and the attenuating medium remains reasonably constant, then a least squares fit may be made to the scatter and the form of the curve assumed to follow equations (1.2) or (1.3).

On the other hand, if the points are not scattered but follow a visible trend, then any deviation from the theoretical curve may be related to differences in the attenuating medium along the wavepath.

In method (a) no such simple formula describing the attenuation could be derived, and thus the form of the curve would be difficult to predict for a uniform attenuating medium.

Now from the section discussing the general appearance of the records (page 46) it can be considered that apart from those stations very near to or far from the noise source, all stations received a predominant 6 cps. signal. The 6 cps. frequency could, however, still be recognised in the areas of interference, and thus the average peak-to-peak amplitude was measured of the 6 cps. peaks only (method b). Since the 6 cps. component can be measured at all stations over the whole area (the station at the network focus being the only exception),

then information on the nature of the attenuating materials over this area should be possible.

Average peak-to-peak measurements were not made on frequencies higher than 6 cps. since only within about 100 metres from the noise source were they sufficiently above the level of the 6 cps. signal to be measured accurately.

Estimation of Errors in Vertical Ground Velocity Values

The errors involved in the measurement and calculation of vertical ground velocity are either systematic or random. Systematic errors are those which remain constant for each measurement made, such as the underestimation in the values of a_0 and f_0 mentioned on page 34 . Such errors will only affect the absolute and not the relative values of ground velocity. Since we are concerned only with relative values such errors do not concern us. Random errors do affect the relative values and thus merit some discussion. The principal causes of such errors are as follows:

- (a) In the measurement of each of the linear parameters in equation (4.3).
- (b) Due to any variation in the degree of coupling throughout the station network.
- (c) Due to interference of the 6 cps. signal by other noise components.
- (d) Due to the variation in instrumental parameters.
- (e) Due to any fluctuations in the 6 cps. level that might have occurred during recording.

Error (a) arises from the large size of the graduated squares on the recording paper in comparison with the scale of precision required. If measurement of a length AB is made by inspection, then errors will be associated with both of the points A and B due to the uncertainty in the estimation of their position inside a mm. square. The estimated % error for average values of such quantities as p , a_o , d and A_p will not exceed about 8%.

In view of the steps taken (page 18) to maintain constant coupling conditions throughout the station network, the magnitude of error (b) is likely to be small -- probably about 1 to 5%. Maximum errors are likely to occur at stations 1 and 5 as well as the one at the network focus, where flooding may have caused reduced coupling. All three stations should thus be underestimates of their true value. Error (e) is likely to be of a similar size since it will be shown in the next section that the 6 cps. level remains almost constant throughout the duration of the fieldwork. However, since no control could be exercised on the 6 cps. output level of the source, there was no guarantee of its stability during recording: small fluctuations in it may well have occurred.

Three principal types of error (c) may be recognised:

- (1) At those stations where the background noise level approaches that of the source noise. Here severe interference may take place between the two, resulting in a distorted 6 cps. component which is difficult to separate from the background noise level. The error in the measurement of average peak-to-peak values at such stations may be as high as 20%.

(2) A slightly larger error (about 30%) is probable for those measurements taken from stations very close to the source, where there is appreciable high frequency noise partially obscuring the 6 cps. trace.

(3) For a good quality 6 cps. trace, errors will still occur in peak-to-peak values measured between the modulation "beats" of the 6 cps. noise. It is here that the 6 cps. level is small and often masked by higher frequencies. Since this region makes up only about 1/5 of the trace, all other measurements being of 6 cps. peaks well above the high frequency noise level, errors in the average peak-to-peak amplitude due only to the high frequency are likely to be very small -- about 1%.

The major component of error (d) is that resulting from variations in f_0 due to mechanical changes in the Neocardiograph. This has already been discussed on page 23 .

The approximate total % error to the nearest 5%, in ground velocity values calculated from equation (4.3), is estimated to be for a good quality 6 cps. trace 10%, and for one distorted by interference, about 30% at the most.

Observations on Noise Variation

In this section the nature and magnitude of the variation of the source output will be given as indicated by the continuous caravan recording described on page 36 . Additional evidence from certain of the field techniques and field records is included in a discussion on the possible extension of this pattern of noise variation to cover the entire period over which field recordings of local noise were made.

Variation of Noise Level with Time as Detected by the Recording Caravan

Random noise samples, at intervals of about one to four hours, were taken over a period of five days from a continuous recording obtained from the caravan unit between the 2nd and 9th of November, 1963.

Two stations monitored in this way were Nos. 26 and 27 (refer to Fig. 1).

It was found from the records so obtained that two noise levels, in the ratio of 4:5, were generated by the plant. During the five days sampled it was concluded that no other noise level was present.

Periods of each noise level alternated throughout the week, the lower noise level being far more prevalent.

The ratio of the total time of duration for the two noise levels over the five days was 120:18 hours. It would thus appear that the lower noise level is the one normally produced by the plant during the working week and that the raised noise level is due to some additional noise, generated by some temporary source at the plant, superimposed on that of the lower noise level.

The higher noise level always occurred between definite times during the day, beginning abruptly at about 7 a.m., remaining constant for about nine hours, then at about 4 p.m. suddenly terminating, with a consequent reduction in noise and return to the lower noise level. Though the increased noise level was always confined to the same interval during the day, its occurrence

was found to be aperiodic through the week, since it was present on only 3 of the 5 days, two of which were consecutive.

An important conclusion that can be drawn from the above is that both noise levels remained constant over the five days of records sampled.

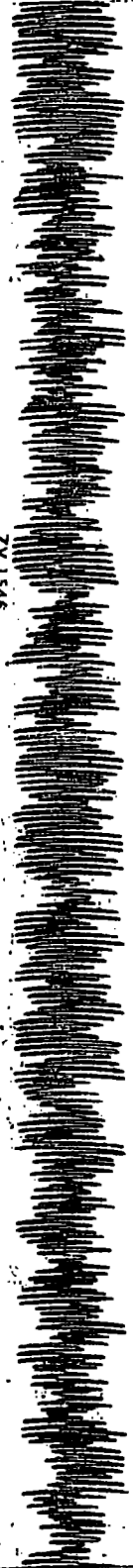
Now there is also a marked difference in the waveform characteristics of the two noise levels. Sample records of the noise levels are shown in Fig. 21, for comparison.

The lower noise level normally consists of a 6 cps. Sinusoidal Wave showing even, regular amplitude modulation. Each "beat" extends over a period of about 2 → 4 seconds. Only minor amounts of higher frequency are present.

The higher noise level still shows a prominent 6 cps. component but there is a noticeable increase in the higher frequency interference, especially in the range 11 → 12 cps. As a result of this increase, the modulation of the 6 cps. signal becomes less distinct. The modulation may take one of two forms, both of which can be distinguished from that in the lower noise level; there may be a pronounced decrease in the period of modulation to about 1 second (see trace on channel 4 in Fig. 21a), or a period of 4 → 8 seconds may be retained and the maximum amplitude of each "beat" controlled by a much longer period modulation (channel 2, Fig. 21a).

By comparing the signal level on Channel 1 for the 2 records in Fig. 21, the relative amounts of high frequency noise present in the two levels can be seen.

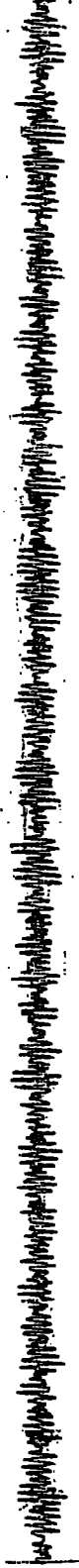
9451 AZ



Channel 1 Station No. 27: Willmore Seismometer.



Channel 2 Station No. 26: Willmore Seismometer.



Station No. 27: A.W.R.E. Seismometer. Direct. Channel 3



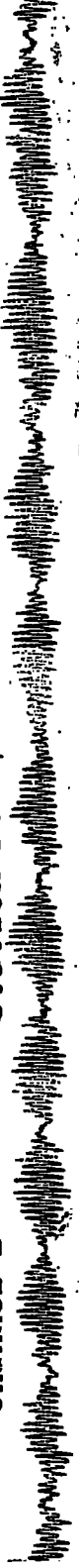
Station No. 27: A.W.R.E. Seismometer. 5.4 cps. Filter. Channel 4

(a)

9451 AZ



Channel 1 Station No. 27: Willmore Seismometer.



Channel 2 Station No. 26: Willmore Seismometer.



Station No. 27: A.W.R.E. Seismometer. Direct Signal. Channel 3



Ch. 4 Station No. 27: A.W.R.E. Seismometer. 5.4 cps. Band-Pass Filter.

(b)

FIG. 21

An important point to note from Fig. 21 is that the rise in noise level is due to an increase in the frequency components above 6 cps. The average peak-to-peak amplitude of the 6 cps. signal remains almost constant regardless of the overall noise level change. This can be seen by comparing the filtered output on channel 4 for the two noise levels.

Information on Noise Level Variation from Field Recording Techniques

1. Field Method (a) - Simultaneous recording

The results of recordings obtained at the base station (near station 19) showed that the character and the level of the noise remained the same practically throughout each day that recordings were made.

The gain and nominal sensitivity of the amplifiers was held constant throughout each day so that direct comparison between records could be made.

Over the five days recorded using this method, the noise level remained constant with the exception of one day which showed an increased noise level.

2. Field method (b2) Looping

On page 22 it was mentioned that the nature and magnitude of noise level variation could be found by the use of method (b2).

This method was applied in particular to the arc profile containing stations 1 → 5 where the 6 cps. noise level at

each station with the exception of numbers 1 and 5 was of the same order of magnitude. Thus the graphs of noise level variation for the three remaining stations should be almost parallel.

The actual graph of the noise variation at these stations proved to be inconclusive due to the high degree of scatter in the results; no trend of noise variation common to all three stations was thus seen. The only thing that may be said about this is that either the variations in the noise are too rapid to be detected, or which is more likely, that the scatter of data reveals that the variation in noise, if any, is below the variation due to the errors inherent in the recording, measurement and calculation of the ground velocity values.

As seen previously the minimum error in such values is likely to be about 10% and thus it is this which is probably causing the observed scatter. If this is the case then the 6 cps. noise level variation cannot be detected in the field with the instruments used, and thus can be regarded as negligible for our purposes.

Conclusions

Now the caravan experiment has shown that two noise levels exist which have different waveform characteristics. It has been found, in addition, that a number of field records show features present in those from the caravan, and thus it should be possible to distinguish both noise levels in the field. Two field stations considered to be showing the upper noise level are 12 (Fig. 11a) and 11, both of which exhibit long period

modulation similar to that on channel 3 in Fig. 18a and also Fig. 21a). Referring to Fig. 12 we also see that a number of stations (e.g., 22, 21, 19, 18 and 9) show waveform characteristics similar to those shown on all channels in Fig. 21b.

Since the field records were made over a period of three weeks either side of the caravan recording, then it would seem from the similarity between the records from the field and caravan, that the noise conditions shown by the caravan to exist over a week, may also be applicable throughout the entire period over which local noise was recorded in the field.

Further support for this may be obtained from information supplied by the field recording methods (a) and (b2), (page 47): it was mentioned previously that the change in noise level is due to a rise in the level of an 11 → 12 cps. component, the intensity of the 6 cps. noise remaining constant. Since the 11 → 12 cps. component is rapidly attenuated, disappearing at about 500 metres from the source (page 21) then it may be supposed that all stations near or beyond this distance would receive an almost constant 6 cps. noise level. The result of the field recording method (b2) which was confined to such stations indicates an approximate constant noise level. Since, in addition, method (a) has shown the presence of 2 noise levels it may be considered that the field and caravan recordings give results generally in accordance with one another.

Since these field methods were used either at the beginning or towards the end of the seven week recording period, then it seems likely that over this time an almost uniform 6 cps. noise level existed.

The conclusions that may be drawn, therefore, are:

(a) that the 6 cps. noise (which is the component measured for attenuation studies) remains at a constant level throughout the duration of the fieldwork except for those days at the weekend when the source was not operating.

(b) that in the immediate vicinity of the source, two noise levels were present caused by the fluctuation of an 11 + 12 cps. noise component.

As a result of the above conclusions, some explanation of the fluctuation in the 11 + 12 cps. noise component detected by the filtering technique described on page 59, can now be given.

Referring to Fig. 18a we see that long period modulation on channel 3 coupled with a prominent 11 + 12 cps. component present in the records from station 25 suggests the presence of the higher noise level at the time of recording.

More regular modulation and a reduced 11 + 12 cps. component, seen on records from stations 19, 10 and 24 (Fig. 19), indicate the presence of the lower noise level.

The fluctuation in the 11 + 12 cps. component can thus be related to the two noise levels generated by the plant.

Plotting of Attenuation Curves

It was mentioned on page 6 that the attenuation is dependent upon two functions, one associated with the geometric spreading of the wavefront and the other an exponential term associated with elastic wave absorption.

Now it will be seen later that all attenuation curves

are drawn using the method of least squares. The reason for this is that the ground velocity values plotted on the graphs are too scattered to show any obvious functional relation between them. In order to apply a least squares fit to a scatter of points it is necessary to know the form of the function that is to be fitted. The form of the equation that we are going to use for this purpose is:

$$A = \frac{A_0}{R} \cdot e^{-\alpha R} \dots\dots\dots (4.4)$$

which is the standard equation expressing the attenuation of body waves from a source at some point inside a homogeneous medium. The equation is considered valid as a first approximation for describing the attenuation of waves from a surface source such as the one at Rookhope. The reasons for this are as follows:

(1) The entire Carboniferous down to a depth of 700' is composed of an approximately cyclic sequence of thin sandstones, limestones, and shales, each unit not exceeding about 70' in thickness. Apart from the 200' thick Whin Sill, at a depth of 700', there are no major changes in lithology throughout the Carboniferous succession, and thus it may be considered to have an overall constant seismic velocity.

In addition, since the minimum estimated velocity for the recorded 6 cps. disturbance travelling in the Carboniferous is that near to the shear velocity (about 3000 meters/second) then each individual layer in the Carboniferous sequence is very

much thinner than the minimum wavelength of the seismic energy. Scattering or reflection at rock interfaces should thus be reduced to a minimum.

It may thus be concluded that propagation of seismic energy is taking place through an essentially homogeneous medium. (2) Since only the vertical ground velocity has been measured, no proof of the exact type of waves with which we are dealing can be obtained. However, the strong vertical component of motion recorded does suggest that the waves may be SV, highly incident P, or Rayleigh. Since Love waves have a transverse motion it is likely that any surface waves are predominantly of Rayleigh type. It can be expected that in the immediate vicinity of the source body waves may predominate; this is due to the fact that, since any surface waves will be propagated with a depth of penetration approximately equal to their wavelength, they may require some distance from the source before they are fully established. It is possible that only at distances from the source greater than a wavelength will a true surface wave be propagated. For a 6 cps. surface wave traveling in carboniferous sediments with an assumed shear velocity of about 3000 m./sec., this distance may be of the order of 500 metres.

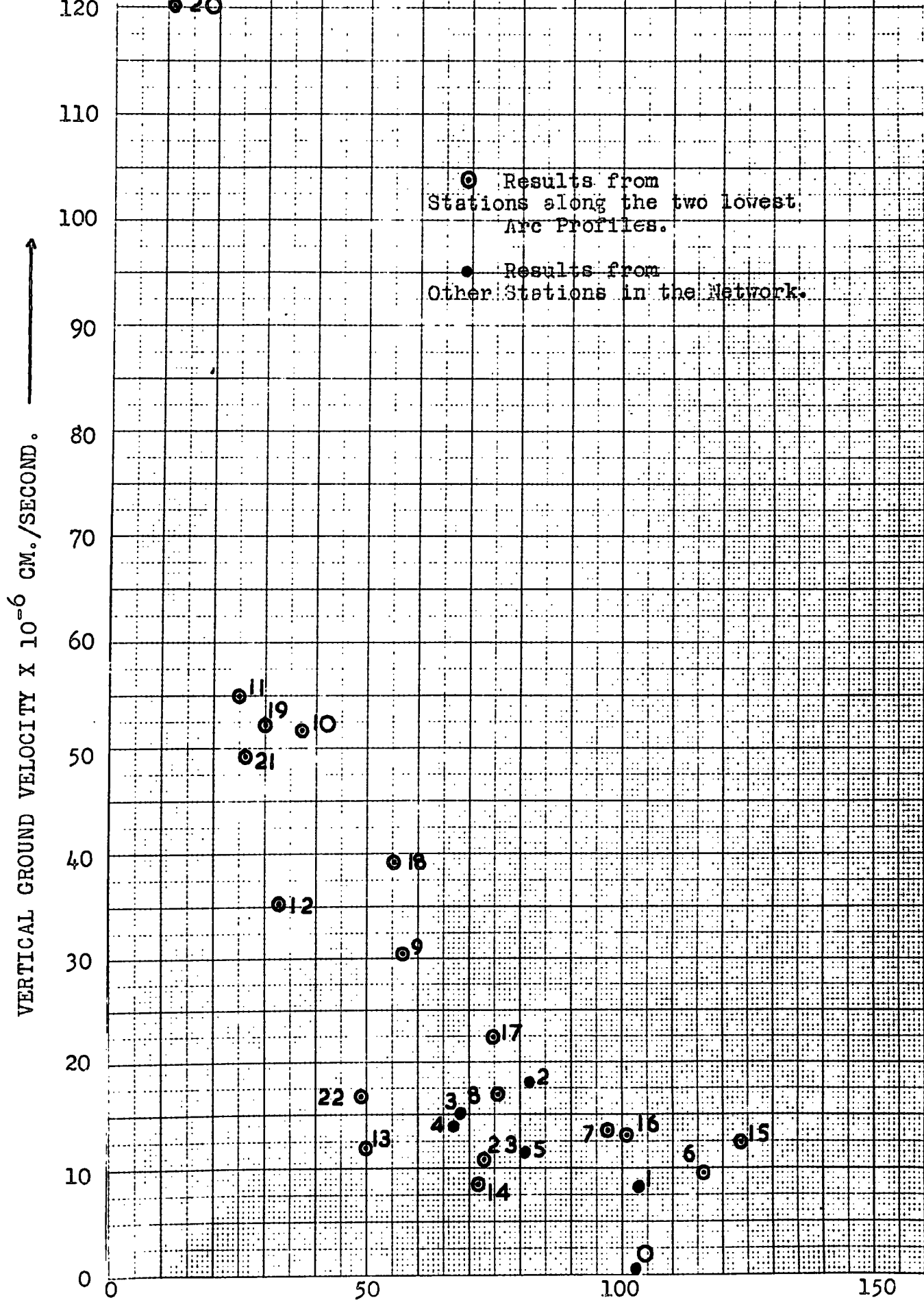
Now in addition it has been shown theoretically by Lamb (1904) that at distances of a few wavelengths from a surface source on a homogeneous halfspace, Rayleigh waves predominate.

Thus over the entire path of a 6 cps. disturbance, body waves may predominate near the source and further away the energy may be mainly in the form of Rayleigh waves. Since we do not know the exact distribution of the predominant wave types we cannot be justified in immediately using equations (1.2) and (1.3) to describe the attenuation. Instead equation (4.4) is assumed to apply as this will give a decay proportional to $1/R$ which is intermediate between $1/\sqrt{R}$ and $1/R^{2 \rightarrow 3/2}$ in equations (1.3) and (1.2); it will thus give the average attenuation over a path of energy, some of which is in the form of body waves and some in the form of Rayleigh waves.

Now according to equation (4.4) if a plot is made of the ground velocity, V , at a station, against the distance R of the station from the source, the attenuation should follow a combined hyperbolic and exponential law. A plot such as this for all stations in the network is shown in Fig. 22. Though a general downward trend can be seen there is appreciable scatter and the results appear inconclusive.

However if we sketch graphs, (figs. 23a and 24) showing the variation in ground velocity at stations along the three arc profiles as a function of distance from the source, we see that there is a markedly different rate of attenuation shown by the areas on either side of the two lower arc profiles. The topmost profile does not show this effect (its significance will be discussed later).

It thus appears that the scatter in Fig. 22 is due to two different rates of attenuation present over the area covered



DISTANCE FROM SOURCE in METRES X 10

FIG. 22

VERTICAL GROUND VELOCITY X 10^{-6} CM./SECOND.

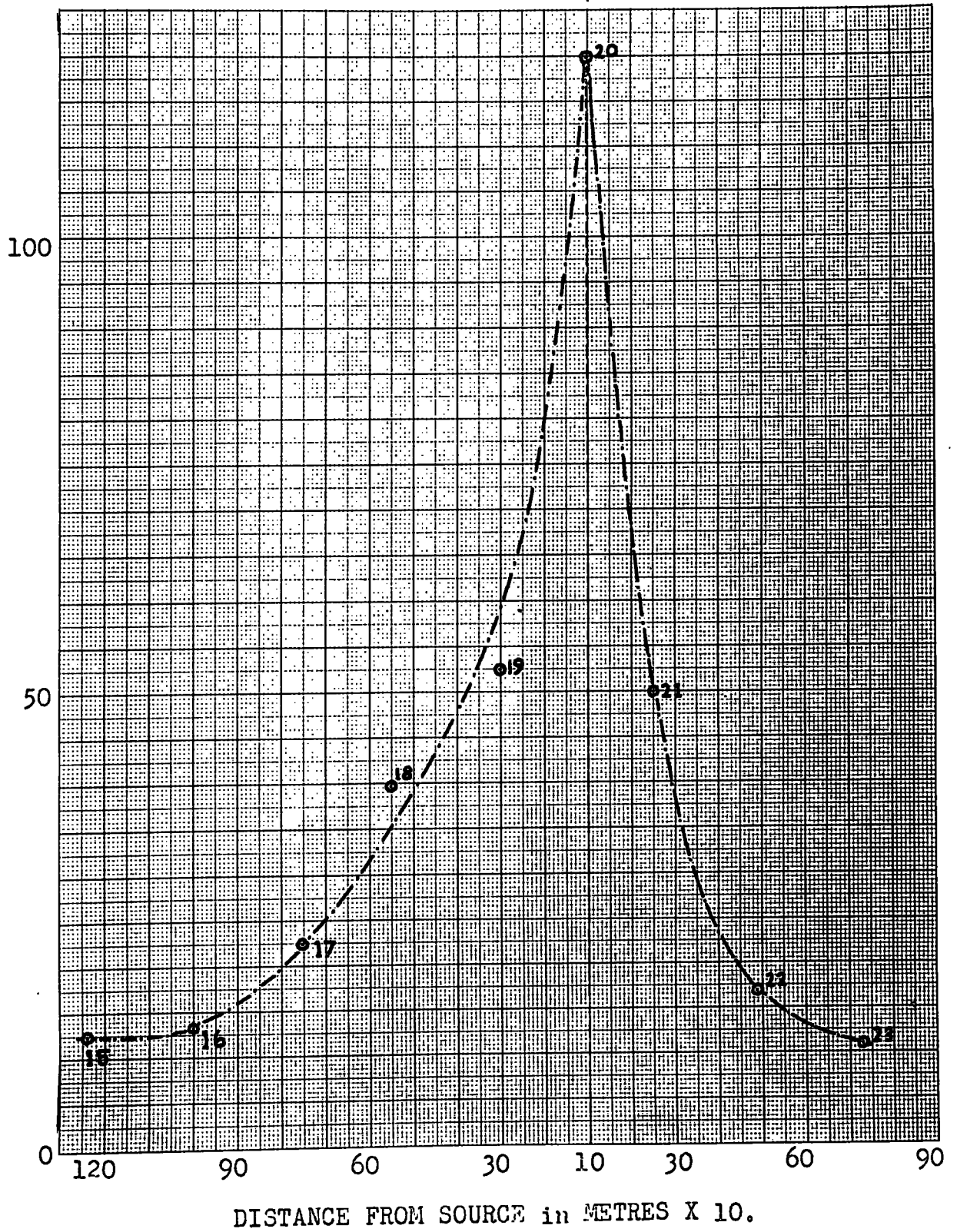
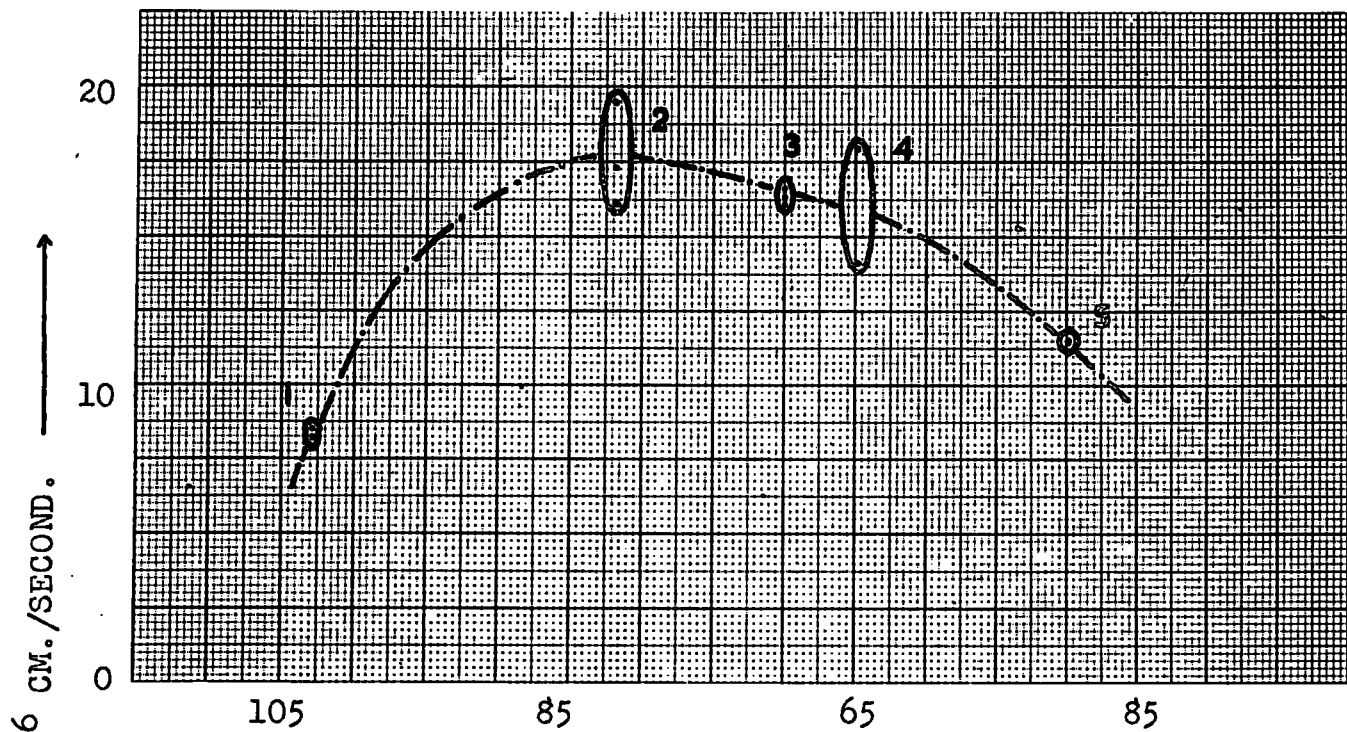
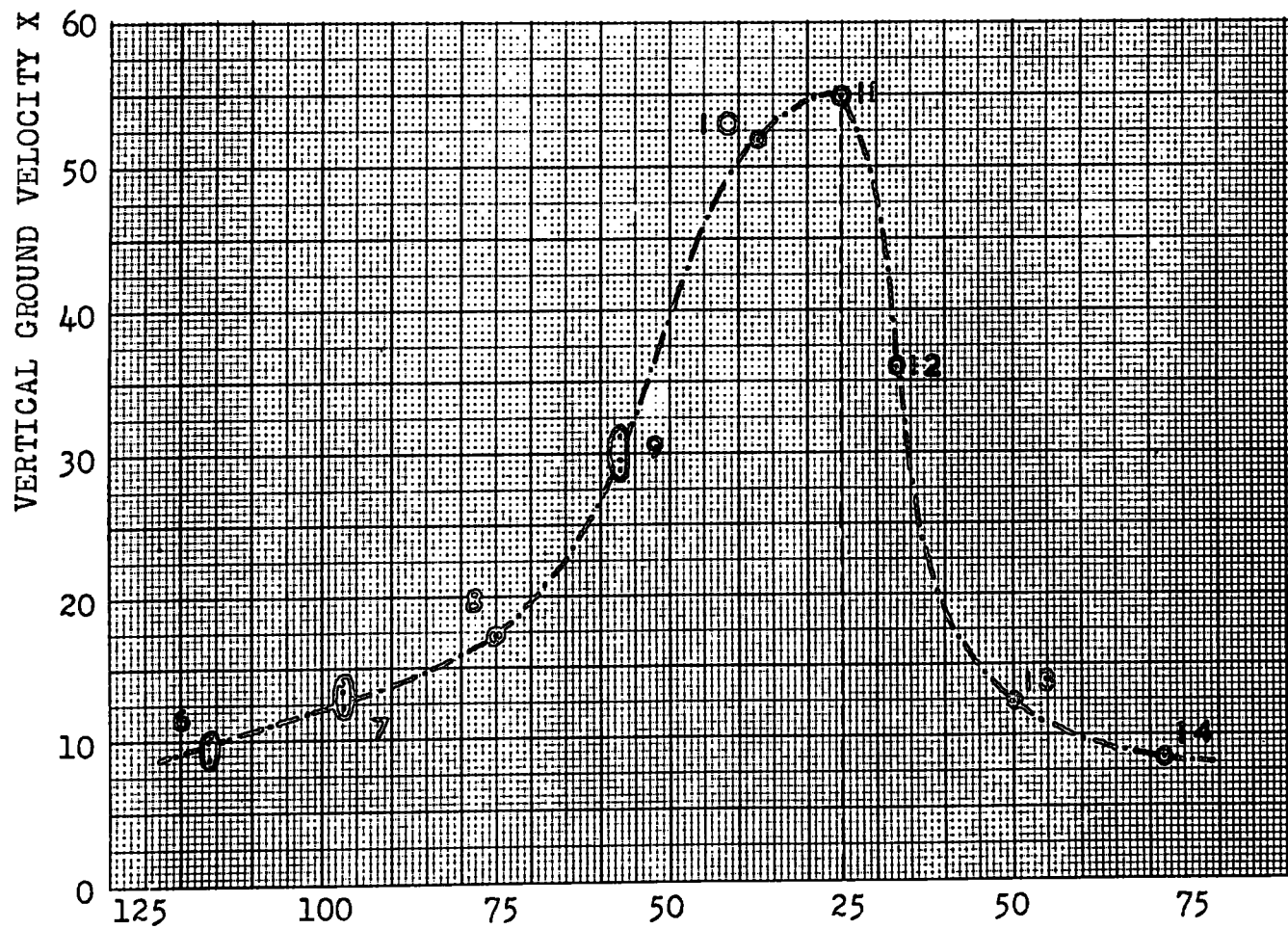


FIG. 23



(a)



(b)

FIG.24

by the two lower arc profiles. In order to examine the nature of this difference, we will confine our attention for the moment to this area and fit least squares solutions to the data obtained from it:-

Ground velocity values from each of the stations along the two lower arc profiles were plotted on an attenuation graph (large circles only in Fig. 22). A least squares fit was made on the resulting two lines of scatter assuming that the form of the attenuation follows equation (4.4). The form of the curves that must be fitted to Fig. 22 are combined exponential-hyperbolic functions. In order to simplify the least squares calculation, the hyperbolic function was eliminated by transferring the scatter of Fig. 22 onto a graph of $V.R$ against R . In this way the form of the least squares fit is exponential and becomes a straight line on the logarithmic scale since:

$$V = \frac{V_0}{R} \cdot e^{-\alpha R}, \text{ and thus, } \text{Log } V.R = -\alpha.R + \text{Log } V_0,$$

which is the form of a straight line. The least squares fit was performed on the logarithmic scale and the resulting two straight line graphs are shown in Fig. 25. By transferring the graphs to the linear scale, exponential curves were formed, (Fig. 26) which are the absorption curves for the two areas of different attenuation. The least squares are plotted on the velocity-distance graph of Fig. 22 if the complete attenuation curves according to equation (4.4) are required.

Now from Figs. 25 or 26 the rate of absorption was measured for the 2 different attenuating regions to the south

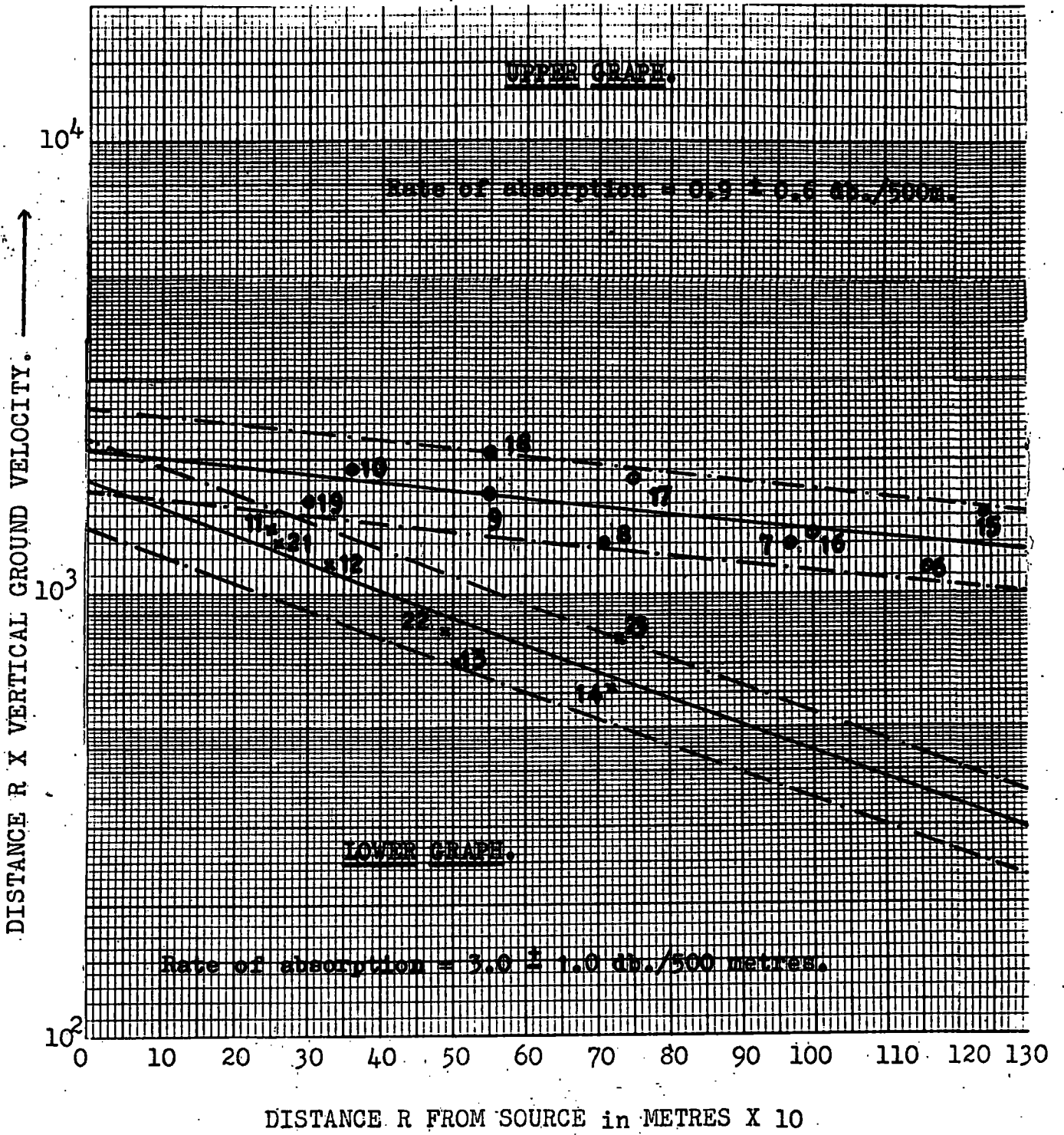


FIG.25

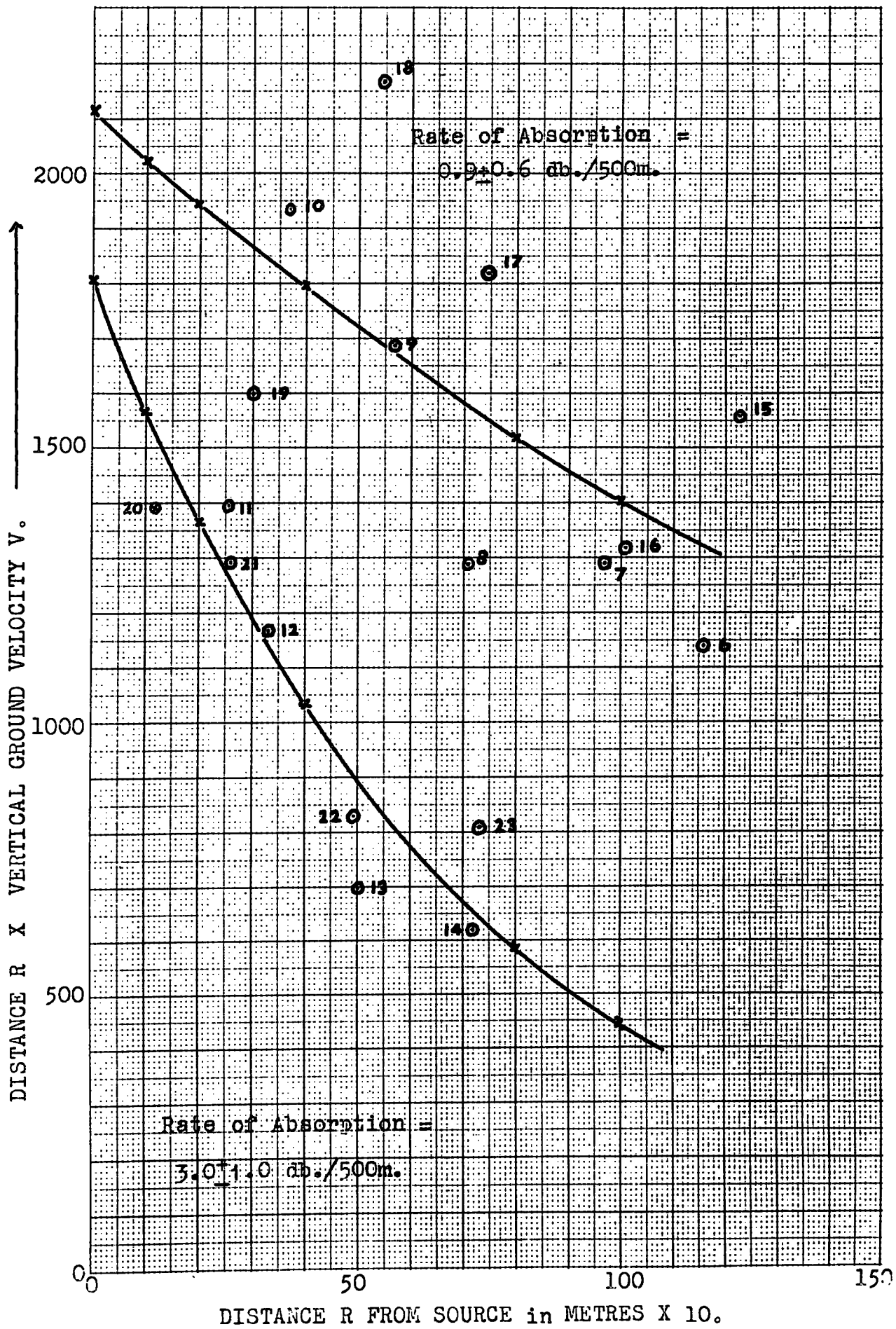


FIG. 26

and west of the plant, and found to be 3.0 ± 1.0 and 0.9 ± 0.6 db./500 metres respectively.

Now the reason why a difference in attenuation is not observed along the topmost arc profile (Fig. 24a) is that each station along it is a similar distance from the source, thus rendering the profile insensitive to any changes in attenuation along its length. It will be noticed that the velocity values at stations 3, 4 and 5 plot on Fig. 22 midway between the lines of scatter for the two regions of different attenuation. This suggests that the noise received at each station along the profile has been attenuated from the source at a rate intermediate between the two values found to exist along the two lowermost arc profiles. A possible explanation for this is that the lower rate of attenuation found to the west of the plant extends over the entire area covered by the station network, with the exception of a region of higher attenuation (shown on Fig. 27) running in a narrow strip along the edge of the valley to the south of the plant, its westerly margin lying about halfway between the edge of the valley and the topmost arc profile. Stations 3, 4 and 5 would thus receive noise which had travelled from the source an equal distance through each of the two areas of different attenuation, resulting in an intermediate value for the overall rate of attenuation.

The northerly margin of the higher attenuating area is considered to lie somewhere between stations 19 and 20, since station 19 shows a marginal velocity value of similar type to those at stations 3, 4 and 5.

Now the high degree of scatter in the attenuation data is principally due to the combined effect of all random errors occurring in the measured values of ground velocity. These errors were discussed in detail on page 65. In addition to this, scatter of data may also result from inhomogeneities present in the ground, causing differential absorption of the seismic energy. However such an effect as this is considered small in comparison with those above owing to the overall homogeneous aspect of the Carboniferous sediments. It would thus appear that the degree of scattering reflects the departure from the ideal case when all points lie on an attenuation curve obtained when true relative ground velocity values are measured over the surface of a perfectly homogeneous medium. Since the method of recording over the station network has been essentially random, then the amount of scattering should give an estimate of the error in any measurements made from a least squares curve drawn through the scatter of points. The error in the calculated rates of absorption may thus be found, by calculating a quantity known as the Standard Error of Estimate which assesses the degree of uncertainty in the two Regression lines of Fig. 25; the limits of uncertainty are shown for each line.

Now a map of the Rookhope Area showing contour lines of equal vertical ground velocity is given in Fig. 27. The advantage of such a map is that it shows at a glance that all the measured noise originates from the Boltsburn Washing plant, and that two areas of different attenuation are present.

From the contour map it will be noticed that values of ground velocity at stations along the lowest arc profile are consistently higher than the corresponding stations of the middle arc profile, despite the fact that towards the extremities of each profile corresponding stations are approximately the same distance from the source. From Fig. 27 it can be seen that this effect is shown by seven out of nine pairs of stations, the only exceptions being the station pairs (10,19) and (7,16). Thus from this it would appear that there is some statistical support for there being a general rise in the ground velocity along the valley edge. However such a change in ground velocity may be due purely to the 10 → 30% error which is present in all the values of ground velocity. If this is the case then no significance can be attached to the observed differences. However it would be expected that if such a change was due to random errors, then there would be no consistency in the direction of the change along the valley edge.

From the above discussion, it thus seems more probable that there is a general rise in ground velocity values along the valley sides which may indicate that there is some sort of channelling effect controlling the propagation of seismic waves along the edge of the valley.

Comparison of Attenuation Results Obtained from Record Measurements
and Power Frequency Analysis

The only stations analysed using the Power frequency analysis were 9 and 6; it will be seen from Figs. 16 and 17 that the ratio of the power density in the 6 cps. peaks at these stations is 2600:160. The ratio of their amplitudes is thus $\sqrt{2600} : \sqrt{160}$ which is 4:1.

From direct measurement of the 6 cps. peaks at these stations the corresponding amplitude ratio is about 3.3:1. The results from both types of measurement are thus in fairly good agreement, the slight discrepancy between them possibly being due to the high 20% error associated with the direct measurement of the 6 cps. peaks at station 6.

CHAPTER V

INTERPRETATIONS AND CONCLUSIONS

1. INTERPRETATIONS

The Nature of the Noise Source

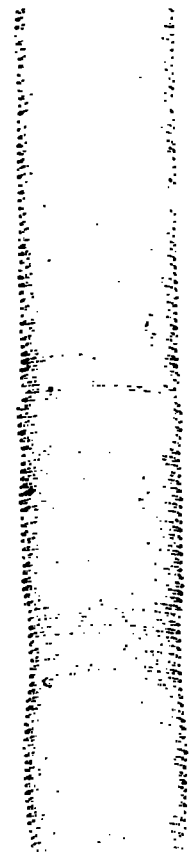
The Nature of the Noise Source as Deduced from the Records

The prominence of the 6 cps. component in the noise, demonstrated from the frequency analyses shows that there is present at the plant some type of 6 cps. sinusoidal wave generator. Modulation of the 6 cps. wave shows that there may be interference between the outputs from two 6 cps. generators with only slightly different working frequencies, such that the mean of them is about 6 cps. and their difference from the mean is equal to the frequency of the modulation (for theory of this see Appendix E). This is further supported by a recording made when the plant was closing down over the weekend (Fig. 28). From this it can be seen that, just before the noise was terminated, modulation ceased and a pure 6 cps. sinusoidal wave resulted. This shows that one of the 6 cps. generators was stopped before the other.

If there are only two generators working, and both give a "sine wave" output, then the form of the modulation should be smooth regular "beats". This is almost the case on the record shown in Fig. 12b.

The variation in the frequency of modulation shown to occur on the records may point to there being a number of sinusoidal wave generators with working frequencies different but close to 6 cps. A change in the number or combination operating at any one instant would also alter the frequency of the recorded modulation (cf. Figs. 12k and j).

Modulation ceases.



Plant noise ceases.



SURFACE

WILLMORE SEISMOMETER.

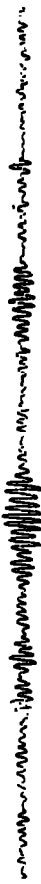


FIG. 28

The fact that the period of modulation varies but the overall 6 cps. noise level remains constant may be due to two possible mechanisms:

- (a) An increase in the number of 6 cps. generators may tend to increase the destructive interference in the resultant noise and this may help to retain it at almost constant level.
- (b) The number of generators may remain constant but different combinations may be used. The period of modulation would depend on the relative positions within the plant of the generators working at any one time.

Now a mixture of frequencies higher than 6 cps. are prominent in the immediate vicinity of the source. It is possibly high frequency noise from the 6 cps. generators, but may also originate from some other type of source within the plant.

Now it was stated earlier that two distinct noise levels exist, the higher one of which contains a greater percentage of frequencies above 6 cps. with a noticeable 11 → 12 cps. component. This increase in higher frequencies will be due to some type of noise generator which is not in operation during the period of lower noise level. The character of the modulation also changes (cf. Figs. 21a and b) which indicates that with the introduction of the higher frequency generator there is an accompanying change in the number or combination of 6 cps. generators operating. Since the 6 cps. modulation is distinctly different for the higher noise level, it would

seem that there is a particular combination of 6 cps. generators which does not occur throughout the duration of the lower noise level.

The Actual Mechanical Cause of the Recorded Noise, as Deduced From Information Supplied by the Plant Management

From discussion with the management of the plant, it would appear that the 6 cps. noise originates from motor-driven pumps which convey the fluorspar in liquid suspension from one processing unit to the next.

There are as many as nine pumps operating, at least two of which are kept going continuously 6 days a week. However some of them only work for short periods at a time, and thus it is these that are probably responsible for the variation in the 6 cps. modulation. The strong 11 + 12 component present in the raised noise level, is thought to be due to a pair of crushers which reduce the blocks of raw fluorspar into smaller, more manageable, sizes. The crushers are only used when the demand arises, but when in operation continue without a break through the day from 7 a.m. to 4 p.m. Since this coincides with the duration of the raised noise level it would appear fairly certain that the crushers are responsible for the increase in noise. The continuous high frequency that is detected at all stations near to the plant may be due to a grinder which is maintained like the pumps, in continuous operation for six days a week. The function of the grinder is to reduce the fluorspar lumps from the crushers into a powder fine enough to be carried in liquid suspension.

The Cause of the Difference in Attenuation

It was shown in the previous chapter that over the station network there exists two areas with noticeably different rates of seismic wave attenuation.

If Fig. 27 is compared with the geological map of Fig. 3 it will be seen that the boundary between these two regions follows fairly closely that of the layer of the drift. It is thus considered that such a surface feature as this may be influencing the propagation of the seismic energy, but whether it is of sufficient thickness to cause the observed change in the attenuation rate is a matter of some conjecture.

The main shortcoming of this theory is that such a thin superficial layer with a maximum thickness of only about 30' may be thought of as having a negligible effect in attenuating waves which may travel wholly or partly in the underlying Carboniferous sediments. Since the noise measured at Rookhope has a pronounced vertical component, it seems likely that the seismic energy travels with a speed near to that of the shear wave velocity, and is thus probably in the form of SV or Rayleigh waves. The possibility that strong highly incident P waves may be present can be discounted since the rapidly changing Carboniferous succession provides no clear-cut velocity changes to give large amplitude reflected waves. Thus the wavelength of a 6 cps. disturbance travelling with a speed of 3000 metres/second (the estimated shear wave velocity in Carboniferous sediments) would be about 500 metres. If the propagating medium is considered to be drift of an assumed transverse wave velocity of about 900 metres/second, then the wavelength of the

seismic energy is reduced to about 150 metres. If this is the case then over the region to the south of the plant body waves will predominate only within a distance of about 150 metres from the source, and Rayleigh waves at greater distances (refer to page 75 for explanation).

The evidence from the topmost arc profile, which indicates the presence of a higher attenuating region around the source, may show that any body waves must have a near surface nature for them to be affected by the layer of drift. Whether in fact SV waves could be propagated in such a thin layer is uncertain. However, it can be shown (Bullen, 1953) that a Rayleigh wave of 150 metres wavelength travels with an approximate depth of penetration of about 110 metres which is far in excess of the thickness of drift expected. It thus appears that Rayleigh waves cannot be set up in the drift layer, but may travel at some velocity which is nearer to that of the Carboniferous rocks beneath.

There is also another uncertainty associated with the 'drift' hypothesis:

It was stated that the boundary between the two areas of different attenuation follows that of the drift. It is possible that such a circumstance may arise as a result of insufficient station coverage in the region of the supposed 'attenuation' boundary. The western margin of the higher attenuating area was established only from evidence provided by the topmost arc profile, which must be considered questionable on the grounds of the small number of stations from this profile showing marginal ground velocity values on the attenuation graph of Fig. 22.

Some support for drift being the cause of the change in attenuation may be obtained from two sources:

(a) Both values of the absorption rate can be shown to be consistent with those found by other workers. It was stated previously that the wavelength of seismic energy propagating through carboniferous rocks is about 500 metres. Such a wavelength as this probably exists over the area to the west of the plant where drift is absent. O'Brien (1961) has stated that laboratory experiments have revealed that the rate of absorption in rocks generally lies within the range $0.1 \rightarrow 1.0$ decibels/wavelength. The rate of absorption found for the western area is 0.9 ± 0.6 decibels/500 metres or 0.9 ± 0.6 decibels/wavelength which is in general agreement with the values stated by O'Brien.

Now for the area to the south of the plant, the rate of absorption is 3.0 ± 1.0 decibels/500 metres. If, due to the presence of drift, the wavelength of the propagating energy is considered to be 150 metres, then the rate of absorption for this area becomes 0.9 ± 0.3 decibels/wavelength which again is consistent with the figures quoted by O'Brien.

(b) The suggestion of channelling of seismic waves along the edge of the valley discussed on page 80, shows that the propagation of seismic energy may be influenced by near surface conditions. This may indicate that a shallow surface feature such as the layer of drift may be responsible for the observed change in attenuation.

Now difference in drainage may play some part in the observed attenuation results. According to Born (1941) and Usher (1962) an increased moisture content increases the energy loss

per cycle, and thus increases the rate of attenuation (the details of this were discussed in Chapter 1). However, this may be just a corollary of supposing that the drift is the cause of the attenuation change, since boulder-clay drift may hold more water than the underlying rocks.

The possibility that the Carboniferous rocks may be causing the difference in attenuation may be eliminated for the following reasons:

- (a) the change in attenuation is seen along the two lowermost arc profiles. Since the Carboniferous rocks are almost horizontal, laterally uniform and unfaulted, and the arc profiles follow the topographic contours, the depth of any one bed below the profiles will remain constant along their length. Thus the Carboniferous sequence should cause uniform attenuation along the profiles.
- (b) Since the Carboniferous has been considered to have an approximately uniform composition, then large variations in its attenuation properties should not occur.

A fourth possible conclusion that may be reached is that the change in the rate of attenuation is due to a difference in the distribution of the predominant wavetypes propagating over the two regions, and not to any change in the attenuating medium.

This theory thus assumes that the Carboniferous rocks are the main controlling factor in the attenuation; little seismic energy being propagated through the layer of drift in comparison with the older rocks beneath.

If, for some reason, body waves predominate over greater distances from the source on its south side than on its west, then it may be that Rayleigh waves only predominate over an area towards the western end of the two lower arc profiles and not at all over their southern extremity.

Thus over the area to the south of the plant, body waves may predominate within about 500 metres from the source and Rayleigh waves after about one kilometre. Over the region to the south of the plant, conditions for some reason are more unfavourable to the propagation of surface waves after about 500 metres and these are relatively suppressed in favour of body waves which predominate over most of the region. If this is the case then it could be argued that equation (4.4)^{p.74} is still a valid description of the attenuation over the area to the west of the plant, but that equation (1.2) is a more correct relation to describe the attenuation over the region to the south of the plant. The continued use of equation (4.4) is further supported since, as we have seen previously, it gives a rate of absorption consistent with those generally found for rock materials.

Now if the layer of drift over the area to the south of the plant has a negligible effect in the attenuation of seismic waves then it will be noticed that if equation (4.4) was applied to this area, then a rate of absorption of 3.0 ± 1.0 decibels/wavelength would be obtained which is a value in excess of those normally found. This discrepancy is rectified, however, if this equation is replaced by equation (1.2) which describes the attenuation of body waves from a surface source. It is found that by

doing this a value for the rate of absorption is obtained which is very close to that found for the area to the west of the plant. The reason for this apparent decrease in the absorption rate is because by changing the equation used, the power of R in the function $1/R$, present in both equations (4.4) and (1.2) has been increased from 1 to $3/2 \rightarrow 2$.

Thus the above theory has demonstrated that the rate of absorption may be the same for the areas to the west and south of the plant. Since body waves may be more predominant over the southern area, and surface waves may have a greater influence over the western region, then the change in the overall attenuation seen in Figs. 23 and 24b is due to differences in the geometrical spreading of the seismic wavefronts over the two areas (the contribution of this factor to the attenuation was discussed in Chapter 1).

Now the "intermediate" values of ground velocity at stations 3, 4 and 5 on the topmost arc profile can be easily explained on the basis of the above theory if it is assumed that, along the wavepaths of the recorded noise, the distance from the source over which body waves predominate is intermediate between that for the areas to the west and south of the plant. In order to clarify this, the area over which body waves may predominate is very approximately shown as the shaded area in Fig. 27. A possible explanation of the asymmetry of this area in relation to the position of the source is that, in some way, the layer of drift is prolonging the propagation of the seismic energy in the form of body waves, or conversely, that it is opposing the establishment of surface waves.

We have already noted that it is unlikely that Rayleigh waves can be set up within the layer of drift itself but whether such a layer could prevent them from forming is uncertain. The fact that the source is at a lower elevation than the layer of drift may play some part in deciding this.

Thus, to conclude, two theories to explain the difference in attenuation have been evolved. Both of them depend on rather debatable mechanisms associated with the propagation of seismic energy through a thin superficial surface layer on an approximately uniform halfspace. Due to this uncertainty, coupled with the lack of precise knowledge of the types and distribution of the waves present, no preference has been given to either of these theories.

CONCLUSIONS

The major conclusions of this research are as follows:

It was shown that the most prevalent component in the local noise over the area studied at Rookhope was a 6 cps. sinusoidal wave. Nearly all local noise was found to originate from a single source.

Horizontal attenuation curves of the 6 cps. component were plotted, and it was discovered that there were two areas of noticeably different rates of attenuation.

Two causes of this change were put forward:

(1) That the change is due to a layer of drift covering the area of higher attenuation. Absorption rates calculated on the basis of the hypothesis yielded results consistent with those of previous workers.

(2) That the difference in attenuation is not directly due to any change in subsurface conditions, but to a difference in the type of wave predominating over the two areas. The calculated rates of attenuation were only found to be in agreement with generally found values, when body waves were chosen as the predominant wave-type propagating over the higher attenuating region, and both Rayleigh and body waves over the lower attenuating area.

Due to the various uncertainties associated with each of these theories, no preference was made.

Waveform and frequency analyses revealed the composite nature of the noise source. It was concluded that the source consisted of a number of closely spaced units, mechanically generating noise of two predominant frequencies, 6 and 11 → 12 cycles per second.

The difference in the rates of attenuation of these components from the source was also demonstrated. Time did not permit a full study of this to be made, but initial results showed that the rate of attenuation increased with frequency which is in accordance with what is generally observed.

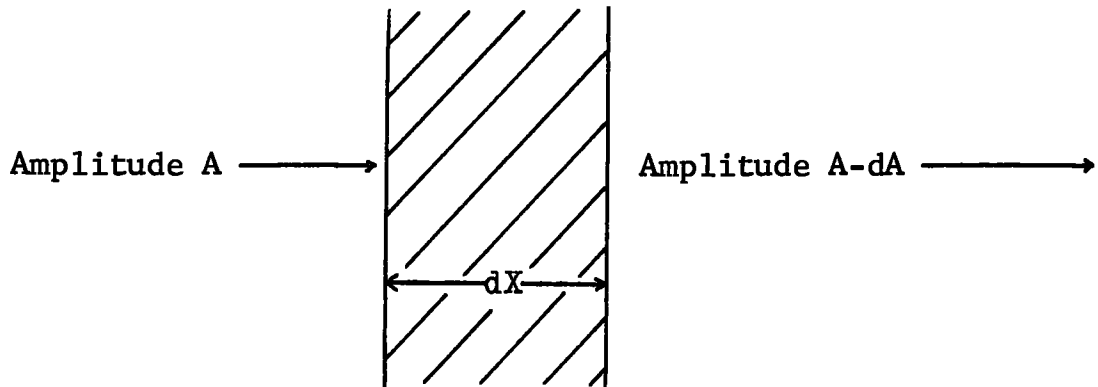
APPENDIX A



DERIVATION OF THE FORMULA $A_R = A_0 \cdot e^{-\alpha R}$

This is the standard form for any equation describing the attenuation by a medium in which α , the attenuation constant is independent of amplitude.

Consider a plane wave of amplitude A passing through an attenuating medium of thickness dX :



Then α is defined by: $-dA = A \cdot \alpha \cdot dX$, i.e., the fractional change in amplitude per unit distance travelled.

Integrating over any distance R , we have:

$$A_R = A_0 \cdot e^{-\alpha R} ,$$

where A_0 is the amplitude at $R = 0$, and A_R is the amplitude of the wave after having passed through a thickness R of the medium.

APPENDIX B

PROOF OF FORMULA $= 0.58 \sqrt{\frac{a_o \cdot f_o}{d}}$, (FROM CARPENTER & MARSHALL, 1957)

The full proof of this formula is somewhat lengthy, so only the major steps in the derivation are included.

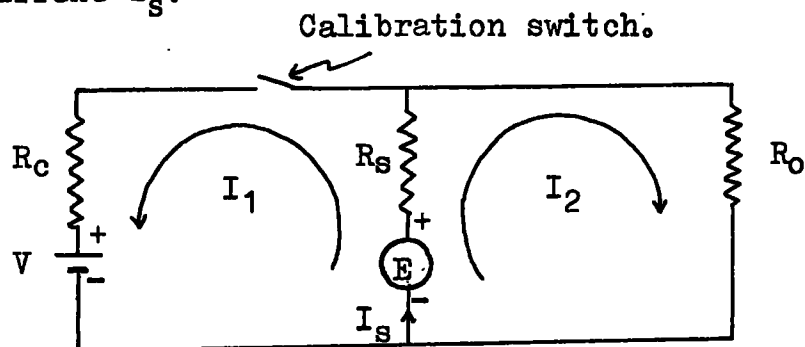
1. The differential equation describing the motion of the seismometer magnet due to ground motion and a current step injected through the coil is given as:

$$M \cdot \frac{d^2 x}{dt^2} + r \cdot \frac{dx}{dt} + c \cdot x = M' \cdot \frac{d^2 z}{dt^2} + S I_s \dots\dots\dots (1)$$

R.H.S. = Restoring forces

L.H.S. = Displacement forces

Where c = stiffness of spring suspension; M = mass of magnet; z = displacement of the ground; x = displacement of the magnet; r = mechanical damping factor; M' = mass of magnet + suspension (approx = M); I_s = the current passing through the coil and S is an instrumental constant such that $S I_s$ is the displacement force due to the current I_s .



2. Now an expression for I_s may be obtained by applying Kirchhoff's laws to the above seismometer calibration circuit, consisting of

the seismometer, amplifier and calibration circuit resistances R_s , R_o , R_c . I_s is expressed in terms of these resistances and the voltage, V , of the calibration battery.

3. Substituting for I_s in (1) we have:

$$\frac{d^2x}{dt^2} + (r/M + S^2/R_1.M) \frac{dx}{dt} + (c/M).x = (S.V/R_2.M) + \frac{d^2z}{dt^2} \dots\dots (2)$$

where $R_1, R_2 = f(R_o, R_c, R_s)$

This has the form of the standing equation for any forced harmonic vibration:

$$\frac{d^2x}{dt^2} + 2nw_o \frac{dx}{dt} + w_o^2.x = f(t) \dots\dots\dots (3)$$

where w_o is the free resonance frequency; n = damping coefficient.

4. Now, considering the seismometer calibration circuit only,

$\frac{d^2z}{dt^2} = 0$, since the motion of the seismometer (due to the current step) is so much larger than the ground motion.

The full general solution of (2) then becomes:

$$x = e^{-nw_o t} (A \cos(pt) + B \sin(pt)) + x_s \dots\dots\dots (4)$$

where

$$p = \sqrt{1-n^2} .w_o, \text{ and } x_s \text{ is the steady state solution.}$$

For steady state:

$$\frac{d^2(\quad)}{dt^2} = \frac{d(\quad)}{dt} = 0, \text{ thus } (c/M).x_s = SV/R_2M. \text{ - Therefore,}$$

$$x_s = SV/R_2c \dots\dots\dots (5)$$

where $R_2 = f(R_c, R_o, R_s)$.

5. The output voltage across the amplifier, V_o , is then found for both switch positions in the seismometer calibration circuit.

Closed Switch

Constants A and B may be found from (4) using the initial conditions of the motion of the mass. By differentiation and substitution, it can be shown from (4) that:

$$\frac{dx}{dt} = x_s \cdot \frac{w_o \cdot e^{-nw_o t}}{(1-n^2)^{1/2}} \cdot \sin(pt) \dots\dots\dots (6)$$

By applying Kirchhoff's laws to the seismometer calibration circuit it can be shown that:

$$V_o = \frac{R_o \cdot R_s V + R_c \cdot S \cdot (dx/dt)}{G} \text{ where } G = R_o \cdot R_s + R_o \cdot R_c + R_c \cdot R_s, \text{ and } S \cdot \frac{dx}{dt}$$

has replaced E, the E.M.F. generated by the motion of the magnet.

Substituting values of x_s and dx/dt obtained from (5) and (6) in

(7), we have:

$$V_o = \frac{R_o R_s V}{G} \left(1 + \frac{R_c}{R_s V} \cdot \frac{S^2 V}{R_2 c} \cdot \frac{w_o \cdot e^{-nw_o t}}{(1-n^2)^{1/2}} \cdot \sin(pt) \right) \dots\dots (8)$$

Open Switch

For the open switch position, a similar type of argument is used leading to:

$$V_o = - \frac{R_o}{R_o + R_s} \cdot \frac{S^2 V}{R_2 c} \cdot \frac{w_o \cdot e^{-n'w_o t}}{(1-n'^2)^{1/2}} \cdot \sin(p't) \dots\dots\dots (9)$$

Now if a_o is the amplitude of the undamped oscillation on open switch (i.e., $n' = 0$), then from (9):

$$a_o = - \frac{R_o}{R_o + R_s} \cdot \frac{S^2 V}{R_2 c} \cdot w_o \dots\dots\dots (10)$$

If d is the steady D.C. level in the output for the closed switch position then from (8):

$$d = \frac{R_o R_s V}{G} \dots\dots(11). \quad \text{Thus from (10) and (11) we have:}$$

$$a_o/d = \frac{G}{R_s(R_o+R_s)} \cdot \frac{S^2}{R_2 M w_o^2} \quad (1/c = 1/Mw_o^2 \text{ by equating coeffs. in (2) and (3)).}$$

Therefore:

$$S^2 = \frac{R_2 R_s (R_o + R_s)}{G} \cdot \frac{2 \pi \cdot M \cdot a_o \cdot f_o}{d}, \quad \text{where } w_o = 2 \pi f_o$$

Substituting in this equation the actual values of R_s , R_o , R_c and M , we obtain:

$$S = 1.16/\sqrt{a_o f_o/d}, \quad \text{for the seismometer calibration circuit,}$$

but it can be shown that:

$$S_{\text{record}} = \frac{R_{sh}}{R_s + R_{sh}} \cdot S_{\text{cal}} \quad \text{where } R_{sh} = \text{damping resistance (see}$$

Fig. 6a, page 27). Since $R_s = R_{sh} = 500$ ohms, then $S_{\text{record}} = 0.58/\sqrt{a_o f_o/d}$

Now S is in fact the velocity sensitivity:

In Open Switch Position:

$$/V_o/ = R_o/I_2/ = R_o/(R_o+R_s) \cdot S/dx/dt / \quad \text{where } / / = \text{"magnitude of"}$$

Since R_o is very much greater than R_s then $R_o/(R_o + R_s) = 1$.

Thus $S = \frac{V_o}{\frac{dx}{dt}}$ which is the ratio of the output to the velocity

of the magnet producing it.

THUS: SENSITIVITY $S = 0.58/a_o f_o/d$ (12)

APPENDIX C

From equation (1) Appendix B, a similar equation may be derived except that the current in the coil is not injected as a step, but is generated by the motion of the coil:

$$M \frac{d^2 x}{dt^2} + r \frac{dx}{dt} + c \cdot x = M' \frac{d^2 z}{dt^2} - JI \dots\dots\dots (1)$$

Now from Fig. 6a, it can be shown that:

$$E = IR_s + R_{sh} \cdot R_o I / (R_{sh} + R_o) \quad \text{But } E = J \frac{dx}{dt}$$

Therefore $J \frac{dx}{dt} = I (R_s + R_{sh} \cdot R_o / (R_{sh} + R_o))$ where I is the current through the seismometer coil.

Thus (1) becomes:

$$M \frac{d^2 x}{dt^2} + (r + J^2/Q) \frac{dx}{dt} + c \cdot x = M' \frac{d^2 z}{dt^2}, \quad (Q = (R_s + R_{sh} \cdot R_o / (R_{sh} + R_o)))$$

but M is approximately equal to M',

Therefore

$$d^2 x / dt^2 + (r/M + J^2/Q \cdot M) \frac{dx}{dt} + (c/M) \cdot x = d^2 z / dt^2 \dots\dots\dots (2)$$

Again this has the form of equation (3) in Appendix B.

Thus $(r/M + J^2/Q \cdot M) = 2n\omega_o$ and $c/M = \omega_o^2$

By substituting $x = x_o e^{i(\omega t - \&)}$ and $z = z_o e^{i(\omega t)}$ in (2),

two expressions are obtained, one relating the real components, and the other equating the imaginary ones:

$$\tan \& = 2n\omega_o \omega / (\omega_o^2 - \omega^2) \quad \text{and} \quad x_o ((\omega_o^2 - \omega^2) \cos \& + 2n\omega \omega_o \sin \&)^{1/2} = \omega^2 z_o$$

These combine to give:

$$x_0 = -z_0 w^2 / ((w_0^2 - w^2)^2 + (2nw_0 w)^2)^{1/2}$$

Substituting for x_0 and z_0 and differentiating:

$$S = \frac{dx/dt}{dz/dt} = w/w_0 \sqrt{(w_0/w - w/w_0)^2 + 4n^2} \dots\dots\dots (3)$$

& becomes equal to zero since the velocity sensitivity is the ratio of the velocities of the ground and magnet for zero lag

$$\text{If } w = 2 \pi f \text{ then } S = f_0 \sqrt{(f_0/f - f/f_0)^2 + 4n^2} \dots$$

APPENDIX D



The A.C. amplifier system present in the recorder will not pass a direct current without distortion. This is due to the coupling capacitor in the amplifier, C, which blocks the D.C. level. On raising the D.C. level the capacitor gradually charges up through the resistance R, (Fig. 9). When the calibration switch is opened, the D.C. level slowly drops as the capacitor discharges through the resistance.

The change in D.C. level is shown on the amplifier calibration curve below.

From Fig. 9, it can be seen that:

$$V_{out} = \frac{R.V. in}{-j/wC + R}, \text{ where } w = \text{frequency of input in radians/second}$$

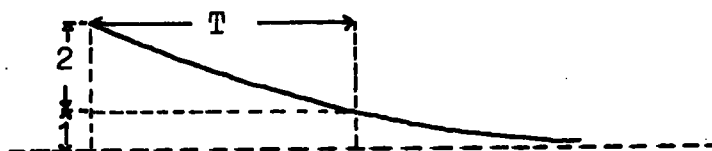
$$\text{Therefore: } V_{out} = \frac{V_{in}}{1-j/wT}, \text{ where } T = CR = \text{Time constant.}$$

$$\text{Therefore: } V_{out}/V_{in} = 1/(1-j/wT).$$

Multiplying the R.H.S. by the complex conjugate:

$$(V_{out}/V_{in})^2 = 1/(1+1/w^2T^2), \text{ Therefore } |V_{out}/V_{in}| = \sqrt{1/(1 + 1/w^2T^2)}$$

An approximate value of T can be estimated from the amplifier calibration curve thus:

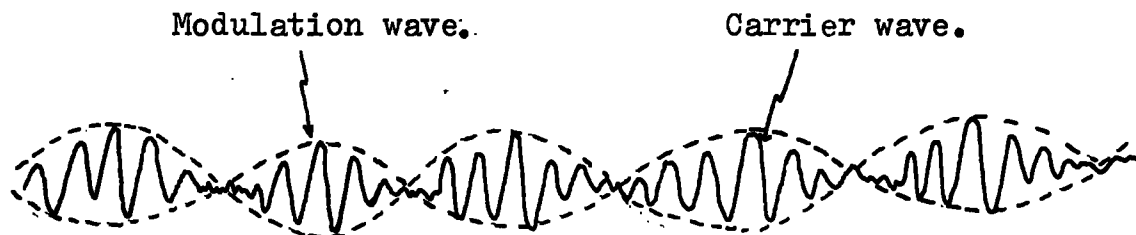


For the Neocardiograph amplifier, T = 2 seconds.

Thus the theoretical response curve for all those frequencies below the experimental limit of 4 cps. may be calculated.

APPENDIX E

A modulated sinusoidal wave such as the one recorded at Rookhope is sketched below:



Suppose that the modulation wave has a frequency df , and the "carrier" wave has a frequency f , then the modulation is due to two "Sine" waves of frequency f_1 and f_2 such that:

$$f_1 = f + df, \text{ and } f_2 = f - df.$$

For the case at Rookhope, where $f = 6$ cps., and $df = 0.1$ to 0.2 cps., we have:

$$f_1 = 6.1 \text{ to } 6.2 \text{ cps.}, \text{ and } f_2 = 5.8 \text{ to } 5.9 \text{ cps.}$$

Thus it is possible at Rookhope that the recorded modulated 6 cps. waveform is in fact due to two "sine" waves showing very similar frequencies with a mean of about 6 cps.

ACKNOWLEDGMENTS

I would like to thank Professor K. C. Dunham for providing the facilities for this research and Dr. R. E. Long for his close supervision during the past year. I would also like to convey my gratitude to Dr. M. H. P. Bott for his valuable assistance in the writing of the computer programmes for the power frequency analysis, and to The Atomic Weapons Research Establishment for the loan of much of the recording equipment.

D.S.I.R. have provided an Advanced Course Studentship for the past year.

BIBLIOGRAPHY

- Biot, M.A., 1956. Theory of propagation of elastic waves in a fluid-saturated porous solid. Part 1: Low frequency range. J. Ac. Soc. Am. 28, No. 2, pp. 168-178.
- Birch, F., and Bancroft, D., 1938. Elasticity and Internal Friction in a Long column of Granite. B.S.S.A. 28, pp. 243-254.
- Blackman, R.B. and Tukey, J.W., 1958. "The measurement of Power Spectra". Dover Publications, Inc., New York.
- Born, W.T., 1941. The attenuation constant of earth materials. Geophysics 6, Part 2, pp. 132-148.
- Bullen, K.E., 1953. "An Introduction to the Theory of Seismology". 2nd ed., Cambridge University Press, p.90.
- Bycroft, G.N., 1956. Forced vibration of a rigid circular plate on a semi-infinite elastic space and on an elastic stratum. Phil. Trans. Roy. Soc. London, 248, pp.327-368.
- Carpenter, E.W. and Marshall, R., 1957. Some notes on the Willmore Seismometer. U.K.A.E.A. Foulness Division Note No. 3/57.
- Donato, R.J., O'Brien, P.N.S. and Usher, M.J., 1962. Absorption and dispersion of elastic energy in rocks. Nature 193, No. 4817, pp. 764-765.
- Dunham, K.C., 1948. Geology of the North Pennine orefield. Mem. Geol. Surv.
- Ewing, M., Jardetsky, W.S., and Press, F., 1957. "Propagation of Elastic Waves in Layered Media". McGraw-Hill, New York. pp. 53-55.

- Fail, J.P., Grau, G. and Lavergne, M., 1962. Couplage des sismographes avec le sol. *Geophys. Prosp.* 10, pp. 128-147.
- Fortsch, O., 1956. Die Ursachen der Absorption Elastischer Wellen. *Annali di Geofisica*, 9, 4, pp. 469-524.
- Howell, L.G., 1961 Absorption of seismic waves in rock. *Bur. Central Seismol. Internat. Pubs., Ser. A, Travaux Sci.* No. 21, pp. 55-64.
- Knopoff, L. and MacDonald, 1958. Attenuation of Small Amplitude Stress Waves in Solids. *Reviews of Modern Physics*, 30,(4), pp. 1178-1192.
- _____, and _____, 1960. Models for Acoustic loss in solids. *Jour. Geophys. Research*, 65, No.7. pp. 2191-2197.
- Lamb, H., 1904. On the propagation of tremors over the surface of an elastic solid. *Phil. Trans. A*, 203, pp. 1-42.
- McDonal, F.J., Angona, F.A., Mills, R.L., Sengbush, R.L., Van Nostrand, R.G., and White, J.E., 1958. Attenuation of Shear and Compressional Waves in Pierre Shale. *Geophysics* 23, (3), pp. 421-439.
- O'Brien, P.N.S., 1961. The nature and magnitude of elastic absorption. *Geophys. Prosp.* 9, pp. 261-275.
- Ricker, N., 1953. The form and laws of propagation of seismic wavelets. *Geophysics* 18, pp. 10-40.
- Runcorn, S.K., (Editor), 1960. "Methods and Techniques in Geophysics" Volume 1, Interscience Publishers Inc., New York.
- Sezawa, K., and Kanai, K., 1935. The rate of damping in seismic vibrations of a surface layer of varying density or elasticity. *Bull. Earthq. Res. Inst. Tokyo*, 13, pp. 1-17.

Usher, M.J., 1962. Elastic behaviour of rocks at low frequencies.

Geophys. Prosp., 10, No. 2, pp. 119-127.

Willmore, P.L., 1950. The theory and design of two types of portable seismograph. Mon. Not. R. astr. Soc.,

Geoph. Suppl. 6.

Wyllie, M.R.J., Gardner, G.H.F., and Gregory, A.R., 1962.

Elastic wave attenuation in porous media. Geophysics

27, No. 5, pp. 569-589.

